AGRADECIMENTOS

Devo o maior dos agradecimentos ao meu orientador Doutor Jorge Lima, pela disponibilidade, partilha de conhecimento, apoio e simpatia.

Agradeço aos membros do Grupo da Biologia do Cancro do IPATIMUP pelas gargalhadas constantes e pela ajuda pontual. Agradeço ao Doutor Valdemar Máximo e à Doutora Paula Soares pelo acolhimento no grupo e à Rute, ao Pedro e à Xana pela ajuda preciosa na aprendizagem das técnicas e na realização do meu trabalho.

Não posso deixar de agradecer aos investigadores que colaboraram na obtenção destes resultados: Doutora Maria Oliveira (INEB), Doutora Ana Teixeira e Doutor Nuno Carinhas (IBET/ITQB).

Pelo apoio amigo dos MBCémicos (quer os mais perto e os mais longe) e dos amigos de longa data.

Finalmente, agradeço aos meus pais pela forma incansável como sempre me apoiam e confiaram em mim, principalmente nos momentos mais difíceis. Não esqueço igualmente a minha irmãzinha Inês, desde a preocupação constante sobre o meu bem-estar até aos textos passados no computador.

Muito obrigada!

INDEX

GLOSSARY

ADP	Adenosine diphosphate
ANOVA	Analysis of variance
ANT	Adenine nucleotide translocator
ATP	Adenosine triphosphate
BrdU	5-bromo-2-deoxyuridine
COX II	Cytochrome oxidase subunit II
Cyt b/c	Cytochromes b or c
DCA	Dichloroacetic acid
DMEM	Dulbecco's modified eagle medium
DMSO	Dimethyl sulfoxide
DNA	Desoxyribonucleic acid
dNTP	deoxyribonucleotide triphosphate
$FAD/FADH_2$	Flavin adenine dinucleotide
FBS	fetal bovine serum
^{18}F-FDG	^{18}F-fluorodeoxyglucose
GFP	Green fluorescence protein
G6P	glucose-6-phosphate

G6PD	glucose-6-phosphate dehydrogenase
GLUT1/3/4	Glucose transporter 1, 3 or 4
H&E	Haematoxylin-eosin
HIF-1	Hypoxia-inducible transcription factor 1
HIF-1α/1β	Hypoxia-inducible transcription factor 1α or 1β
HK	Hexokinase
HKII	Hexokinase II
HSV	Herpes simplex virus
IBET	Instituto de Biologia Experimental e Tecnológica
ITQB	Instituto de Tecnologia Química e Biológica
INEB	Instituto de Engenharia Biomédica
LDH	Lactate dehydrogenase
LDH-A/-B	Lactate dehydrogenase subunit A or B
MtDNA	Mitochondrial DNA
MtPTP	Mitochondrial permeability transition pore
NAD/NADH	Nicotinamide adenine dinucleotide
ND1/2/3/4L/4/5/6	NADH:ubiquinone oxidoreductase subunit 1, 2, 3, 4L, 4, 5 and 6
nDNA	Nuclear DNA

OXPHOS	Oxidative phosphorylation
PBS	Phosphate buffered saline
PCR	Polymerase chain reaction
PDH	Prolyl hydroxylases
PDKI	Pyruvate dehydrogenase kinase 1
PEG	Polyethylene glycol
PET	Positron emission tomography
RNAi	RNA interferance
ROS	Reactive oxygen species
rRNA	Ribosomal RNA
RT-PCR	Reverse transcriptase PCR
SDH	Succinate dehydrogenase
SDHA/B/C/D	Succinate dehydrogenase subunit A, B, C or D
shRNA	short hairpin RNA
STS	Staurosporine
tRNA	Transfer RNA
tRNA	Transfer RNA
$tRNA^{Leu(UUR)}$	Transfer RNA for leucine UUR

TUNEL	Terminal deoxynucleotidyl transferase-mediated d-UTP Nick End Labeling assay
VDAC	Voltage-dependent anion ion channel
VHL	Von Hippel-Lindau
Wt	Wild-type

ABSTRACT

In addition to the six hallmarks of cancer proposed by Hanahan & Weinberg in 2000 (Hanahan and Weinberg, 2000), a seventh, and the first biochemical hallmark to be identified, has been highlighted throughout the last 50 years: the "Warburg effect", also known as aerobic glycolysis. This phenomenon was initially described by Otto Warburg who reported a high consume of glucose and release of lactate by malignant cells comparing to non-neoplastic cells in presence of oxygen. Warburg hypothesised that this aerobic glycolysis was irreversible and due to an impairment of mitochondrial respiration (Warburg, 1956). This property of cancer cells has been exploited through the use of positron emission tomography (PET) but its causal relationship with cancer progression remains unclear. Many models have been advanced and one proposes that mutations in oxidative phosphorylation (OXPHOS) genes lead to mitochondrial dysfunction, being responsible for the acquisition of the "Warburg effect" (Frezza and Gottlieb, 2009). However, the latter hypothesis has not been consistently evaluated.

The aim of this work was to establish cellular models of mitochondrial dysfunction caused by mutations in the mitochondrial DNA (mtDNA) or in nuclear DNA (nDNA)-encoded mitochondrial proteins. We also wanted to demonstrate that these models present the "Warburg effect" and this is essential for the progression of tumorigenesis. To achieve our purposes, we made use of the cybrid (transmitochondrial hybrid) technology, a technique that allows the analysis of mtDNA mutations against a common nuclear background (143B osteosarcoma cells) (Swerdlow, 2007). We have constructed a cybrid cell line harbouring a mutation in the mtDNA gene for $tRNA^{Leu(UUR)}$. We have also performed silencing of the mitochondrial succinate dehydrogenase subunit B

(SDHB) protein (encoded by the nDNA) using RNA interference in a cybrid cell line with wild-type mtDNA.

We analysed the metabolic phenotype of these cell lines, by assessing the fluxes of glucose, lactate, glutamate and glutamine across the plasma membrane and the expression of some key enzymes in bioenergetic pathway. We have concluded that both the SDHB silencing and the mtDNA mutation alters the cellular metabolism, increasing glycolysis. To assess the influence of the mtDNA mutation and the "Warburg effect" in tumourigenesis, cybrids with the mtDNA mutation were analyzed for markers associated to tumourigenesis such as cell growth, cell death, and motility and migration. Although mutant cybrids showed no differences in the population doubling time, they displayed more resistance to apoptosis and more motility and migration ability.

Finally, by injecting both wild-type and mtDNA-mutated cybrids in nude mice, we saw tumours formation only in mice injected with mtDNA mutated cybrids; in addition some mice already displayed invasion and metastasis, clearly demonstrating the tumourigenic potential of this specific mutation *in vivo.*

Although these results are yet superficial, they show that mitochondrial dysfunction caused either by mtDNA mutation or SDHB silencing, results in altered cellular metabolism, which, in the case of the mtDNA mutation is associated with an increased tumourigenic potential. Further studies will help to understand the mechanisms behind this so common phenomenon in tumour cells.

Keywords: "Warburg effect", aerobic glycolysis, mitochondrial dysfunction, cancer, metabolism, cybrids.

RESUMO

Para além dos seis "hallmarks" do cancro propostos por Hanahan & Weinberg em 2000 (Hanahan and Weinberg, 2000), um sétimo e o primeiro "hallmark" bioquímico a ser identificado tem sofrido destaque ao longo destes últimos 50 anos: o "efeito de Warburg", também conhecido como glicólise aeróbia. Este fenómeno foi inicialmente descrito por Otto Warburg, que mostrou que um elevado consumo de glucose e secreção de lactato em células malignas, em comparação com células não-neoplásicas, na presença de oxigénio. Warburg sugeriu que a glicólise aeróbia seria irreversível e devia-se a defeitos na respiração mitocondrial (Warburg, 1956). Esta propriedade das células cancerígenas tem sido explorada através da tomografia de emissão de positrões (PET) apesar de a relação causal com a progressão do cancro permanecer pouco clara. Vários modelos têm sido propostos, sendo que um deles sugere que mutações nos genes da cadeia fosforilativa (OXPHOS) originam uma disfunção mitocondrial e são responsáveis pela aquisição do "efeito de Warburg" (Frezza and Gottlieb, 2009). No entanto, esta última hipótese não tem sido avaliada consistentemente.

O objectivo do nosso trabalho foi estabelecer modelos celulares de disfunção mitocondrial causada por mutações em genes de proteínas mitocondriais codificadas pelo DNA mitocondrial (mtDNA) ou pelo DNA nuclear (nDNA).

Com vista a se atingirem estes objectivos, tirou-se partido da tecnologia dos cibridos (híbridos transmitocondriais), que permite uma análise de mutações no mtDNA face a um "background" nuclear comum (células de osteosarcoma 143B) (Swerdlow, 2007). Construiu-se uma linha celular de cibridos com uma mutação no gene do $tRNA^{Leu(UUR)}$ do mtDNA. Procedeu-se ainda ao silenciamento da proteína mitocondrial succinato

desidrogenase subunidade B (SDHB) (codificada pelo nDNA) usando RNA de interferência num cibrido com mtDNA "wild-type".

Analisamos o fenótipo metabólico destas linhas celulares, medindo os fluxes de glucose, lactato, glutamato e glutamina através da membrana e a expressão de enzimas-chave da via bioenergética. Concluímos que tanto o silenciamento da SDHB como a mutação no mtDNA altera o metabolismo celular, aumentando a glicólise.

Para estudar a influência das mutações no mtDNA e o "efeito de Warburg" na tumorigenese, os cibridos com a mutação no mtDNA foram analisados em termos de marcadores associados à tumorigenese, como o crescimento celular, a morte celular e a capacidade de mobilidade e migração.

Por fim, através da injecção em ratinhos "nude" dos cibridos "wild-type" e dos cibridos com o mtDNA mutado, foi observada a formação de tumores apenas nos ratinhos injectados com estes últimos cibridos; para além disso, alguns destes ratinhos apresentaram invasão e metástases, demonstrando claramente o potencial tumorigénico desta mutação específica *in vi*vo.

Apesar destes resultados serem por agora superficiais, eles mostram que a disfunção mitocondrial causada pela mutação no mtDNA ou o silenciamento da SDHB leva à alteração do metabolismo celular, que, no caso da mutação no mtDNA, está associada com um potencial tumorigénico aumentado. Estudos adicionais ajudarão à compreensão dos mecanismos por detrás deste fenómeno tão comum nas células do cancro.

Palavras-chave: "efeito de Warburg", glicólise aeróbia, disfunção mitoconrial, cancro, metabolismo, cibridos.

Chapter 1 Introduction

1.1 Cancer

According to the World Health Organization, cancer is a leading cause of death worldwide, being responsible for 13% of all deaths. Cancer can affect almost any part of the body and the most frequent types are lung, breast, colorectal and stomach cancer (WHO, 2010).

Cancer is a generic term for a large group of diseases characterized by neoplasia, i.e. new growth of cells caused by a genetic and/or environmental deregulation of homeostasis. A tumour can invade surrounding tissues and spread to other organs, creating metastases. Metastases are the major cause of death from cancer (WHO, 2010).

A significant proportion of cancers can be treated by surgery, radiotherapy or chemotherapy, with good results being achieved in those that are detected early. However, the number of clinically approved drugs is low, comparing to other diseases (Kamb *et al.*, 2007). The development and achievement of efficiency of drugs in this area is more difficult because these drugs are targeted to essential cell functions, thus affecting not only neoplastic but also non-neoplastic cells. Moreover, sometimes target selectivity is not achieved and drugs activate other unwanted cellular process, leading to toxicity. Tumours also have an exceptional cellular heterogeneity and are very adaptable, resulting in a large variety of responses to the drug and resistance. Considering these and other problems, drugs are being developed and the two most popular therapeutic modalities are low-molecular-mass drugs, which inhibit elements in key signalling pathways and unconjugated biologicals (although traditional cytotoxics) which block essential function and kill dividing cells (Kamb *et al.*, 2007).

Hanahan & Weinberg (2000) described cancer investigation as "logical science" based on "a small number of underlying principles" (Hanahan and Weinberg, 2000). Carcinogenesis is associated with the manifestation of a succession of changes called the hallmarks of cancer: self-sufficiency in growth signals, insensitivity to growth-inhibitory signals, evasion of apoptosis, limitless replicative potential, sustained angiogenesis and tissue invasion and metastasis (Hanahan and Weinberg, 2000). This increased survival, proliferation and immune evasion by cancer cells is the result of alterations in key signalling pathways. For example, oncogenes, such as RAS or c-MYC or tumour suppressor genes, such as p53 or RB are frequently altered in cancer, leading to deregulation of signalling pathways involved in the above-mentioned hallmarks of cancer (Yeung *et al.*, 2008).

A tumour is now recognized as an organ. As a result the interaction between different cell types within the tumour and its surrounding supporting tissue, the tumour's stroma, has also been highlighted as it can largely determine the tumour phenotype, being a potential therapeutic target (Mueller and Fusenig, 2004). More recent models propose that the microenvironment has an important role in tumour progression and include increased glycolysis as a phenotypic strategy of cancer cells to overcome natural barriers (Gatenby and Gillies, 2004).

Recently, the existence of a 7^{th} hallmark of cancer has been under discussion: the aerobic glycolytic metabolism or "Warburg effect" that defines a state in which cells rely on glycolysis, rather than oxidative phosphorylation (OXPHOS), as a way to obtain energy, even in the presence of abundant oxygen. The shift from OXPHOS to glycolytic metabolism is not a simple adaption caused by rapid cell proliferation but is considered

as involved in transformation, being associated with a higher metastatic potential and survival advantage (Yeung *et al.*, 2008).

1.2 Warburg Effect

In the middle of the XXth century, Otto Warburg, a German scientist, described a phenomenon that would alert the scientific community for the metabolism of tumours and the importance of mitochondria: "the respiration of all cancer cells is damaged" (Warburg, 1956).

Measuring oxygen consumption and lactate production at the same time in tumour slices, Warburg reported that in the presence of oxygen, the proliferating tumour cells consumed glucose at a much higher rate compared to normal cells and secreted most of the glucose-derived carbon in the form of lactate (Warburg, 1956). A century ago, Louis Pasteur had already demonstrated that glucose flux was reduced by the presence of oxygen so pyruvate is conducted to the mitochondria to be oxidized. In the presence of oxygen, the key enzymes of glycolysis are inhibited by the high levels of ATP, leading to a lower uptake of glucose. This "Pasteur's effect" plays an important role in maintaining energy production throughout a range of oxygen concentrations in mammalian cells (Gatenby and Gillies, 2004; Shaw, 2006). However, in the case of tumour cells, increased glycolysis happens even in aerobic conditions.

Warburg hypothesized that this "aerobic glycolysis" was due to an impairment in respiration, in the mitochondrial metabolism and it was the origin of cancer cell transformation (Warburg, 1956).

After a period with declining interest in the metabolism of cancer cell, a new imaging technique based on Warburg's principle brought it up to the stage again. PET (Positron Emission Tomography) is based on the detection of photons released by annihilation of positrons emitted by radiopharmaceuticals ^{18}F-fluorodeoxyglucose (^{18}F-FDG), the most widely used PET tracer. This use of this glucose analogue has shown that most primary and metastatic human cancers have a significantly increased glucose uptake (Boss *et al.*, 2008; Gatenby and Gillies, 2004).

Genes involved in glycolysis are overexpressed in more than 70% of human cancers (Yeung *et al.*, 2008). It has been demonstrated that glucose uptake and criteria of aggressiveness of tumours and prognosis (invasion, size, and metastasis) are positively correlated in gastric cancer (Mochiki *et al.*, 2004), oesophageal cancer (Kato *et al.*, 2005), oral squamous cell carcinoma (Kunkel *et al.*, 2003) and soft tissue sarcomas (Schwarzbach *et al.*, 2005), among others.

The "Warburg effect" has been associated with mutations in "classical" oncogenes and tumour suppressor genes, as well as mutations in metabolic enzymes and mutations in mitochondrial DNA (mtDNA), leading to the exploration of the mitochondrial function in tumour cells and travelling beyond the bioenergetics point of view to the general metabolism of tumour cells.

1.3 Metabolic shift glycolysis – OXPHOS: causes

Warburg observed that tumour cells had increased glycolysis even in the presence of oxygen. During the years after, a lot of research was done concerning the "Warburg

effect" and several hypotheses on the origin of this phenotype and its consequences for tumorigenesis were raised (Yeung *et al.*, 2008).

One of the models proposed that the changes in the metabolism of cancer cells may arise from the selection exerted by the microenvironment, especially by restriction in oxygen availability - hypoxia. This hypothesis is based on the fact that the glycolytic phenotype confers a selective advantage for survival and proliferation during somatic evolution of cancer in the unique tumour microenvironment (Hsu and Sabatini, 2008).

The microenvironment of a solid tumour generally has an increased interstitial pressure, disorganized microvasculature or is avascular and consequently has regions of hypoxia (Pries *et al.*, 2009; Yeung *et al.*, 2008). These hypoxic zones develop near the oxygen diffusion limit (Fig. 1).

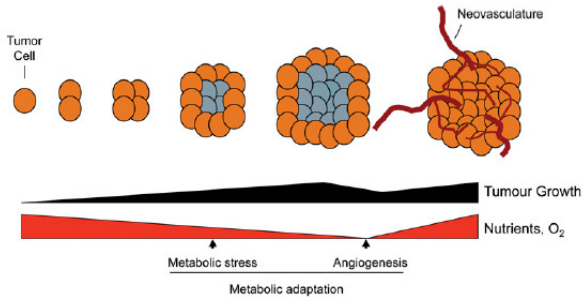

Figure 1: Metabolic stress during tumour development. Tumour cells experiencing hypoxia are depicted in gray (Jones and Thompson, 2009).

The defenders of this hypothesis propose that persistent metabolism of glucose to lactate, even in aerobic conditions, is an adaptation to hypoxia. Glycolytic phenotype is also seen in non-hypoxic conditions. It is believed that there is a moment where the upregulation of glycolysis in response to hypoxia in tumour cells becomes oxygen-

independent, resulting in the "Warburg effect". This may be caused by cyclic behaviour of hypoxia and by genetic and epigenetic alterations (Gatenby and Gillies, 2004). This phenomenon is thought to be crucial to the selection of the glycolytic phenotype. The upregulation of glycolysis, initially an adaptation to a local hypoxia, becomes constitutive (Gatenby and Gillies, 2004).

Lack of oxygen is responsible for inhibiting the mitochondrial OXPHOS and favouring the glycolytic metabolism for production of energy. Glucose uptake is thought to increase, as well as the secretion of lactate. Acidosis is a crucial component in this model of selection the glycolytic phenotype. The upregulation of glycolysis leads to increased lactate secretion, lowering the extracellular pH, which could suggest that the glycolytic metabolism is unfavourable to tumour cells. However, tumour cells have upregulation of H^+ transporters that maintain neutral intracellular pH and are important for cell survival in this environment, turning this disadvantage into growth advantage, favouring also invasion by eliminating other populations (Gatenby and Gillies, 2004). Suppression of pyruvate oxidation in the mitochondria preserves oxygen under hypoxia in order to sustain other oxygen-dependent activities and to avoid necrotic death. It may also protect cells from the hypoxia-mediated production of cytotoxic amounts of reactive oxygen species (ROS) (Frezza and Gottlieb, 2009).

Thus, the glycolytic phenotype in presence of oxygen favours the phenotypes adapted to this environment, resistant to hypoxic and acid-induced cell toxicity (Gatenby and Gillies, 2004; Yeung *et al.*, 2008). Cells undergo a variety of biological responses in hypoxic conditions, including glycolysis as an anaerobic alternative to oxidative

phosphorylation, activation of signalling pathways that regulate proliferation, invasion, angiogenesis and death.

It has been discussed if the glycolytic phenotype caused by the microenvironment is an event that happens early or later in the process of carcinogenesis. Some, like Gatenby & Gillies, argue that the transition to an invasive cancer coincides with the adoption of increased glucose uptake and this happens before the "angiogenic switch", emerging early in carcinogenesis (Gatenby and Gillies, 2004). Some studies concluded that the molecules that mediate hypoxia and enhanced glycolysis are highly expressed under normoxic conditions, especially in cell lines aggressively metastatic (Robey *et al.*, 2005).

Several general signalling proteins related to oncogenesis, such as RAS, c-MYC, SRC and p53 can influence energy substrate utilization by affecting cellular targets, leading to metabolic changes that favour cancer cell survival. In some cases, oncogenesis results in a dependency on a specific substrate or causes sensitivity to specific substrate deprivation. Consequently, genetic alterations in these pathways, very commonly observed in human cancers, can alter the glycolytic rate (Frezza and Gottlieb, 2009; Hsu and Sabatini, 2008; Jones and Thompson, 2009; Yeung *et al.*, 2008).

Mitochondrial defects have been proposed as playing an important role in the acquisition of tumours' aerobic glycolysis, although little investigation has addressed this hypothesis (Frezza and Gottlieb, 2009; Lee and Wei, 2009).

A probable scenario that has also been discussed is that these hypotheses interact in the cell and do not occur alone. Some authors propose "waves" of gene expression

reprogramming that promote metabolic changes of carcinogenesis. These waves include all the above described hypotheses, acting sequentially or even simultaneously all contributing for an altered metabolism (Smolkova *et al.*).

1.3.1 HIF-1: a molecule in the crossroad of several hypotheses

One of the most important mediators of hypoxia, oncogenic, metabolic stress and mitochondrial dysfunction response is hypoxia-inducible transcription factor 1 (HIF-1). HIF-1 is a transcription factor complex that binds to hypoxia-responsive elements. This heterodimer is formed by constitutive β subunits (also known as aryl hydrocarbon receptor nuclear translocator) and α- subunits and it was first described in 1992 by Semenza & Wang (Semenza and Wang, 1992). The α-subunit or HIF-1α is constitutively expressed, but, in the presence of O_2, HIF-1α is targeted for proteosomal degradation by the E3 ubiquitine ligase, VHL (von Hippel-Lindau) after proline hydroxylation catalysed by PHD enzymes (prolyl hydroxylases). When there is a low concentration of O_2, prolyl hydroxylation of HIF-1α is reduced and so VHL cannot bind to the newly synthesized subunit. This leads to HIF-1α stabilization and accumulation in the cytosol. Then, eventually this subunit is translocated to the nucleus where occurs the association with the HIF-1β subunit to form an active transcription factor (Harris, 2002) (Fig. 2).

HIF-1α can also be stabilized by numerous intermediates of signalling pathways (tumour suppressors and oncoproteins) in an oxygen independent manner (reviewed in Gatenby and Gillies, 2004). Cancers of the Von-Hippel Lindau spectrum (characterized by VHL mutations) are thought to develop mainly due to HIF stabilization (Shaw,

2006). Mitochondria, through ROS and Krebs cycle subproducts (e.g. succinate) can be involved in PHD inhibition and, consequently, HIF-1 induction during normoxia (Selak *et al.*, 2005). Tumour-associated mutations on complex II of the respiratory chain can lead to this effect by one or both pathways (ROS and succinate) (Guzy *et al.*, 2008).

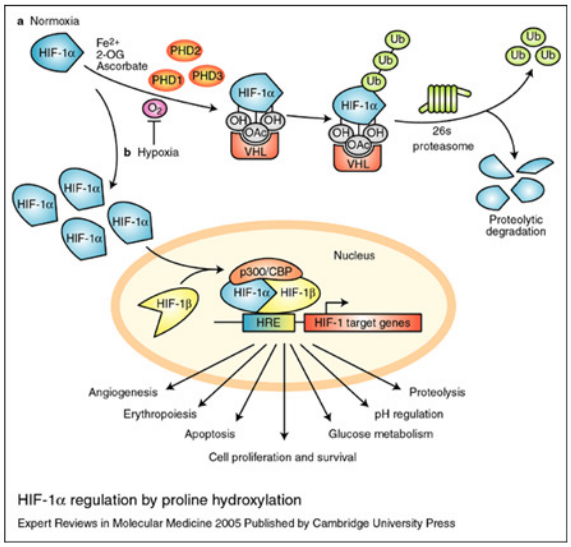

Figure 2: HIF-1 regulation (Carroll and Ashcroft, 2005).

A study of Favaro *et al.* (2008) where HIF-1α was silenced shows that this leads to cellular death in hypoxic conditions because of a high energy demand and cycle arrest. It also reported that the addition of glucose into the medium prevents this hypoxic-induced cell death, highlighting the importance of this substrate for the maintenance of the intracellular ATP levels under hypoxia (Favaro *et al.*, 2008).

1.3.2 Glycolytic phenotype

Specific expression of genes has been characterized as contributing to the tumours aerobic glycolysis – the "bioenergetic signature". These genes encode mostly enzymes that are crucial for the direction of the metabolic pathways and whose expression can be

altered by HIF-1 or by activation of oncogenes / inactivation of tumour suppressor genes. Some of these molecules are glucose transporters 1 and 3 (GLUT1 and GLUT3), hexokinase II (HKII), pyruvate dehydrogenase kinase (PDK1) and lactate dehydrogenase A (LDH-A) (Gatenby and Gillies, 2004).

Glucose transporters (GLUT) facilitate the diffusion of glucose across the plasma membrane and their expression is normally tissue-specific. The rate of glucose transport in a given tissue is determined in part by the translocation of preexisting transporters to the plasma membrane (McGowan *et al.*, 1995). GLUT3 and GLUT4 have a higher affinity for glucose than GLUT1, ensuring that glucose transport will be maximal in tissues containing these isoforms even when glucose concentrations are low. GLUT1 is thought to play a constitutive role and is responsible for basal glucose uptake. GLUT4 is an inducible transporter and is classically associated with glucose uptake in response to insulin in specific target tissues. GLUT3 is responsible for glucose uptake in times of low circulating glucose levels and is expressed in the brain, which relies on glucose as its only source of energy (Medina and Owen, 2002).

HK catalyses the irreversible first step of the glycolytic pathway, where glucose is phosphorylated to glucose-6-phosphate (G6P) via phosphate transfer from ATP (see Annex I). The enzyme plays a very important because it traps G6P inside the cell for commitment to either the glycolytic pathway or the shutting of this metabolite to the ribose-phosphate synthesis. The first insight into the cause of aerobic glycolysis came from the discovery that hepatomas express HKII, instead of the IV isoform or glucokinase (Parry and Pedersen, 1983). HKII is predominantly localized on the outer mitochondrial membrane (Mathupala *et al.*, 2009).The binding of HKII to voltage-

dependent anion ion channel (VDAC) in the outer mitochondrial membrane allows a preferred access of HKII to ATP synthesized via the mitochondrial adenine nucleotide translocator (ANT) and confers protection from inhibition by its product G6P. This facilitates the increase of glucose metabolism and inhibits apoptosis (Pedersen, 2007).

PDK1 is the enzyme that catalysis pyruvate dehydrogenase (PDH) phosphorylation. PDH catalyses the oxidation of pyruvate to acetyl-CoA and is tightly regulated in order to modulate carbon metabolism according to energy demands in the cell (see Annex I). Once phosphorylated by PDK1, PDH becomes inactivated diverting pyruvate away from OXPHOS and leading to its accumulation of pyruvate which, by turn, is converted into lactate by LDH (lactate dehydrogenase) (Semenza *et al.*, 1996).

LDH is a tetrameric enzyme comprising two major subunits A and B, which can catalyze the forward and backward conversion of pyruvate to lactate. LDH-A (LDH-5, M-LDH, or A4), which is the predominant form in skeletal muscle, kinetically favours the conversion of pyruvate to lactate. LDH-B (LDH-1, H-LDH, or B4), which is found in heart muscle, converts lactate to pyruvate that is further oxidized (Le *et al.*, ; Malmqvist *et al.*, 1991).

It was shown that the glucose uptake of lung carcinomas is correlated with a reduced expression level of β-F1-ATPase (the catalytic subunit of the mitochondrial H^+-ATP synthase) which is considered a "bioenergetic signature" and a useful prognostic marker in this kind of tumours (Lopez-Rios *et al.*, 2007). These authors suggested that the shift to a glycolytic phenotype is hardwired in cancer cells because glycolysis is the metabolic pathway required for cellular proliferation, hence differences in the

bioenergetic signature of tumour specimens might also arise as a result of diverse rates of cellular proliferation in the tumour (Lopez-Rios *et al.*, 2007).

Recent investigations demonstrated that mitochondrial uncoupling caused by uncoupling proteins can promote the "Warburg effect" in absence of permanent and transmissible alterations to the oxidative capacity of cells. It was proposed that aerobic glycolysis represents a metabolic shift to the use of non-glucose carbon sources to maintain mitochondrial function. Uncoupled mitochondria can also be associated with chemoresistance (Samudio *et al.*, 2009).

1.4 Advantages of the aerobic glycolysis

Oncogenesis and tumour growth seems to be positively influenced by an enhanced glycolytic metabolism and other related metabolic alterations.

As deduced by the microenvironment hypothesis, a glycolytic phenotype allows cells to survive in conditions of intermittent oxygen tension (Gatenby and Gillies, 2004). Besides, the acidosis resulting from this kind of metabolism is thought to favour tumour invasion (Swietach *et al.*, 2007) and suppress anticancer immune effectors (Fischer *et al.*, 2007). Recently, it has been also proposed that stromal cells are the ones that exhibit aerobic glycolysis and promote tumour growth by the secretion of energy-rich metabolites, such as pyruvate and lactate. This idea has been named "the reverse Warburg effect" (Pavlides *et al.*).

A bioenergetic advantage seems a paradox since glycolysis is a less efficient pathway for producing ATP when compared to OXPHOS (Warburg, 1956). However, using a mathematical model conjugated with flux data, it has been proved that the "Warburg effect" is a favourable catabolic state for rapid proliferating mammalian cells. The production of ATP is said to be regulated by the number of glucose transporters and by the cytoplasmic solvent capacity for allocating the components of the ATP generation pathways. In cancer cells, the uptake of glucose is not limiting but, when it reaches certain level, cells cannot further increase the concentration of mitochondria and the respiration rate. So, in these conditions, a gradual activation of glycolysis and a slight decrease of mitochondrial respiration results in the highest rate of ATP production (Vazquez *et al.*).

Aerobic glycolysis is not found exclusively in cancer cells, but is also observed in "normal" rapidly proliferating cells. The metabolism of cancer cells and indeed all proliferating cells, is adapted to facilitate the uptake and incorporation of nutrients into the biomass (e.g., nucleotides, amino acids, and lipids) needed to produce a new cell (Vander Heiden *et al.*, 2009) (Fig. 3).

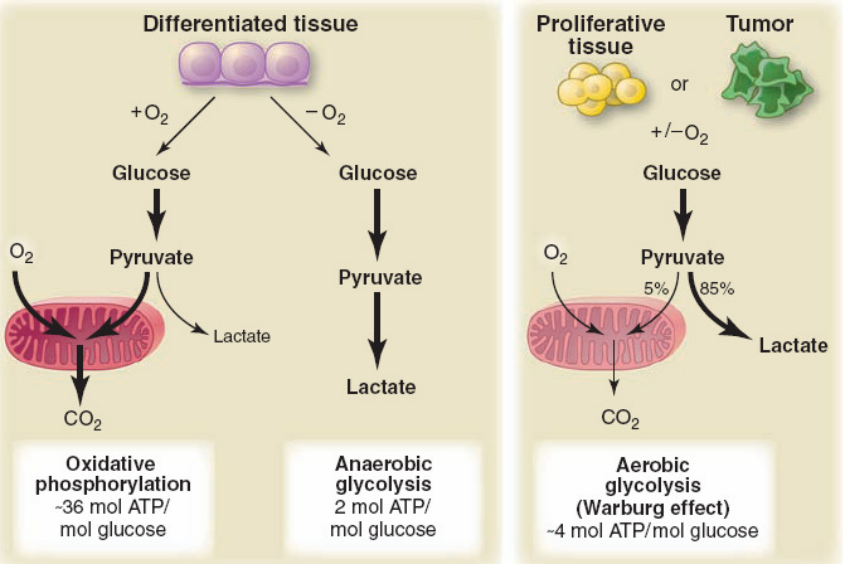

Figure 3: Differences in the glycolytic metabolism in differentiated and proliferating tissue. Tumours share the bioenergetic metabolism with proliferating cells (Vander Heiden *et al.*, 2009).

Fatty acids synthesis is also very important for cell signalling and growth. It requires anaplerosis and NADPH production. PI3K/Akt/mTOR pathway positively regulates the expression of lipogenic genes, glucose transporters and inhibits β-oxidation. Particularly ribose-5-phosphate and fatty acids and lipids synthesis are essential to cellular proliferation in tumours (DeBerardinis *et al.*, 2008). NADPH requirements for fatty acids synthesis are, in part, overcome by this pathway.

On the other hand, glutamine metabolism can provide intermediates and is a source of NADPH (DeBerardinis *et al.*, 2008). Citrate (a Krebs cycle intermediate) is needed for lipogenesis. This molecule is exported from Krebs cycle from the mitochondria but, in order to keep the citrate source, there must be compensation by replacement of oxaloacetate. Glutamine can also originate malate, a very important source of NADPH

in tumour cells. Glutaminolosis is relevant because the depletion of the glycolytic and Krebs' cycle intermediates could cause a decrease in ATP supply and, in this case, it allows tumour cells to sustain Krebs cycle activity and produce NADPH during proliferation (Hsu and Sabatini, 2008) (Fig. 4).

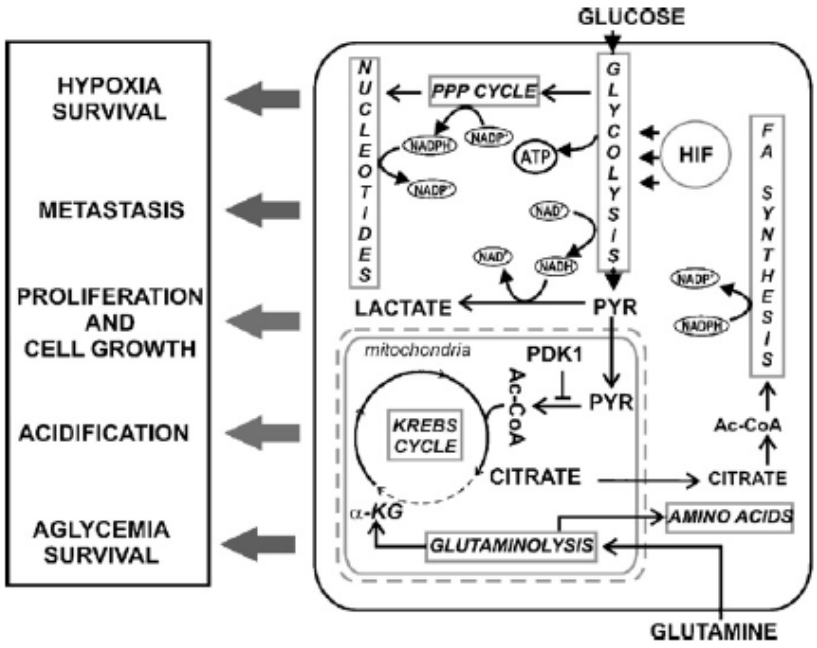

Figure 4: Major features of cancer cell metabolism, which support proliferation and cell growth (Smolkova *et al.*).

1.5 Mitochondria

Mitochondria are semi-autonomous cellular organelles that constitute more than 25% of the cytoplasmic volume in eukaryotic cells. Mitochondria are maternally inherited, due to their transmission from the egg to the zygote. Paternal mitochondria from the sperm are selectively marked with ubiquitin and degraded (Sutovsky *et al.*, 1999). The identity of an individual mitochondrion is short-lived, because it will fuse with a neighbouring

mitochondrion in the near future. Therefore, the entire mitochondrial population is in constant flux, driven by continual fusion and division of mitochondria (Chan, 2006).

Mitochondria are bounded by two membranes, the outer and the inner mitochondrial membranes, composed by lipids and proteins. The outer mitochondrial membrane is more permeable than the inner because of integral proteins called porins or VDAC. The inner mitochondrial membrane area is increased by a large number of infoldings or cristas that protrude into the mitochondrial matrix and maximize its function. The matrix is the local where pyruvate and fatty acids are metabolized into acetyl-CoA, which, by turn, is oxidized in Krebs cycle (Lodish, 2004).

This organelle has essential functions in cellular metabolism, particularly the production of energy, but also has a central role in apoptosis or programmed cell death.

Mitochondria are a repository for several apoptotic proteins. The mitochondrial permeability transition pore (mtPTP) is formed by Bax and Bcl-2 family proteins, porin, the ADP/ATP translocator (ANT), cyclophilin D and benzodiazepine receptor. mtPTP is responsible for the apoptotic function of mitochondria. As it opens, in result of excessive Ca^{2+}, increased oxidative stress or decreased mitochondrial membrane potential, ADP and ATP (which can be due to OXPHOS inhibition and overproduction of ROS), the potential energy stored in membrane potential is freed and mitochondria starts swelling leading to the release of the contents - many of them cell-death promoting factors, such as cytochrome *c*, caspases and SMAD/Diablo - of the intermembrane space into the cytosol (Wallace, 2005).

It also generates the majority of the endogenous ROS and plays a role in regulation of cell proliferation, membrane potential, cellular metabolism and calcium signalling, among others.

Some electrons, which are transported through the respiratory chain during mitochondrial respiration, may escape or leak from the complexes and react with molecular oxygen to form superoxide radicals (O_2^-). This diversion of electron flow occurs mainly at complexes I and III (Carew and Huang, 2002; Petros *et al.*, 2005). Superoxide anion is the first of the ROS and it can be converted to hydrogen peroxide (H_2O_2) by mitochondrial manganese superoxide dismutase. So, ROS are generated as a toxic byproduct of mitochondrial OXPHOS. However, in low levels they are mitogenic (Petros *et al.*, 2005). ROS may induce mutations and oxidative damage to mtDNA but also to proteins, cell membranes and nDNA (reviewed in Addabbo *et al.*, 2009) (Fig. 5).

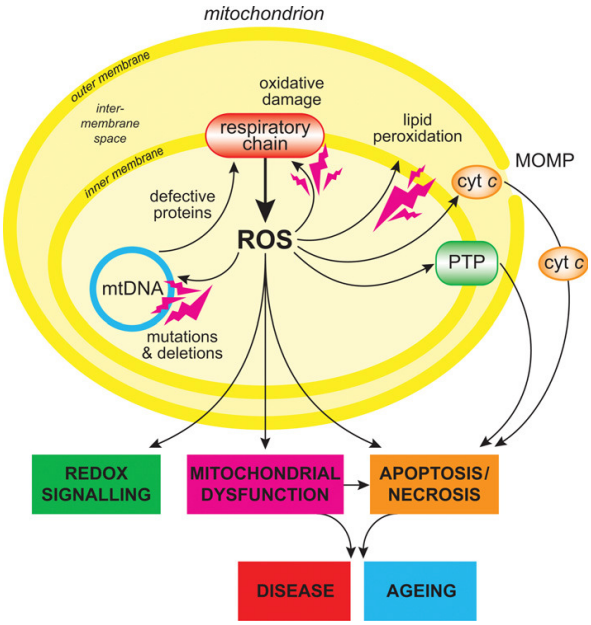

Figure 5: Mitochondrial ROS production and potential effects (Murphy, 2009).

Unless adequately detoxified, superoxide causes mitochondrial oxidative stress and may contribute to the decline in mitochondrial functions through mtDNA damage and nDNA encoded mitochondrial proteins (Addabbo *et al.*, 2009).

Numerous tumours have been found to have increased ROS production (Czarnecka *et al.*, 2006; Kumar *et al.*, 2008) and mitochondrial ROS production has been proposed appears to be a factor that links mitochondrial defects to neoplastic transformation (Brandon *et al.*, 2006).

1.5.1 Mitochondrial respiration

Mitochondria are the main sites of ATP production in aerobic cells. In aerobic conditions, pyruvate from glycolysis is actively transported into the mitochondrial matrix and oxidized to acetyl-CoA, entering the Krebs cycle. However, its fate in intermediary metabolism varies depending on the organism and on whether conditions are aerobic or anaerobic (Fig. 6).

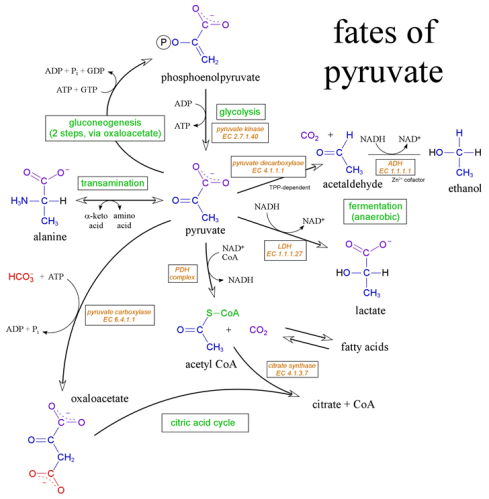

Figure 6: The fates of pyruvate

(guweb2.gonzaga.edu/faculty/cronk/biochem/images/pyruvate_fates.gif)

In Krebs cycle, nicotinamide coenzymes NAD and FAD are reduced to NADH and $FADH_2$ and then transfer their electrons to protein complexes located in the inner mitochondrial membrane, ultimately reducing oxygen. The protein complexes, collectively known as the respiratory chain are encoded by both nDNA and mtDNA (Carew and Huang, 2002). These complexes are formed by flavoproteins, ubiquinone (or coenzyme Q), cytochromes (Cyt), iron-sulfur proteins and cupric protein. OXPHOS is composed of the electron transport chain, encompassing complexes I, II, III and IV and the ATP synthase, complex V.

Coenzyme Q accepts electrons released from the NADH-Coenzyme Q reductase complex (I) and the succinate-Coenzyme Q reductase complex (II) and donates them to the CoQH2–cytochrome c reductase complex (III). Then, electrons from cyt are transferred to cyt c oxidase complex (IV), where they reduce oxygen to water (Fig. 7).

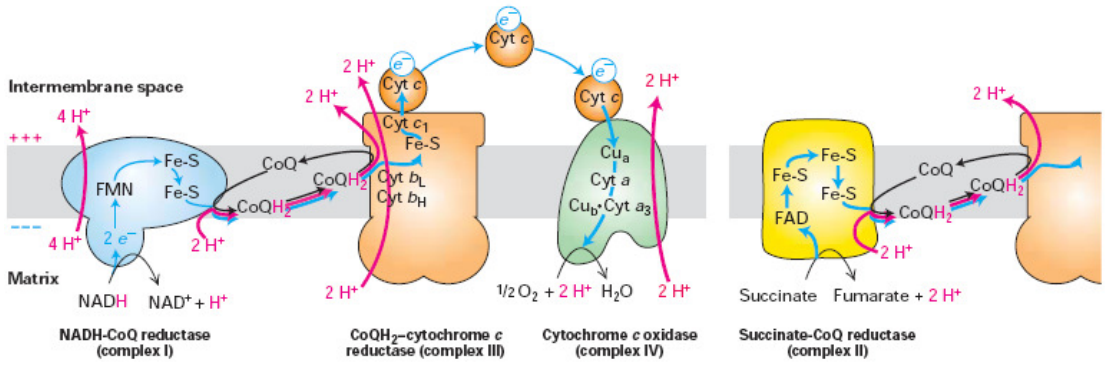

Figure 7: The respiratory chain (Lodish, 2004).

The electron transport chain generates a proton concentration gradient and an electric potential (voltage gradient), collectively called proton-motive force. This chemiosmotic coupling is responsible for drive the energy-requiring process, ATP synthesis (Fig. 8).

ATP synthase is a member of ATP-powered proton pumps. Protons flow through ATP synthase from the exoplasmic to the cytosolic face of the membrane promoting ATP synthesis by the enzyme (Lodish, 2004). ANT is involved in the exportation of mitochondrial ATP and cytosolic ADP (Brandon *et al.*, 2006)

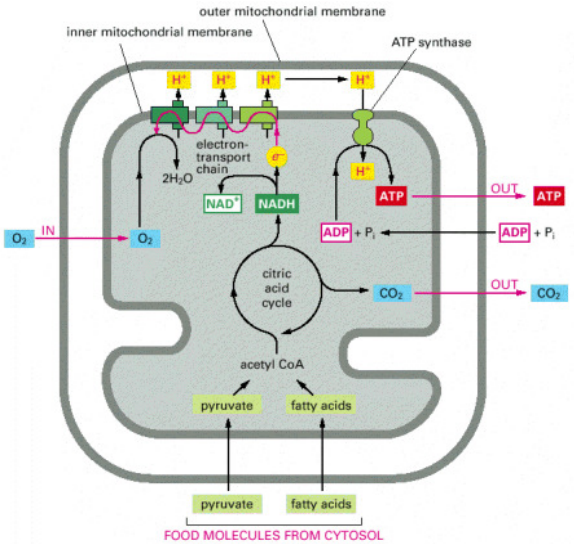

Figure 8: Energy-generating metabolism in mitochondria (Alberts, 2002).

The process of energy production is highly regulated in response to physiological and environmental conditions. This requires a constant cross-talk between the mitochondrial and the nuclear genome.

1.5.2 MtDNA

Mitochondria have DNA in the matrix - the mtDNA – that harbours 13 genes that encode structural subunits of OXPHOS enzyme complexes. These include 7 (NADH:ubiquinone oxidoreductase subunit 1, 2, 3, 4L, 4, 5, 6) of the 46 polypeptides of complex I, one (cyt b) of the 11 polypeptides of complex III, 3 (cyt c oxidase I, II,

III) of the 13 subunits of complex IV and 2 (ATP 6 and 8) of the 16 proteins of complex V. The mtDNA genome also encodes 22 transfer RNAs (tRNA) and two ribosomal RNAs that are required for protein synthesis in mitochondria. Because of its limited repair ability, lack of protective histones proteins and high rate of generation of ROS in mitochondria, mtDNA is more susceptible to oxidative damage and has a higher mutation rate compared with nDNA (Lee and Wei, 2009). Moreover, considering the fact that mtDNA lacks sizeable introns, mutations in the coding sequences have a high probability of changing the aminoacid composition of the encoded proteins. Thus, many of the mtDNA mutations are likely to have physiological consequences and might confer a cellular advantage or disadvantage in growth or survival.

1.6 Mitochondrial Dysfunction

Mitochondrial impairment is found in many types of diseases, namely neurodegenerative diseases like Huntington's, Parkinson's, Alzheimer's, hereditary mitochondrial diseases and cancer. Mitochondrial dysfunction plays a central role in majority of pathological processes largely due to their critical function in controlling the cellular energy status, signalling systems and the pathways of cell death (Seppet *et al.*, 2009).

The advantage for cancer cells of mitochondrial dysfunction may seem a little contradictory and hard to understand and even more if we take into consideration the adverse role of mitochondrial dysfunction in neurodegenerative diseases. However, it is important to underscore that this advantage is many times coffered with an oncogenic nuclear background.

Mitochondrial impairment was the first hypothesis proposed by Warburg for the "aerobic glycolysis" phenomenon (Warburg, 1956). By the time it was also reported that biochemical defects in mitochondria might be responsible for hypermetabolic state of some diseases (Luft *et al.*, 1962). This dysfunction could be due to genetic alterations either in mtDNA or in nDNA that encode mitochondria proteins or to biochemical defects of mitochondria caused by deregulated pathways and oncogenic activation or inactivation of tumour suppressor genes (Fig. 9).

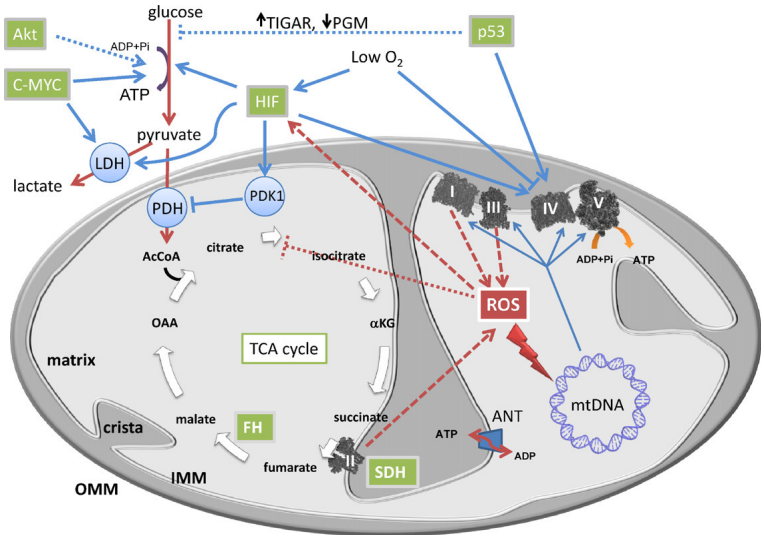

Figure 9: Metabolic pathways in mitochondria that can be altered in tumour cells and lead to the shift OXPHOS- glycolysis (Frezza and Gottlieb, 2009).

Brandon *et al.* consider that there are two types of mtDNA mutations: tumorigenic and adaptative. Tumorigenic mutations, more severe mutations which increase ROS production, are advantageous in the initial phases of tumour growth, leading to cell proliferation; on the other hand, adaptative mutations, milder mutations also seen in different human populations, may allow tumour cells to flourish in new environments, when the tumour becomes vascularized and/or metastasizes by facilitating the return to

an oxidative metabolism (Brandon *et al.*, 2006). These authors also suggest that severe mutations impairing OXPHOS may be lost once the tumour cells return to a high-oxygen environment during cell culture (Brandon *et al.*, 2006).

1.6.1 Biochemical defects of mitochondria

This line of thought proposes that the mitochondria activity is not damaged. Rather, the rate of OXPHOS is reduced by a dramatic increase in glycolysis and lactate production. Mitochondrial dysfunction is defended as a second hit of shift to an increased aerobic glycolysis (Frezza and Gottlieb, 2009). The diminished oxidative metabolism can be caused by low oxygen levels, changes in metabolic fluxes and gene expression reprogramming, resulting in down-regulation of the phosphorylative machinery (Frezza and Gottlieb, 2009). So, in this case, oncogenic transformation and HIF-1 are the responsible for the metabolic shift.

The inhibition of OXPHOS by glycolysis is often called the Crabtree effect, named after the author who first reported it (Crabtree, 1929). It was suggested that there was a competition to regenerate ATP between glycolysis and mitochondria and ADP and Pi become limiting. In addition, the acidic pH induced by lactate generation may affect highly pH-sensitive mitochondrial oxidative enzymes (Moreno-Sanchez *et al.*, 2007). However, it is argued that the aerobic glycolysis phenotype observed in cancer is not full explained by the Crabtree effect (Frezza and Gottlieb, 2009).

1.6.2 Defective mitochondrial proteins

Alterations in mitochondrial proteins may occur as a consequence of mutations in mtDNA or in nuclear genes that encode mitochondrial proteins.

MtDNA mutations have been described (and still are) in various types of human cancers (reviewed in Carew and Huang, 2002; Chatterjee *et al.*, 2006; Czarnecka *et al.*, 2006) (Fig. 10). In fact, the majority of cancer cell lines harbour mutant mtDNA. Mutations in mtDNA appear in both the non-coding and coding regions and the majority seem to be homoplasmic in nature (Chatterjee *et al.*, 2006). The mutations can either arise in female germ line and predispose to cancer or in the mtDNAs of the tissues and participate in tumour progression, being called respectively oncogenic germline mutations and tumour-specific somatic mutations (Brandon *et al.*, 2006).

Figure 10: Mitochondrial mutations present in different types of tumours

(Chatterjee et al., 2006).

1.6.2.1 MtDNA mutations in cancer

Mammalian cells can have hundreds to thousands of mitochondria and each mitochondrion contains several mtDNA genomes. This challenges the investigation of

mtDNA mutations and their functional consequences. Deleterious mutations of mtDNA often affect some but not all mitochondrial genomes. This fact leads to the possibility of co-existence of wild-type and mutant mtDNA in the same cells in a state called heteroplasmy. Unlike nDNA, mtDNA is not a binary system and different ratios of wild-type (wt) and mutant mtDNA species can reside within a cell, with the heteroplasmic mutation being present in varying degrees of high to low abundance. When all the mtDNA copies have the same genome, either wild-type or mutated, a state of homoplasmy is said to exist. Non-deleterious mutations of mtDNA (neutral polymorphisms) are typically homoplasmic, whereas pathogenic mutations are usually, but not invariably, heteroplasmic.

The biological impact of a given mutation may vary, depending on the proportion of mutant mtDNAs carried by the individual (Wallace, 2005). Threshold refers to how much of an mtDNA mutational load is required within a cell for the mutation to cause a biochemical or phenotypic consequence. In this case it is logical to predict the more pathogenic the mutation, the lower the mutant heteroplasmy required to alter mitochondrial or cell physiology (Swerdlow, 2007). Moreover, in the case of mutation that are associated with defects in mitochondria, the pathogenic threshold concentration of mutant mtDNAs is lower in tissues that are highly dependent on oxidative metabolism than in tissues that can rely on anaerobic glycolysis (Chan, 2006).

Cells do not lose respiratory function until high loads of pathogenic mtDNA are present, ranging from 60% to 90% depending on the specific mutation. This compensation likely depends, at least partially, on the ability of mitochondria to fuse and divide within cells, thereby allowing complementation of mtDNA gene products (Chan, 2006).

1.6.2.1.1 Germline mtDNA mutation in cancer

There are mtDNA polymorphisms associated with increased risk of breast and endometrial cancer. These mtDNA polymorphisms are localized in genes that encode complex I subunits, and so it was proposed that it can lead to decreased efficiency of the respiratory chain and consequently to an increased ROS production (Canter *et al.*, 2005). The role of mutations in COI (gene that encodes an OXPHOS complex IV subunit) and ATP6 (component of the ATP synthase – complex V) was also addressed in the context of prostate cancer (Petros *et al.*, 2005) and it was demonstrated that these mutations can enhance carcinogenesis (Brandon *et al.*, 2006).

According to DiMauro & Schon (2001), there are two main types of mtDNA mutations: those that affect mitochondrial protein synthesis and those in protein-coding genes (DiMauro and Schon, 2001). Mutations in tRNA genes are one type of mutation from the first group.

The A3243G transition is the most extensively investigated tRNA gene mutation (Chomyn *et al.*, 2000). It is located in the $tRNA^{Leu(UUR)}$ mtDNA gene, at the 14 residue in the D-stem which coincides with the middle of the binding site for the mitochondrial transcription termination factor (Kruse *et al.*, 1989; Wittenhagen and Kelley, 2002) (Fig. 11). This mutation is associated in MELAS syndrome (Myopathy, Encephalopathy, Lactic Acidoses and Stroke-like syndrome) (Goto *et al.*, 1990), among others (van den Ouweland *et al.*, 1992). This mutation induces the dimerization of the tRNA that strongly self-associates under physiological conditions which is partially responsible for the observed loss of function (Wittenhagen and Kelley, 2002).

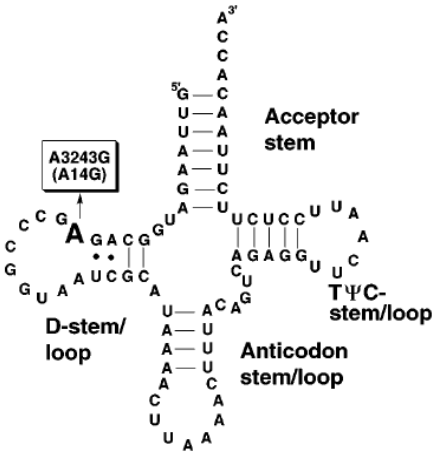

Figure 11: Proposed cloverleaf secondary structure of $tRNA^{Leu(UUR)}$ mtDNA gene, predicted by MFOLD (Wittenhagen and Kelley, 2002).

1.6.2.1.2 Somatic mtDNA mutation in cancer

Between 40 and 70% of all types of tumours harbour somatic mtDNA alterations (Kaipparettu *et al.*).

Unlike studies linking germline mtDNA mutations to cancer, those concerning somatic mtDNA mutations can be more definite since cancer cells should have the neoplastic mtDNA mutation while the normal tissue should not (Brandon *et al.*, 2006). Most of the mtDNA mutations found in cancer cells are somatic mutations (Czarnecka *et al.*, 2006). However, only few mutations in non-coding or coding sequences result in substantial aminoacid changes, raising questions about their biological impact (Chatterjee *et al.*, 2006).

D-loop has been shown to be a mutation "hot spot" in human cancers because of its unique triple-stranded DNA structure (Czarnecka *et al.*, 2006; Zhou *et al.*, 2007). MtDNA can suffer point mutations, deletions, insertions, tandem duplications and copy

number changes (reviewed in Lee and Wei, 2009). According to Brandon *et al.* (2006) the first clear demonstration of the functional significance of mtDNA mutations in cancer cells came from Horton *et al.*, 1996, who reported that half of the renal adenocarcinomas studied had a 294 nucleotide in-frame deletion of the ND1 gene (NADH dehydrogenase 1 which takes part of complex I of the OXPHOS) resulting in a truncated mRNA. The patients manifest severe mitochondrial disease (Brandon *et al.*, 2006; Horton *et al.*, 1996). In thyroid cancer, for example, the majority of the mutations occur in the genes coding for complex I subunits (Maximo *et al.*, 2002) and are closely related with the oncocytic phenotype of thyroid tumours. Oncocytic refers to lesions whose cells have an abnormally high number of mitochondria (Maximo and Sobrinho-Simoes, 2000). In a study where it was applied the long-range gene synthesis technique for cloning a gene which would generate nuclear-transcribed and mitochondrial-targeted ND2 (mitochondrial NADH dehydrogenase subunit 2) protein, it was demonstrated that mutants formed more colonies and had an increased growth (anchorage dependent and independent). The development and maintenance of the malignant phenotype caused by ND2 mutation might involve HIF-1α induction and ROS production, which were higher in mutants. The aerobic glycolytic phenotype, deduced from an elevated pyruvate and lactate concentrations in the mutant-transfected cell lines may also have an important role (Zhou *et al.*, 2007). Nevertheless, the authors considered that these mitochondrial mutations are not sufficient to cause the malignant transformation (Zhou *et al.*, 2007). ND6 (mitochondrial NADH dehydrogenase subunit 6) gene was also shown, when mutated, to be associated with metastatic potential (Ishikawa *et al.*, 2008). It was suggested that the disruption of mitochondrial complex I leads to ROS overproduction which, in turn, upregulate nuclear genes like MCL-1, an antiapoptotic protein, HIF-1α

and VEGF, involved in neoangiogenesis and, consequently, regulate tumour cell metastasis. Although the effect of these mutations can be generalized to other tumour cell lines, the same does not happen with non-transformed cells and upregulation of glycolysis is not involved on this process of metastasizing (Ishikawa *et al.*, 2008).

A variety of mutations in COI (cytochrome oxidase subunit I) gene have been described in prostate cancer (Petros *et al.*, 2005). Since complex IV dysfunction is associated with overproduction of ROS, this mutation can be associated with tumourigenesis.

Besides all the aforementioned information, the ROS mediated mitochondria-to-nucleus retrograde signalling induced by mitochondrial dysfunction result in elevated cytosolic free Ca^{2+}, an important second messenger in the activation of different nuclear transcription factors which control the expression of genes involved in cancer progression and invasion (Amuthan *et al.*, 2001).

1.6.2.2 Nuclear-encoded mitochondrial proteins

The first example of unequivocal causality between mitochondrial dysfunction and tumorigenesis was the observation that the genes encoding for succinate dehydrogenase (SDH) and fumarate hydratase or fumarase (FH) predispose to hereditary neoplasias (Gottlieb and Tomlinson, 2005).

These two enzymes belong to the Krebs cycle and SDH is also a functional member of OXPHOS.

1.6.2.2.1 SDH (OXPHOS complex II)

Complex II of the respiratory chain is the only one whose subunits are all encoded by nDNA. This complex, that links the Krebs cycle to OXPHOS, is formed by four subunits: SDHA, SDHB, SDHC, SDHD and several prosthetic groups (Gottlieb and Tomlinson, 2005; Guzy *et al.*, 2008). SDHA collects the electrons resulting from oxidation of succinate in the Krebs cycle, reducing FAD prostetic group, and passes them to the iron-sulphur components in SDHB (iron-sulphur protein). Then, the electrons are transferred to the cytochrome b and ubiquinone associated components SDHC and SDHD, which anchor this complex to the mitochondrial inner membrane.

Germline loss-of-function mutations in SDHB, SDHC and SDHD genes (as well as the newly discovered SDHA and SDH5) cause predisposition to paragangliomas and phaeochromocytomas, neuroendocrine neoplasias. Interestingly, SDH seems to predispose either for cancer or for neurodegenerative diseases, depending on the severity of the mutation and affected gene (reviewed in Burnichon *et al.*, ; Gottlieb and Tomlinson, 2005; Hao *et al.*, 2009). In 2003, Lima *et al.* discovered a syndrome characterized by familial non-RET C cell hyperplasia that was associated with a mutation in SDHD (Lima *et al.*, 2003).

Deleterious mutations in these subunits can lead to failure of complex II assembly, so that the catalytic and electron transport function become compromised. Many studies demonstrate that the transformation due to mutants of this complex is not simply the result of energy deficiency.

Lower activity of SDH and, consequently, retardation of the electron flow, caused by mutations in SDHC gene, could increase the production of ROS resulting in increased mutagenesis (Ishii *et al.*, 2005). In previous reports, suppression of SDHD failed to

produce oxidative stress (Selak *et al.*, 2005), but these results might be due to the technique used (Guzy *et al.*, 2008). In fact, Guzy *el al.* (2008) found that inhibition of the SDHB leads to overproduction of ROS which were involved in stabilization of HIF-1α under normoxic conditions, enhancing growth rates *in vitro* and *in vivo*. On the other hand, loss of SDHA does not increase normoxic ROS production since it blocks the entry of electrons into complex II and decreases tumour growth rates. It was suggested that complex II functions as a protooncogene capable of activating HIF when defects in SDHB, SDHC or SDHD cause an increase in ROS production, leading to the stimulation of HIF-dependent gene expression and cell proliferation" (Guzy *et al.*, 2008).

The FH gene encodes the homonymous Krebs cycle enzyme that converts fumarate into malate, having been identified as the tumour suppressor gene responsible for HLRCC syndrome (hereditary leiomyomatosis and renal cell carcinoma) (Tomlinson *et al.*, 2002). Deficiency in FH leads to accumulation of fumarate and succinate. Accumulation of fumarate due to FH mutations, as well as succinate, can inhibit PHD, acting as a competitive inhibitor (figure 14). This leads to stabilization of HIF-1α and induces the Warburg effect (Isaacs *et al.*, 2005). Certain types of gliomas also present alterations in $NADP^+$-dependent isocitrate dehydrogenases. A recent survey has revealed that mutations in IDH1 and IDH2 (isocitrate dehydrogenase 1 and 2, respectively) are common events in malignant gliomas emphasizing the importance of mitochondrial dysfunction in tumourigenesis. The IDH1 and 2 mutations may not be inactivating but allow other substrates to be used by the enzyme (Yan *et al.*, 2009).

1.7 Cancer therapy

Anti-neoplastic therapy has long relied on the rapid proliferation of tumours in order to be an effective treatment. However, the lack of specificity is precisely its biggest disadvantage because it often leads to undesirable side effects.

Despite the heterogeneity of tumours, which dictates an individual approach to anti-cancer treatment, almost all of them demonstrate enhanced uptake and utilization of glucose. It has been proved that cancer abolishes the tissue-specific differences in the bioenergetic phenotype of mitochondria. This alteration of the bioenergetic signature strongly supports a relevant role for the mitochondrial impairment of the cancer cell in progression of the disease (Acebo *et al.*, 2009).

In fact, the basis of several mechanisms of tumour resistance to both radiotherapy and chemotherapy is in the aberrant metabolism of a tumour (Tennant *et al.*).

With the exploration of the "Warburg effect" new therapeutic targets started to emerge. These include glycolytic, Krebs cycle and OXPHOS inhibitors. They can also target HIF-1α, the biosynthesis activity driven by high levels of glycolysis (including glutaminolysis), mitochondria redox status and its apoptotic machinery (reviewed in Pathania *et al.*, 2009).

The extent of the role of metabolism in tumourigenesis should not be underestimated and drugs that can selectively target the tumour metabolic phenotype and tumour microenvironment are likely to at least delay if not halt tumour progression. The so-

called “metabolic addition” has been extensively studied. Besides, targeting several different functions can potentiate the therapeutic benefits.

1.8 Cybrids

In 1989, King and Attardi showed for the first time that ρ^0 human cells can be repopulated with exogenous human mitochondria (King and Attardi, 1989). Since then, the use of cybrid technology has been growing exponentially.

Cybrids are cytoplasmatic trans-mitochondrial hybrids used to study mtDNA-related mitochondrial biology. Direct cloning of mitochondrial genes into conventional expression vectors is not possible, because direct translation of mitochondrial sequences results in incorrect protein formation, as translation is different in the nuclear and the mitochondrial genetic code (Zhou *et al.*, 2007). One way to circumscribe this problem is by using cybrids. They are obtained by the fusion of a cell line completely depleted of mtDNA, called ρ^0 (rho 0) with an enucleated cell line that has the desirable mtDNA mutations (Fig. 12). This technology allows the differentiation of the effects caused by mtDNA mutations from those caused by nDNA, since the cybrids cell lines have the same nuclear background (Swerdlow, 2007).

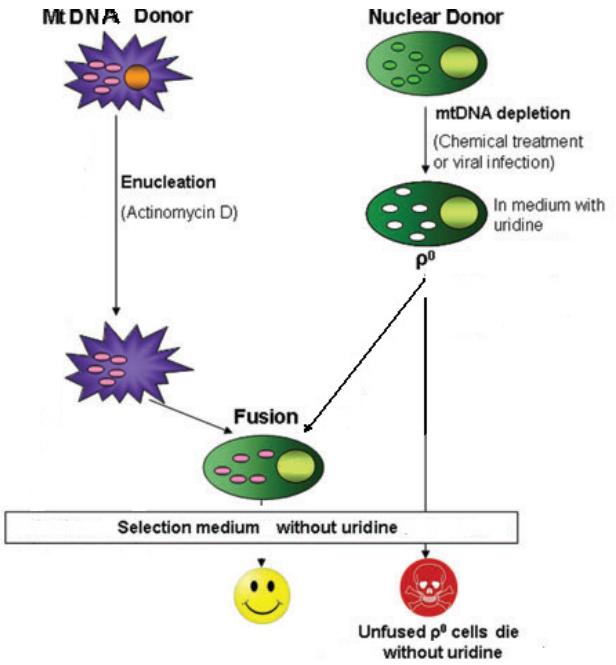

Figure 12: Cybrid construction method (adapted from Kaipparettu *et al.*).

This relatively recent technique is a fundamental tool in studies assessing the ROS production, dysfunction of the related complex of the oxidative phosphorylation, phenotypic implications (apoptosis, proliferation, invasion, mobility) or tumourigenic potential of mtDNA mutations (Ishikawa *et al.*, 2008; Petros *et al.*, 2005; Shidara *et al.*, 2005; Zhou *et al.*, 2007).

1.9 Aims

Taking in consideration the importance of the Warburg effect, the uncertainty regarding its causes and tumourigenic effects, as well as its potential use in cancer therapy we undertook a project with the following main aims:

- Establish cell lines with defects in OXPHOS proteins (both encoded by nDNA and mtDNA);

- Assess the metabolic alterations in OXPHOS deficient cells and see whether they are consistent with the "Warburg effect";

- Determine the effects associated with tumourigenesis *in vitro* and the *in vivo* oncogenic properties induced by OXPHOS defects.

Chapter 2 Materials and Methods

2.1 Materials

Dulbecco's modified Eagle's medium (DMEM), inactivated fetal bovine serum (FBS), the antibiotics used in the culture medium (penicillin and streptomycin), amphotericin B, trypsin-EDTA were purchased from GIBCO, as part of Invitrogen Life Technologies (Carlsbad, California, USA). Uridine, actinomycin D, the cocktail of phosphatases inhibitors, the Ponceau S solution and Tween-20 were purchased from Sigma-Aldrich (Saint Louis, Missouri, USA). GoTaq® Flexi DNA Polymerase kit was obtained from Promega (Madison, Wisconsin, USA). Agarose was acquired from Lonza (Basel, Switzerland) and the buffer SGTB from Grisp (Porto, Portugal). The nucleic acid staining solution (Gel Red) was obtained from Biotium (Hayward, California, USA). The enzymes exonuclease I and shrimp alkaline phosphatase were purchased from Fermentas (Canada). BigDye Terminator version 3.1 Cycle Sequencing kit and Real Time reagents were bought from Applied Biosystems (Carlsbad, California, USA). Sephadex G-50 Fine, nitrocelulose membranes and x-ray films were acquired from GE Healthcare (United Kingdom). Polyethylene glycol (PEG) was purchased from Fluka Analytical, as part of Sigma-Aldrich (Saint Louis, Missouri, USA). Short hairpin RNA constructs against SDHB were obtained from OriGene Technologies (Rockville, Maryland, USA). The transfection reagent LipoGen was purchased from InvivoGen (San Diego, USA). For TUNEL assay, the "*In situ* cell death detection kit" (Fluorescein) was obtained from Roche (Mannheim, Germany), as well as the cocktail of proteases inhibitors. Bovine serum albumin (BSA), Triton X-100 and dimethyl sulfoxide (DMSO) were obtained from AppliChem (Darmstadt, Germany). Acrylamide/Bis solution 29:1 (3.3%C), the running buffer TGS10x were obtained from

Bio-Rad (Hercules, California, USA). Staurosporine was purchased from LC Laboratories (Massachusetts, USA).

Antibodies for SDHB and COXII were commercialized by MitoSciences (Eugene, Oregon, USA), HK II and GLUT 1 by Abcam (Cambridge, UK) while β-actin antibody was bought to Santa Cruz Biotechnology (California, USA).

All other reagents were obtained from Merck (Darmstadt, Germany), Sigma-Aldrich (Saint Louis, Missouri, USA), AppliChem (Darmstadt, Germany), and Bio-Rad (Hercules, California, USA).

All solutions were aqueous (type II water) except those prepared in DMSO.

2.2 Cell culture

All cell lines used were cultured in Dulbecco's modified Eagle's medium (DMEM) high-glucose supplemented with 10% (v/v) inactivated FBS, 100units/mL penicillin, 100µg/mL streptomycin and 1.25µg/mL amphotericin B (all from GIBCO, Invitrogen). This culture medium was designated as "complete DMEM". Cells were maintained at 37ºC, 5% CO_2 in a humidified incubator and cultured as a monolayer.

XTC.UC1 is derived from a mammary gland metastasis of a thyroid follicular carcinoma (Hürthle cell) (Zielke *et al.*, 1998). It harbours a C insertion at bp3571 in the mtDNA gene *ND1*, generating a premature stop codon at amino acid 101 of ND1 protein, which will be truncated, as a result. This frameshift mutation leads to complete absence of the protein which prevents OXPHOS complex I assembly. This cell line also has a missense substitution in the cytochrome *b* gene. These mtDNA mutations were

proved to be responsible for bioenergetic defects (Bonora *et al.*, 2006). XTC.UC1 was cultured in complete DMEM, but uridine (50µg/mL) (Sigma) was added to this medium to try to increase the rate of mitochondria with the *ND1* mutation.

143B and 143Bρ^{0}sm are osteosarcoma-derived cell lines and were a kind gift from Dr Keshav Singh (Roswell Park Cancer Institute, Buffalo USA). The 143Bρ^{0}sm is derived from the 143B after depletion of mtDNA, hence they share the same nuclear background.

The 143Bρ^{0}sm cells were generated using herpes simplex virus (HSV). A transient expression of UL12.5, a protein encoded by the HSV *UL12* gene with mitochondrial localization, leads to the degradation of mtDNA, through nuclease activity, leaving nuclear DNA intact. Mitochondrial mRNAs are also depleted as rapidly as the mtDNA after HSV infection (Saffran *et al.*, 2007). Comparing to long-term exposure to ethidium bromide, this method of depletion of mtDNA brings the advantage of a selective degradation, without the problem of inducing undesirable nuclear DNA mutations (as it may happen with ethidium bromide).

Cybrid cell lines (see Results Section for details on cybrid production) were cultured in complete DMEM without uridine.

Regarding transfections, stable clones were generated by selection with 0.5µg/mL puromycin (see Results Section for details), which was, according determined as the ideal concentration of puromycin for the selected cells.

After having been established, all cell lines were cultured in complete medium supplemented with uridine, standardizing the culture conditions. This is because

143Bρ^0sm are pyrimidine and pyruvate auxotrophs, dependent on uridine and pyruvate for growth, because of the absence of a functional respiratory chain (King and Attardi, 1989).

2.3 Evaluation of mtDNA mutations in *ND1* and tRNA$^{Leu(UUR)}$ genes

MtDNA from cell lines, before or after selection, was evaluated for *ND1* and tRNA$^{Leu(UUR)}$ mutations by polymerase chain reaction (PCR) flowed by direct sequencing.

2.3.1 Isolation of genomic DNA

Total DNA was extracted from cell lines using a standard salt-precipitation method. Plated cells (70-90% confluence) were washed in PBS 1x (phosphate buffered saline), trypsinized (0.05% trypsin-EDTA), pelleted (1200rpm, 5minutes) and digested overnight in SE solution (75mM sodium chloride [NaCl], 25mM EDTA), 1% SDS (v/v) and in 180µg/ml proteinase K at 55ºC with shaking. To dehydrate and precipitate cellular proteins, it was used a pre-heated saturated solution of 1.2M NaCl. Equal volume of chloroform, an organic solvent, was then added and the tubes were kept shaking for 30 minutes at room temperature and centrifuged for 10 minutes at 2500rpm. Following DNA purification, the DNA was precipitated with isopropanol (1x volume) and washed in 70% ethanol. In the end, DNA was eluted in deionized water and quantified in NanoDrop Spectrophotometer ND-1000 (ThermoScientific).

2.3.2 PCR

Since the primers available for amplifying *ND1* gene include the region where the mutation A3243T of the $tRNA^{Leu(UUR)}$ gene is located, these were used to monitor both mutations. For analysing the sequence of $tRNA^{Leu(UUR)}$ gene, the reverse primer was more suitable.

Genomic DNA extracted from cell lines was used for PCR amplification with the GoTaq® Flexi DNA Polymerase kit (Promega). Amplifications were performed using 1xbuffer, 2.5mM $MgCl_2$ (magnesium chloride) solution, 0.1mM each deoxyribonucleotide triphosphate (dNTP), 10 pM of each primer (forward and reverse), 0.5U of *Taq* polymerase and 50-200 ng/µL of template DNA in a 25-µL volume. The primer pairs for *ND1* and $tRNA^{Leu(UUR)}$ amplification, designed according to the Cambridge Reference Sequence of the *ND1* gene, were: foward (5'-ACACCCACCCAAGAACAGGGTTT-3') and reverse (5'-GTAGAATGATGGCTAGGGTACT-3'). PCR conditions were: 1 cycle of 5 minutes at 94ºC for initial denaturation, followed by 35 cycles of 30 seconds at 94ºC for denaturation, 30 seconds at the appropriated annealing temperature (58ºC) and extension of 30 seconds at 72ºC; the final extension was performed in 1 cycle of 5 minutes at 72ºC. Electrophoresis of the PCR products was carried out in 2% agarose (Lonza) in 1x SGTB (Grisp) gels at 80V. The running was performed in 1x SGTB and the visualization was carried out with a fluorescent nucleic acid gel stain (gel red, Biotium).

2.3.3 MtDNA sequencing

PCR products were subjected to a purifying treatment using 1U/µL exonuclease I and 0.05U/µL shrimp alkaline phosphatase (Fermentas) at 37ºC for 20 minutes, followed by heat inactivation for 15 minutes at 80ºC.

Then, samples were used for direct sequencing with BigDye Terminator version 3.1 Cycle Sequencing kit (Applied Biosystems) using the aforementioned primers (forward for ND1 analysis and reverse for $tRNA^{Leu(UUR)}$ analysis). After a purification with Sephadex G-50 Fine (GE Healthcare) and resuspension in formamide, sequences were run in an automated sequencer (3130 Genetic Analyser, Applied Biosystems).

2.4 Successive serial dilutions and single-cell cloning

In order to enrich the population of mutant mtDNA in the cell lines, we performed successive serial dilutions. The employment of this technique was based on the assumption that there will be a positive selection and these mutations confer advantage to the cells (Zhidkov *et al.*, 2009). This was also the method used for achieving a population enriched by cybrid cells after fusion and for generation of monoclonal stably transfected cells culture.

1.0×10^2 to 20.0×10^2 cells were plated, using a Neubauer-counting chamber, in 6-wells. Independent colonies were picked with the help of cloning-rings, expanded and mutation levels determined by sequencing.

2.5 Isolation of platelets from peripheral blood

Platelets (mitochondria donors) used for the construction of cybrids cell lines were isolated from a patient's peripheral blood collected in EDTA tubes and kept at 4ºC until its procession. This patient was diagnosed with a maternally inherited mitochondrial myopathy due to a germline mtDNA mutation, a A3243T transition in the $tRNA^{Leu(UUR)}$ (Shaag *et al.*, 1997). The platelets were obtained by mixing the blood with 1/10th (v/v) of a 10x warm salt solution of citrate (0.15M NaCl and 0.1M trisodium citrate dehydrated pH 7.0), which was then centrifuged for 20 minutes at 200g. To pellet the platelets, the top three-fourths of the platelet-rich plasma (supernatant) were centrifuged for 20 minutes at 1500g. The platelets were resuspended in physiological saline (0.15M NaCl and 15mM Tris-HCl [Tris-hydrochloric acid] buffer, pH 7.4 at 25ºC) as previously described (Chomyn *et al.*, 1994).

2.6 Cybrid construction

Cybrids clones were constructed using three types mitochondria donors: the cell line XTC.UC1 (or the sub clone C of XTC.UC1 – see Results), which harbours a mutation in *ND1* gene (C insertion at bp3571) and in the cytochrome *b* gene (Bonora *et al.*, 2006), platelets of a patient with the A3243T mutation in the $tRNA^{Leu(UUR)}$ and platelets from a healthy individual (wild-type mtDNA).

As mitochondria acceptor, it was used the 143Bρ^0sm cell line.

2.6.1 MtDNA donor: XTC.UC1

In the case of cybrids resulting from the fusion of 143Bρ^{0}sm and XTC.UC1, it was first necessary to enucleate the mitochondria donor cells. For that, XTC.UC1 was plated ($2.0x10^5$cells/well) in a 6-well. When adherent to the well, the cells were washed with PBS1x and, then, culture medium with 20µg/mL actinomycin D was added. Actinomycin D is an antibiotic (produced by bacteria of the genus *Streptomyces*) that intercalates into DNA duplexes, inhibiting transcription and DNA replication. This treatment was shown to be severe enough not to allow cells to recover after the drug is removed, but mild enough to preserve mtDNA integrity and cytoplast viability. Besides, actinomycin D does not block mtDNA replication or damages mtDNA as severely as it does to the nuclear DNA (Bayona-Bafaluy *et al.*, 2003). To confirm that the observed death is due to the effect of actinomycin D, one well was left without the antibiotic. The formation of cytoplasts was controlled by observation on the microscope.

72 hours following the enucleation with actinomycin D and formation of cytoplasts, the culture medium with actinomycin D was removed and cells washed three times with PBS1x. $1.0x10^6$ 143Bρ^{0}sm cells suspended in the appropriated culture medium were then added over the cytoplasts. One well was left without 143Bρ^{0}sm, to control for the absence of recovery of enucleated cells. This well was checked after for existence of total cell death, confirming that the enucleation process was severe enough to prevent non-fused cells to recover. At least three hours later, the cells were washed 3 times in plain DMEM. The cell fusion was performed by adding 2.5mL of polyethylene glycol (PEG) 45% (v/v) solution (4.5g PEG, 4.5mL complete DMEM and 1mL DMSO). After one minute of incubation at room temperature, the PEG solution was removed from the wells and cells were washed three times with DMEM 10% DMSO for 5 minutes and once with plain DMEM, after which complete DMEM with uridine was added.

Whenever we observed floating cells, the medium was exchanged. 48 hours later, selection began by replacing complete DMEM with uridine for complete DMEM without uridine. The selection was kept constant in some wells as other experienced an alternate selection with medium with uridine. In this medium, only fused cells (cybrids) were expected to survive since ρ^0 cells do not grow in the absence of uridine (King and Attardi, 1989).

2.6.2 MtDNA donor: wild-type and A3243T platelets

Platelets do not need to be enucleated as they are naturally enucleated. After their isolation, the suspension was centrifuged for 15 minutes at 1500g and the supernatant discharged. $1.0x10^6$ 143Bρ^0sm cells were carefully added to the platelets' pellet, which was then centrifuged for 10 minutes at 180g. The cellular fusion was achieved when the pellet was resuspended in 0.1mL of PEG 45% (v/v) and incubated for 1 minute. Next, 10mL of complete DMEM with uridine was added and cells were plated in Petri dishes with serial dilutions: 1:1, 1:10 and 1:100. Selection began 48 hours later by replacing complete DMEM with uridine for complete DMEM without uridine and was prolonged for approximately a month.

2.7 Isolation of tumour cell lines with stable knockdown of SDHB

To evaluate the influence of SDHB on tumour cell metabolism and phenotype, cybrids with wt mtDNA (CMPBR3, which will be used as control cells) were transfected with shRNA constructs.

2.7.1 Plasmids

Short hairpin RNA constructs against *SDHB* gene were obtained from OriGene Technologies, including four sequences against different parts of the *SDHB* gene (expression plasmids with gene-specific shRNA cassetes), as well as two negative control plasmids, one without shRNA cassette insert (TR30007) and other containing non-effective 29-mer scrambled shRNA (TR30013) (table I). All vectors had a pCMV driven tGFP gene which expresses tGFP protein constitutively, enabling monitoring of the transfection efficiency. The bacterial selection marker was kanamycin. The vector had also a puromycin-N-acetyl transferase gene located downstream of the promoter, resulting in resistance to this antibiotic.

Table I: Sequences from the constructs

Designation	**Sequences**
B1	CATTCTCTGTGCCTGCTGTAGCACCAGCT
B2	CCTATCGCTGGATGATTGACTCCAGAGAT
B3	CTCTCTATACCGCTGCCACACCATCATGA
B4	ACATCAATGGAGGCAACACTCTAGCTTGC
TR30013 (scramble)	GCACTACCAGAGCTAACTCAGATAGTACT

2.7.2 Determination of the ideal concentration of puromycin for selection

Puromycin was added to CMPBR3 cells plated in a 6-well in several concentrations. The tested concentrations were 0.5, 0.6, 0.7, 0.8, 1.0, 1.5 and 2.0µg/mL. The selected concentration (0.5µg/mL) was the lowest concentration of antibiotic that results in the

onset of massive cell death after approximately six days, and kills the entire non-resistant population within two weeks.

2.7.3 Transfection

One day prior to transfection, $2.0x10^5$ CMPBR3 cells, in a 6-well culture plate, were diluted 1:2. After 24h of growth, transfection was carried out using LipoGen (InvivoGen) reagent.

The introduction of SDHB shRNA into cells via transfection and posterior creation of stable cell lines were performed according to the manufacturer's protocol (OriGene Technologies).

24hours after transfection, the puromycin selection was started.

2.8 Real-time PCR

All the real-time PCR reagents were bought from Applied Biosystems. RNA isolation was performed with TRI Reagent® Solution, DNA removal using DNase I and real-time PCR with TaqMan® Assays in 96-Well Plates, all in accordance with the manufacturer's protocol. RNA was quantified using NanoDrop Spectrophotometer ND-1000 (ThermoScientific). The gene expression analysis was carried out for SDHB, HK II, GLUT 1, GLUT3, GLUT 4, PDK I, G6PD and LDHA and normalized for β-actin. The standard curve was made for 143B cell line.

2.9 Western blotting

Total cell extracts, achieved with RIPA buffer (50mM Tris-HCl, 1% NP-40, 15mM NaCl and 2mM EDTA, pH 7,5) and cocktails with inhibitors of proteases (Roche Applied Science) and phosphatases (Sigma-Aldrich), were quantified using Bradford protein assay (BSA standards: 250, 500, 750, 1000, 1500 and 3000µg/mL). The absorbance change was read in at 655nm in microplate reader (Bio-rad). Standard curves were accepted for an r^2 >0.97. Protein from the cell extracts, denaturated with 4x loading buffer, were resolved by sodium dodecyl sulphate (SDS)-Page with a gel 40%bisacrylamide 29:1 (Biorad) concentration of 16-10% (v/v) at 100V. Loaded volumes of each input were determined so that the applied protein mass was the same for each lane (25-100µg). Proteins were, then, electrotransferred onto a nitrocellulose membrane (GE Healthcare) for 2 hours at 100V or alternatively overnight at 30V and 4ºC. In the case of low amount of protein, it was loaded half of the protein extract.

After staining the membrane with Ponceau S dye to check the uniformity and overall effectiveness of protein transfer from the gel to the membrane, membranes were blocked for 1h at room temperature (or overnight at 4ºC) in PBS1x containing 0.5% (v/v) Tween-20 (PBS-T) and 5% (w/v) low-fat dry milk. Incubation with primary antibodies, diluted in PBS-T containing 0.5% (w/v) low-fat dry milk (except when stated differently) was carried out according to the manufacturer's instructions (table II) with gentle agitation. Membranes were then washed with PBS-T (5 times, 5 minutes each) and subsequent incubation with suitable horseradish peroxidase conjugated secondary antibody diluted 1:2000 in the above solution was performed for 1 h at room temperature. Membranes were washed again (once 5 minutes and 3 times 10 minutes)

and protein bands were detected by chemiluminescense and x-ray film exposure (GE, Healthcare).

Table II: Antibodies

Protein	Dilution	Incubation	Animal origin	Molecular weight (kDa)	Commercialized by
SDHB	1:1000 (milk 5%)	3h; RT	mouse	30	MitoSciences
HK II	1:800 (BSA 5%)	2h; RT	rabbit	100-150	Abcam
GLUT 1	1:400 (BSA 5%)	2h; RT	rabbit	55	Abcam
COX II	1:1000 (milk 5%)	3h; RT	mouse	22	MitoSciences
β-actin	1:2000 (milk 5%)	1h; RT	goat	44	Santa Cruz Biotechnology

2.10 Main fluxes across the plasma membrane assay

To have a general picture of the metabolism of the aforementioned cell lines, we measured the levels of glucose, lactate, glutamine and glutamate in the culture medium.

The medium from $3.0x10^4$ cells of each cell line growing in 6-well culture plate with 2.5mL of culture medium (complete DMEM with uridine) was collected, centrifuged for removal of floating cells (1200rpm, 5minutes) and frozen at 80ºC until the time of measurement. This procedure was done immediately after the seeding, 4 hours later and in successive timepoints of 12 hours, for 5 days. At the same time, cells were counted

using a Neubauer-counting chamber and in four timepoints (T3, T5, T7 and T8) cells were freezed at -80ºC for posterior analysis of protein lysates (Figure 13). Glucose, lactate, glutamine and glutamate content in the culture medium was measured in IBET/ITQB (Instituto de Biologia Experimental e Tecnológica/Instituto de Tecnologia Química e Biológica) using a Y SI 2300 STAT Plus Glucose Lactate Analyser and HPLC for glutamine and glutamate. The quantification was done always normalizing the values for a sample of culture medium where no cell was cultured (that contains already glucose and l-glutamine).

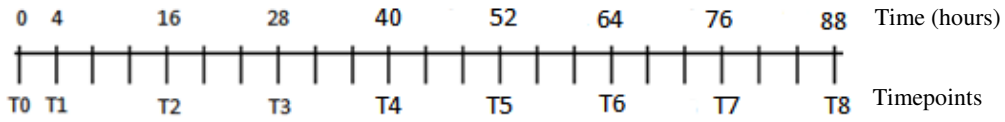

Figure 13: Time scale of the measurements of the main fluxes across the plasma membrane assay.

2.11 *In vitro* cellular growth assay

Cells were plated at a density of 5.0×10^4 cells/ well in a 6-well tissue culture plate. Cells were trypsinized, collected, and counted after seeding and in 12h timepoints for 4 days (84 hours), using Z Series Particle Count and Size Analyzer (Beckman Coulter). For each cell line, cell growth was assessed by calculating the time in which the population number doubles, the population doubling time (PDT). It was used the following formula (Davis, 1994):

$$PDT = 1 / (3{,}32\ (\log N_H - \log N_I)/(t_2 - t_1))$$

Being, N_H the number of cells counted in t2 (after 84 hours)

N_I the number of cells counted in t1

t1 time 0

t2 time - after 84 hours

2.12 *In vitro* cell death assay using TUNEL assay (flow cytometry)

To evaluate and quantify cell death in the described cell lines, DNA strand breaks were labelled using TUNEL assay ("In *situ cell* death detection kit, fluorescein" [Roche]). The analysis was performed by flow cytometry.

TUNEL (Terminal deoxynucleotidyl transferase-mediated d-UTP Nick End Labeling assay) is based in one of the hallmarks of apoptosis, the activation of endonucleases that cleave chromosomal DNA preferentially at internucleosomal. TUNEL assay is based on labelling of DNA stand breaks (and not only single-strand breaks) with modified nucleotides - fluorescein-dUTP -, in a reaction catalysed by the exogenous enzyme terminal desoxynucleotidyl transferase. This assay has the advantage of revealing early DNA sections breaks during apoptosis, prior to the loss of any significant DNA content. However, the presence of DNA strand breaks is not unique to apoptosis, although it marks preferentially apoptosis. To clearly discriminate apoptosis from other forms of cell death, this assay should be run together with other methods to show the specificity of the measurement (Darzynkiewicz *et al.*, 2008). As a result, this method was regarded as a cell death assay.

Cells were treated with staurosporine (LC Laboratories), a microbial alkaloid which is a strong inhibitor of protein kinases and an inducer of apoptosis (Chae *et al.*, 2000). The concentrations of staurosporine (STS) in DMSO used were 25nM, 50nM and 100nM. 4hours post-treatment, cells were fixated using 4% paraformaldehyde and permeabilized with a solution of 0.1%Triton X-100 in 0.1% sodium citrate dehydrate. Then cells were labelled with TUNEL reaction mixture. As negative control, we used a reaction mixture without the enzyme that catalysis polymerization of labelled nucleotides to free 3'-OH DNA ends. The fluorescence was detected in the range of 515-565nm (filter FL1) using a flow cytometer. Analysis of the results was performed in FlowJo software (Tree Star, Oregon, USA) and geometric mean of the curves was calculated. Whenever necessary, a gate was draw to exclude unspecific fluorescence.

2.13 *In vitro* motility and migration assays

To assess individual motility and migration, cells were filmed for 14 hours using an inverted fluorescence microscope (Zeiss Axiovert) equipped with a camera and temperature- and CO_2-controlled chamber at INEB (Instituto de Engenharia Biomédica).

Each cell line was plated in a well of 24-well plate, prior to the experiment. To evaluate individual cell motility, $1.0x10^4$ cells per well were plated (cellular density meant to reach a low confluence after the time frame of incubation). To assess migration, we performed the "scratch assay": $5.0x10^5$ cells were plated in order to reach confluence and the cell monolayer was scratched with a p200 pipette tip in several diagonal lines.

The cell debris was removed and the edge of the scratch was smoothened by replacing the culture medium (Liang *et al.*, 2007).

Five 20x fields were identified per well and marked for return; images were automatically collected in each field every 5 minutes using Axion Vision software.

Time-lapse images were further processed using Zeiss LSM Image Browser software. Appropriate groups of images corresponding to the same field were joined to make the film. We quantified the individual cell motility by determining the total length of the route described by an individual cell (five replicas were made). Dividing or dying cells were not considered. Regarding cell migration, we measured the time that cells took to travel 300µm in the leading edge of the scratch (five replicas were made).

2.14 Nude mouse xenograft tumour experiments

Six-week-old female N:NIH(s)II:nu/nu nude mice were obtained previously from the Medical School, University of Cape Town in 1991 and then reproduced, maintained and housed at IPATIMUP Animal House at the Medical Faculty of the University of Porto, in a pathogen-free environment under controlled conditions of light and humidity. Nude mice, female, aged 6-8 weeks, were used for *in vivo* experiments. Animal experiments were carried out in accordance with the Guidelines for the Care and Use of Laboratory Animals, directive 86/609/EEC. Mice were subcutaneously injected in the dorsal flanks using a 25-gauge needle with $1.0x10^6$ of 3243CY9.7, 143Bρ^0sm or CMPBR3 cell lines. Mice were weighed, and tumour width and length were measured with callipers every week. Mice were euthanized 4 weeks after tumour development (6 weeks after

injection) when the weight of one mouse was less than 20% of its original weight. Moreover, the tumour's volume of one of the mice was too high and might start to affect its life. After fixation with 4% neutral buffered formalin and paraffin-embedded, histopathology of the tumours and other organs (liver, ganglia and lungs) was evaluated using 2μm sections and conventional Hematoxilin and Eosin (H&E) staining.

The slides were examined with a light microscope (Zeiss) using a 1×100 or 1×200 lens. Images were captured with a coupled device camera.

2.15 Statistical Analysis

Whenever adequate, the results are presented as mean ± standard deviation. Statistical analysis was performed using the Mann-Whitney non-parametric test as well as One-Way ANOVA and for multiple comparisons Tukey test, with $p < 0.05$ as the level of significance, in SPSS software.

Chapter 3 Results

3.1 Establishment of Cell Lines

In order to evaluate the role of mitochondrial dysfunction in tumourigenesis by the induction of the metabolic transition from OXPHOS to glycolysis even in the presence of oxygen – the "Warburg effect" -, it was necessary to create suitable cell models. Thus, we decided to create models characterized by a genetic impairment of OXPHOS and Krebs cycle proteins; it should be noted that OXPHOS has both proteins encoded by the mtDNA and the nDNA, whereas Krebs cycle only presents nuclear encoded proteins.

In the case of mtDNA encoded proteins, the aim was to investigate the consequences of mutations in the OXPHOS genes themselves or mutations in transfer RNA genes, which will indirectly affect all other genes. To specifically study the functional effect of mtDNA mutations, nuclear effects must be excluded and, so, cybrid technology was used (see below for details on cybrids).

On the other hand, RNAi (RNA interference) silencing was the strategy selected to address the effects of nuclear encoded genes.

3.1.1 Cybrid (cytoplasmic hybrids) Cell Lines

With the purpose of discriminating the effect of mutations in the mtDNA that can disrupt OXPHOS from alterations at the nDNA level, cybrid cell lines harbouring the desired mtDNA mutations with a constant nuclear background were constructed. Cybrid cell lines are obtained from the fusion of a mtDNA depleted ρ^0 cell line with enucleated cells that harbour the mtDNA mutation of interest; in this way the only variable is the

mtDNA mutation that is present in the same nuclear background (mtDNA depleted cell line). Cybrids are often used to gain insight into the pathogenic mechanism underlying disease-associated mtDNA mutation.

3.1.1.1 Construction of cybrids displaying a mutation in *ND1* mitochondrial gene

ND1 mtDNA gene encodes a peptide that is part of OXPHOS complex I. Its function is possibly crucial for the assembly and function of the complex (Lazarou *et al.*, 2009) and alterations in genes affecting complex I have been shown to increase the susceptibility to thyroid tumourigenesis (Maximo *et al.*, 2002).

3.1.1.1.1 Mitochondria mutation load in XTC.UC1 cell line

XTC.UC1 cell line, as previously stated, harbours a frameshift mutation in the mtDNA *ND1* gene (3571InsC), however, since cells contain hundred to thousand mtDNA copies and this cell line in particular, is derived from a follicular thyroid carcinoma of Hürthle cells (or oncocytic) which is characterized by an even higher number of mitochondria (Maximo *et al.*, 2002), we evaluated the heteroplasmy status of the mutation by mtDNA sequencing. It was observed that XTC.UC1 cell line displays the *ND1* mutation in approximately 50% of mtDNA molecules (Fig. 14).

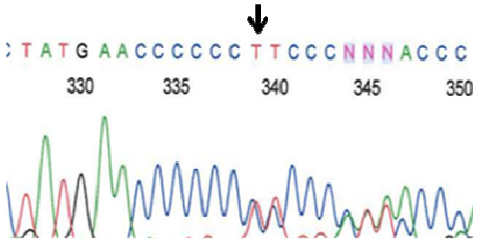

Figure 14: Sequence analysis of the *ND1* gene in XTC.UC1: electropherogram showing the C insertion at bp3571, according to the Cambridge Reference Sequence. The arrow points the insertion place.

XTC.UC1 cell line also displays a mutation in cytochrome *b* gene. However, this mutation was in a very low level of heteroplasmy in the cell line available (data not shown). Therefore, the analysis was focused on the *ND1* mutation.

3.1.1.1.2 Construction of cybrids using XTC.UC1 cell line

In a first attempt to perform cybridization, the cell line 143Bρ^{0}sm was used as recipient cell line, whereas the cell line XTC.UC1 (harbouring the mtDNA with ND1 mutation) was used as donor cell line. 143Bρ^{0}sm cell line has already been used in other studies concerning mitochondrial activity with cybrid cell lines (Kaipparettu *et al.*, ; Singh *et al.*, 2005). A western-blot for the mtDNA encoded protein COXII (cytochrome oxidase subunit II), confirmed that the cybridization was successful because the resulting cybrids show gain of COXII expression as opposed to the lack of COXII expression in the 143Bρ^{0}sm (data not shown). However, after sequencing several cybrid clones, we observed that the percentage of mtDNA molecules with the mutation in the cell population was very low (Fig. 15) and any effects of the mutation would most probably be masked.

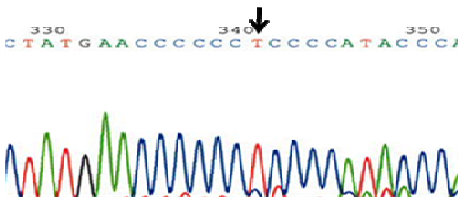

Figure 15: Sequence analysis of the *ND1* gene in XTCBR7 cybrids: electropherogram showing the C insertion at bp3571, according to the Cambridge Reference Sequence. The arrow points the insertion place.

According to Gasparre *et al.* (2007), 70% of heteroplasmy is considered to be above the likely threshold for a damaging effect (Gasparre *et al.*, 2007), therefore we decided to increase the mutation load in the XTC.UC1 cell line, which would likely increase the probability of obtaining cybrids with higher mutation load.

3.1.1.1.3 Selection of a subclone with a higher level of *ND1* mutation

Gasparre *et al.* (2007) established primary cell cultures in a medium supplemented with 50µg/mL uridine to allow growth of cells with impaired mitochondrial function (Gasparre *et al.*, 2007). As XTC.UC1 cell line presents a defective activity of complex I (Bonora *et al.*, 2006), this approach, complemented with serial dilutions, was done to achieve a higher degree of heteroplasmy of the mutation.

XTC.UC1 cells were first cultured in complete DMEM with 50µg/mL uridine and the level of heteroplasmy of *ND1* mutation was assessed periodically by sequencing analysis. After several weeks of cells growing in these conditions, the number of mtDNA copies displaying the mutation had increased, comparing to XTC.UC1 cell line cultured in complete medium without uridine (Fig. 16).

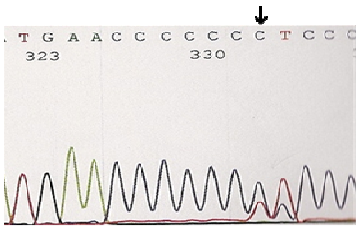

Figure 16: Sequence analysis of the *ND1* gene in XTC.UC1 cell line culture in medium with uridine: electropherogram showing the increased level of the C insertion at bp3571, according to the Cambridge reference sequence, comparing to XTC.UC1 cell line cultured in complete medium without uridine. The arrow points the insertion place.

Then, 200 and 1,000 cells of XTC.UC1 cell line cultured in complete DMEM with uridine were plated in 10mm dishes and "single cell" clones were picked. The rate of mutated mtDNA copies increased in all of the subclones of XTC.UC1. The chosen one, harbouring the highest level of mutation, was named XTC SCC (Fig. 17) and, by an analysis of the electropherogram, presented approximately 70% of the mutation (Fig. 18). This clone was, in fact, the first to be isolated.

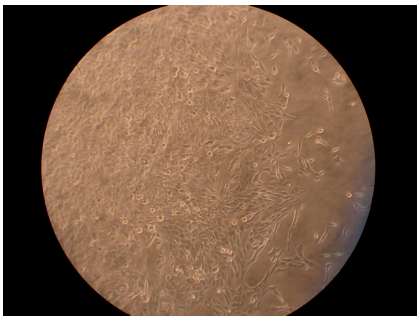

Figure 17: Isolation of clone c of the XTC.UC1 cell line – XTCSCC: microscope visualization using a bright field inverted microscope (amplification 100x).

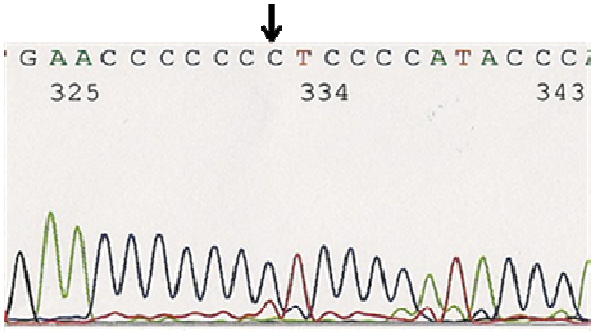

Figure 18: Sequence analysis of the *ND1* gene in XTC.SCC cell line culture: electropherogram showing the increased level of the C insertion at bp3571, according to the Cambridge Reference Sequence, in XTC.UC1 cell line cultured in complete medium with uridine. The arrow points the insertion place.

3.1.1.1.4 Construction of cybrids using the selected clones of XTC.UC1

Once more, the recipient cell line used was 143Bρ^{0}sm, whereas the mtDNA with a ND1 mutation was donated by the XTC.UC1 cell line, after culture in medium supplemented with uridine.

First, we tried to create cybrids from XTC.UC1 cell line cultured in medium with uridine. However, the few clones growing in selective medium revealed to be "false cybrids", as their sequence resembled the 143Bρ^{0}sm one.

After the selection of a subclone of XTC.UC1 with more *ND1* mutation load, XTCSCC, the construction of cybrid using this subclone as mtDNA donor, was attempted. The efficacy of the actinomycin treatment was always confirmed, so no tetraploid nuclei are formed (See Materials and Methods Section for more detail). Clones were successively

picked and cultured individually, but, again, the few clones growing in selective medium revealed to be "false cybrids", as their sequence resembled the 143Bρ^0sm one.

At the moment, we have not managed to establish a stable cybrid cell line from XTC.UC1 cell line with a desirable level of *ND1* mutation that would have phenotypic consequences.

3.1.1.2 Construction of cybrids displaying a mutation in tRNA$^{Leu(UUR)}$ mitochondrial gene – A3243T cybrids

Taking into consideration that our purpose was to inactivate OXPHOS, we decided to take advantage of a known pathogenic mitochondrial mutation – an A-to-T transition at mtDNA nucleotide position 3243 in the tRNA$^{Leu(UUR)}$ gene – that will presumably affect all complexes with mtDNA encoded proteins (I, III, IV and V). To build the A3243T cybrids, platelets were extracted from a patient with mitochondrial myopathy due to a germline A3243T mutation. Platelets were then fused 143Brho0 cell line.

During selection, plated cells grew in "single-cell" clones (Fig. 19) which were, then, picked. Most of them were individualized from the plates with the lowest dilution. The majority of these clones were cybrids without the mutation (8/13) and some were not cybrids (4/13), as proved by sequencing. One of the clones was proven to be a cybrid harbouring the A3243T transition in tRNA$^{Leu(UUR)}$ gene (Fig. 20). This cybrid was called 3243CY9.

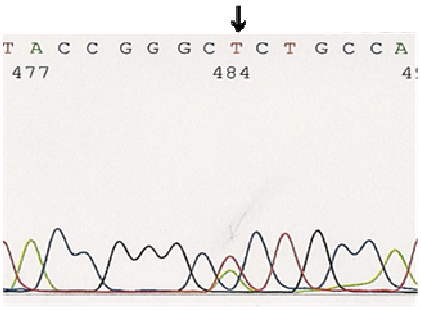

Figure 20: Sequence analysis of the tRNA$^{Leu(UUR)}$ gene in the clone 3243CY9: electropherogram showing the A-to-T transition at mtDNA nucleotide position 3243, according to the Cambridge Reference Sequence. The arrow points the substitution place.

Having a stable cybrid cell line with the tRNA$^{Leu(UUR)}$ mutation - 3243CY9 - the goal was to increase of the mutation load. This was accomplished by the same process used for XTC.UC1 cell line (successive serial dilutions). Four weeks after, it was obtained the subclone 3243CY9.7 (Fig. 21) which presents approximately 50% of mutant. From this last cybrid, and 2 months after the fusion, a sub-subclone with more than 50% presence of the mutation was selected. It was called 3243CY9.7.10 (Fig. 22).

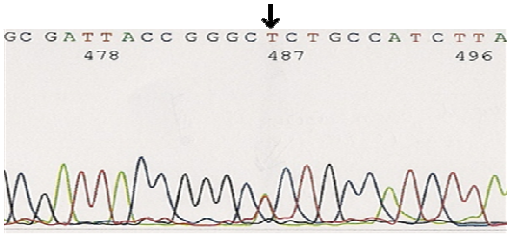

Figure 21: Sequence analysis of the tRNA$^{Leu(UUR)}$ gene in the clone 3243CY9.7: electropherogram showing the increased level of A-to-T transition at mtDNA nucleotide position 3243, according to the Cambridge

Reference Sequence (superimposed peaks suggest 50% mutated mtDNA).

The arrow points the substitution place.

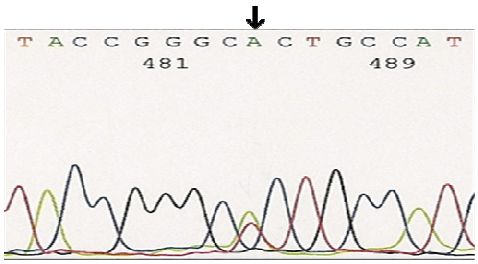

Figure 22: Sequence analysis of the $tRNA^{Leu(UUR)}$ gene in the clone 3243CY9.7.10: electropherogram showing the increased level of A-to-T transition at mtDNA nucleotide position 3243, according to the Cambridge Reference Sequence. The arrow points the substitution place.

In addition to the aforementioned cybrid cell lines produced, we had already available a cybrid cell line resulting from the fusion of 143Bρ^0sm and platelets from a healthy individual - CMPBR3. This cybrid cell line was obtained as the ones previously described and was used as a control for the experiments.

3.1.2 Tumour Cybrid Cell Lines with a Stable Knockdown of SDHB

Human complex II from the respiratory chain is composed by four subunits, all of them encoded by the nuclear DNA. SDHB, one of the subunits, is considered to be a tumour suppressor and its dysfunction is related to tumorigenesis (Bayley *et al.*, 2005). Considering that SDHB is a tumour suppressor and that it takes part both in OXPHOS and Krebs cycle, we decided to inactivate SDHB by short hairpin RNA (shRNA). With the purpose of comparing SDHB-silenced with the inhibition of complex I or all the

complexes achieved by cybrid construction, the silencing was performed in the mtDNA wildtype cybrid, CMPBR3.

The first step was to determine the ideal concentration of puromycin, the antibiotic whose gene of resistance is expressed with the plasmid, to use for the selection of CMPBR3 cells which incorporated the plasmid. The lowest concentration of antibiotic that results in the onset of massive cell death after approximately six days, and kills the entire non-resistant population within two weeks was 0.5µg/mL.

CMPBR3 were transfected with the different plasmids and, two days following the transfection and one day after starting the selection, cells were visualized in an inverted fluorescence microscope and incorporation the plasmid was confirmed. Cells were emitting fluorescence in the wavelength of green, meaning they were expressing GFP, whose gene was contained in the plasmid. Stable cell lines were achieved by picking clones from the cells transfected with the different plasmids, taking advantage of the GFP fluorescence and growing them in the selection medium. Selection with culture media containing 0.5µg/mL of puromycin was performed for approximately 2 months.

In order to do a basic screen of the silencing, Western blotting analysis was performed in the clones obtained from the transfection with all four vectors (Fig. 23).

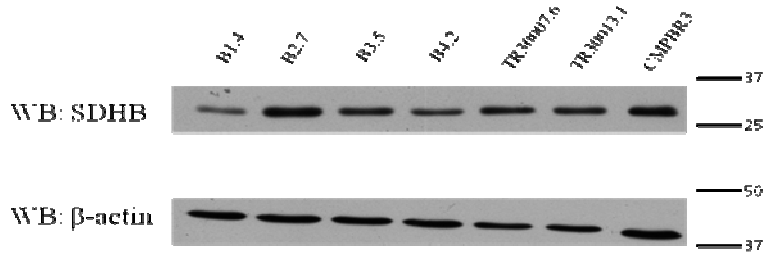

Figure 23: Screening of four clones of the various plasmids expressing the shRNA's targeting succinate dehydrogenase subunit B. Molecular weight markers are indicated in kDa.

From the screened four hairpins sequences, the hairpin sequence B1, particularly clone B1.4, had the most efficient knockdown, as determined through Western-blot. The scrambled plasmid chosen was TR30013.1. This plasmid was used as a negative control for the gene-specific knockdown experiments, with the purpose of specifically ruling out the potential non-specific effect induced by expression of the product.

Cell lysates were used for Western blot analysis with an antibody against SDHB to perform a semi-quantification and verify the functionality of the shRNA vector (Fig. 24).

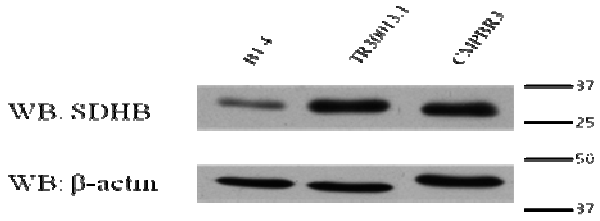

Figure 24: SDHB silencing using a plasmid expressing the shRNA in cybrid CMPBR3 cell line: shRNA for SDHB B1.4, in comparison with the scramble control TR30013.1, effectively diminished SDHB protein levels. Molecular weight markers are indicated in kDa. A representative immunoblot of two experiments is shown. SDHB: succinate dehydrogenase subunit B.

Densitometric analysis showed a 65.8±4.8% reduction of SDHB protein expression, compared to scramble vector (Fig. 25). The results indicate that shRNA-SDHB was specific and efficient for *SDHB* gene silencing in CMPBR3 cell *in vitro*.

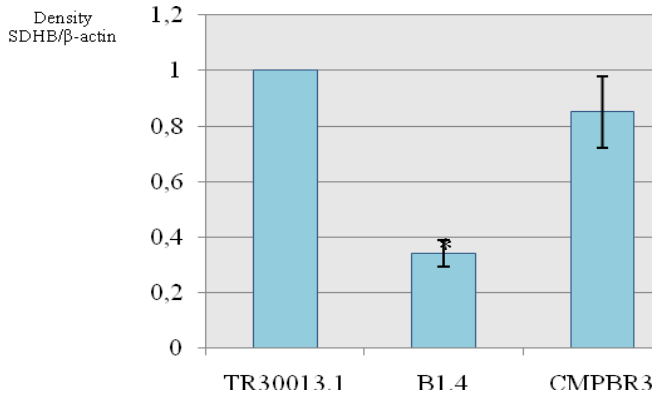

Figure 25: SDHB silencing using a plasmid expressing the shRNA in cybrid CMPBR3 cell line. β-actin was used to normalize for any differences in protein loading between lanes. Data was also normalized to TR13.1 cell line. Data are expressed as density of SDHB band per the density of the β-actin band. Bars, standard deviation; columns, mean. Statistical significance is indicated with an asterisk ($p<0.05$). Data were subjected to one-way ANOVA and a posterior Tukey test.

3.1.3 Sequencing of the 143B, 143Bρ0sm and CMPBR3 cell lines

In order to be sure the mtDNA mutation under study was specific of the 3243CY9.7, we confirmed its absence in 143B, 143Bρ^0sm and CMPBR3. As seen in Fig 26, 27 and 28, no cell line other than 3243CY9.7 and 3243CY9.7.10 presents the A3243T mutation. It should be stated that we could obtain a PCR product from 143Bρ^0sm; however, after sequencing, it displayed numerous point mutations which can be due to fragmentation of mtDNA or to amplification of nuclear pseudogenes of mtDNA (Parr *et al.*, 2006).

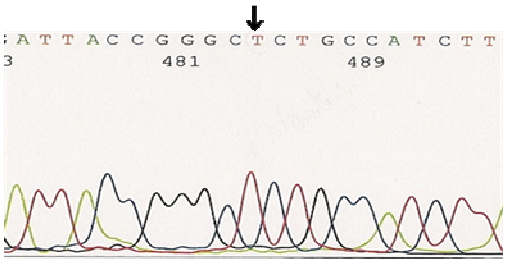

Figure 26: Sequence analysis of the $tRNA^{Leu(UUR)}$ gene in the 143B cell line: electropherogram showing the absence of the A-to-T transition at mtDNA nucleotide position 3243. The arrow points the theoretical substitution place.

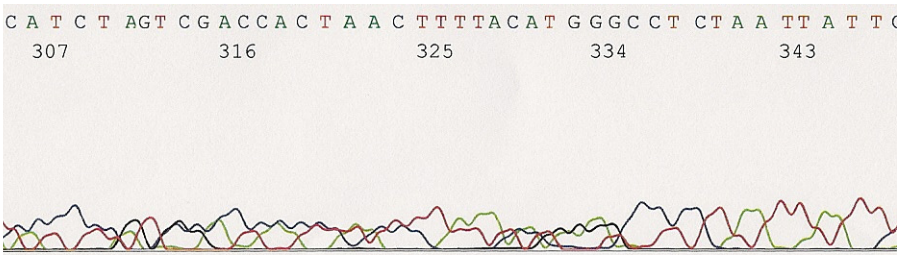

Figure 27: Sequence analysis of the *ND1* gene in 143Bρ^0sm cell line: electropherogram showing mutations all over the sequence.

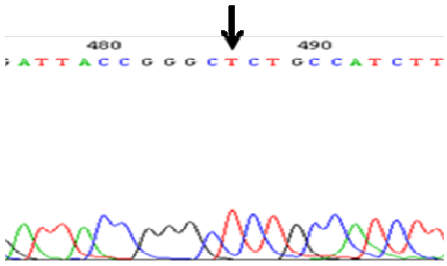

Figure 28: Sequence analysis of the $tRNA^{Leu(UUR)}$ gene in the CMPBR3 cell line: electropherogram showing the absence of the A-to-T transition at mtDNA nucleotide position 3243. The arrow points the theoretical substitution place.

To ensure absence of mtDNA in 143Bρ^{0}sm, the expression of mtDNA-encoded COX II protein was assessed. Figure 29 shows that 143Bρ^{0}sm does not express this enzyme, comparing to the parental 143B cell line, CMPBR3 and 3243CY9.7, confirming the mtDNA depletion in 143Bρ^{0}sm whereas both cybrids cell lines showed expression of this enzyme.

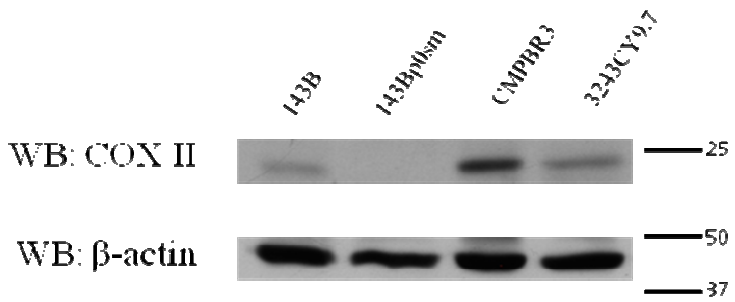

Figure 29: Lack of COXII expression in 143Bρ0sm cell line. Molecular weight markers are indicated in kDa. A representative immunoblot of two experiments is shown.

3.2 *In vitro* Experiments

3.2.1 Metabolic phenotype of the established cell lines (A3243T cybrids and SDHB silenced cell line)

3.2.1.1 Measurement of the main fluxes across the plasma membrane

To understand the metabolic effects of mutations/downregulation of OXPHOS, the flux of glucose, lactate, glutamine and glutamate across the plasma membrane was evaluated in 143B, 143Bρ^{0}sm, CMPBR3, 3243CY9.7 and 3243CY9.7.10 (hereafter designated as cybrid cell lines), as well as B1.4 (SDHB silencing) and respective control - TR30013.1.

This experiment was done only once. The data presented corresponds to the exponential growth phase (after 40h of culture) because the goal was to investigate cellular metabolism when there is a maximum proliferation rate. To ensure this, cells were counted every timepoint and a growth-curve was made. Increased uptake of a metabolite was regarded as increased consume and more secretion as more production. 3243CY9.7 cells presented the lowest glucose uptake and lactate secretion, comparing to CMPBR3 and 143Bρ^{0}sm. In opposition, 143Bρ^{0}sm was the cell line which consumed more glucose and excreted more lactate (Fig. 30). However, 3243CY9.7 presented a higher ratio of lactate produced per unit of glucose consumed ($Y_{lac/glc}$) than to CMPBR3 and 143Bρ^{0}sm (Fig. 31).

The uptake of glutamine or secretion of glutamate did not appear to differ between the cell lines (Fig. 32).

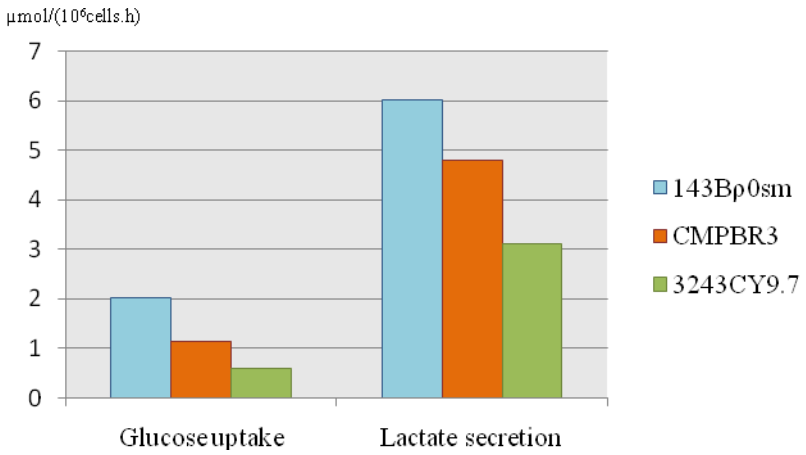

Figure 30: Glucose/lactate fluxes across the plasma membrane in cybrid cell lines. Data are expressed as micromoles of the metabolite per the increase of 1 million cells per hour.

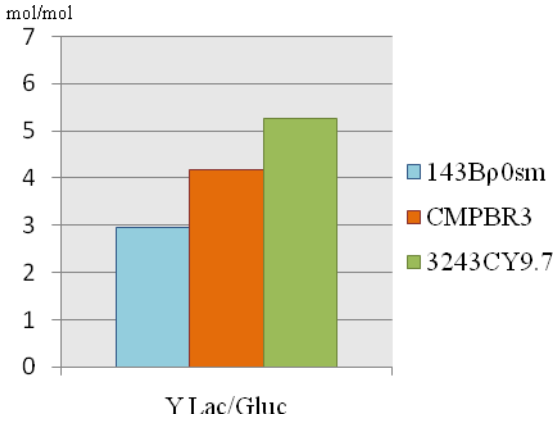

Figure 31: Lactate production per unit of consumed glucose ($Y_{lac/glc}$) in cybrid cell lines. Data are expressed as mole of lactate per mole of glucose.

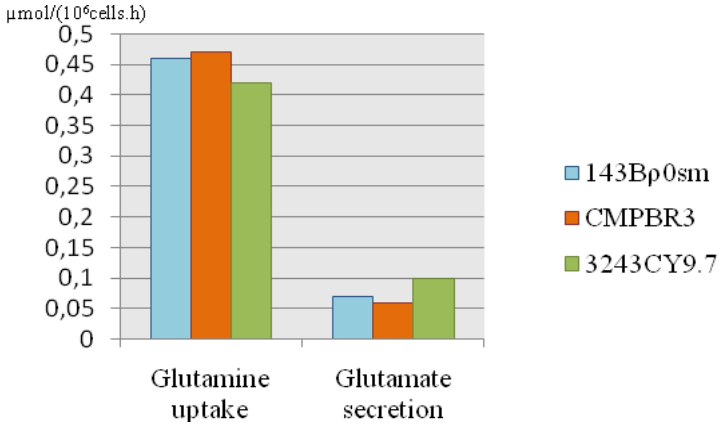

Figure 32: Glutamine uptake and glutamate secretion across the plasma membrane in cybrid cell lines. Data are expressed as micromoles of the metabolite per the increase of 1 million cells per hour.

The SDHB-silenced cell line (B1.4) had, comparing to the control (TR30013.1), the same glucose uptake rate, but an increased lactate secretion (Fig. 33). This increase was

probably the cause for the increased $Y_{lac/glc}$ observed in B1.4 (Fig. 34). Glutamine uptake and glutamate secretion rates seem to increase slightly (Fig. 35).

Silencing of SDHB seems to result in altered cellular metabolism, with increased uptake of glucose and elevated production of lactate.

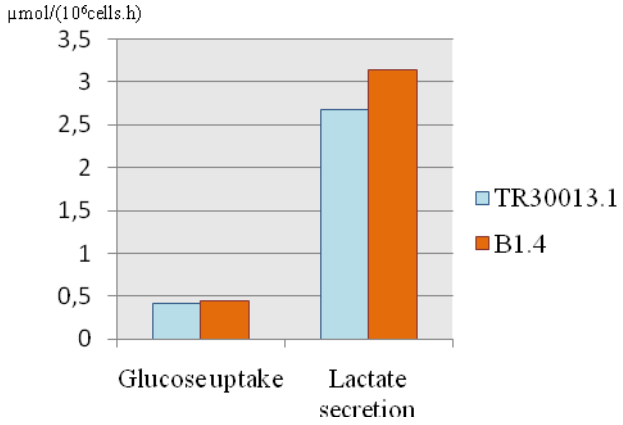

Figure 33: Glucose/lactate fluxes across the plasma membrane in SDHB silenced (B1.4) and control (TR30013.1) cell lines. Data are expressed as micromoles of the metabolite per the increase of 1 million cells per hour.

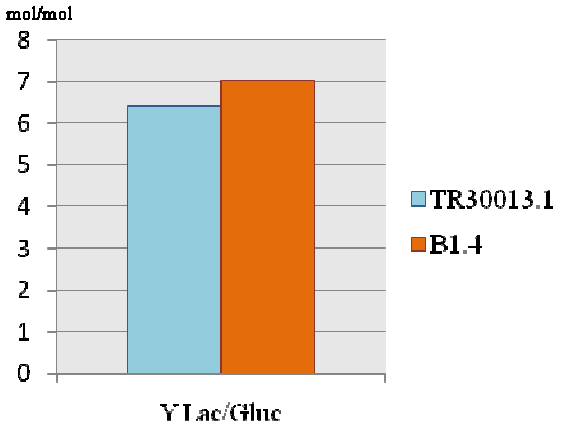

Figure 34: Lactate production per unit of consumed glucose ($Y_{lac/glc}$) in SDHB silenced (B1.4) and control (TR30013.1) cell lines. Data are expressed as mol of lactate per mole of glucose.

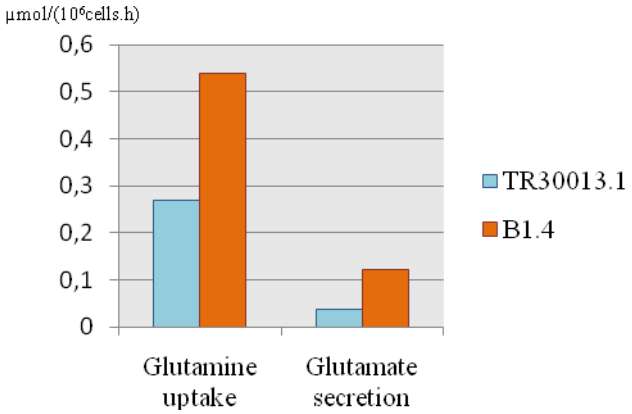

Figure 35: Glutamine uptake and glutamate secretion in SDHB silenced (B1.4) and control (TR30013.1) cell lines. Data are expressed as micromoles of the metabolite per the increase of 1 million cells per hour.

3.2.1.2 Analysis of the expression of key enzymes in glucose metabolism

In an attempt to establish a correlation between the fluxes of the metabolites studied and the expression levels of enzymes that play a key role in glucose metabolism, real-time and Western blotting analyses were performed in all the cell lines.

In three timepoints of the previously described assay cells were stored at -80ºC and cell lyses for protein isolation was carried out. The results of Western-blot presented here concern timepoint 5 (52 hours after the seeding) in order to match with the exponential growth phase (like the previous assay).

Unfortunately, we did not manage to extract RNA from the same cells used in the metabolite measurements and western-blot analyses, therefore, the real-time PCR results concern the same cells but in other passage.

3.2.1.2.1 Protein levels

Western blotting analysis was performed in cell lysates from T5 timepoint of the metabolite measurement. Expression levels of HKII and GLUT1 were measured.

The B1.4 cell line was not silenced for SDHB, in what seems to be a problem associated with the time cells are under culture (see below). Although HKII levels are higher in B1.4, this difference is not statistically significant. GLUT1 showed identical levels (Fig. 36). No statistically significant differences were also observed for 143Bρ^{0}sm, CMPBR3 and 3243CY9.7 cell lines, even though 3243CY9.7 and 143Bρ^{0}sm showed higher levels of HKII than CMPBR3 (Fig. 37).

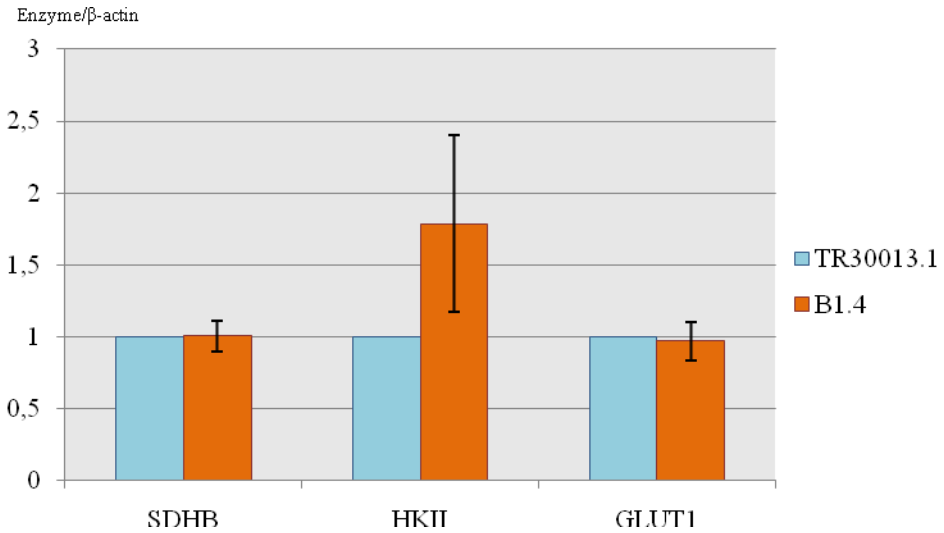

Figure 36: Expression of SDHB, HKII and GLUT1 in SDHB silenced (B1.4) and control (TR30013.1) cell lines: β-actin was used to normalize for any differences in protein loading between lanes. Data reflects fold-change of TR30013.1 cell line. Data are expressed as density of SDHB, HKII or GLUT1 band per the density of the β-actin band. Bars, standard deviation; columns, mean. Statistical significance woud be considered if $p<0.05$. Data were subjected to Mann-Whitney test.

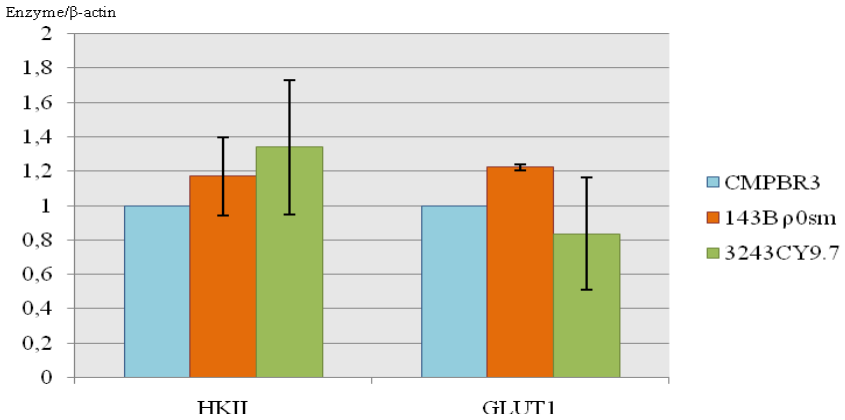

Figure 37: Expression of HKII and GLUT1 cybrid cell lines: β-actin was used to normalize for any differences in protein loading between lanes. Data reflects fold-change of CMPBR3 cell line. Data are expressed as density of HKII or GLUT1 band per the density of the β-actin band. Bars, standard deviation; columns, mean. Statistical significance would be considered if $p<0.05$. Data were subjected to one-way ANOVA and a posterior Tukey test.

As previously mentioned, we observed that the silencing in B1.4 cell line was lost during the time of the metabolites measurement assay (Fig. 38).

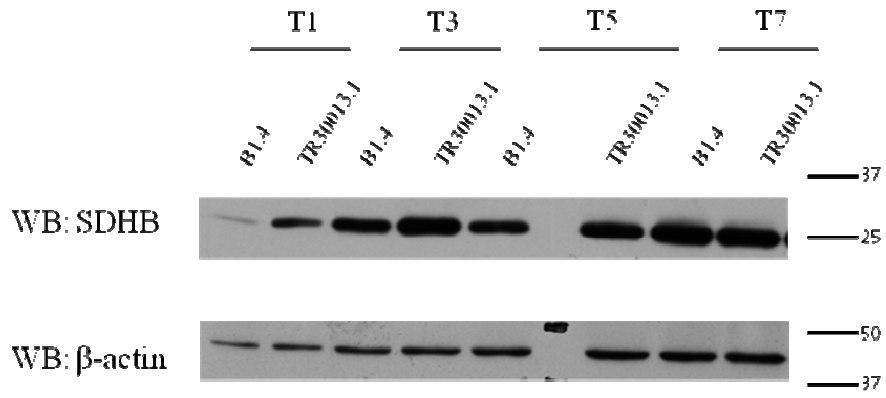

Figure 38: SDHB expression during the metabolite flux assay: SDHB expression is lost during the assay. Molecular weight markers are indicated in kDa. A representative immunoblot of two experiments is shown.

3.2.1.2.2 – Expression of HKII in the A3243T cybrid clone CY9.7.10

After the metabolite flux assay, we managed to obtain, a sub-clone of 3243CY9.7 (3243CY9.7.10) harbouring higher load of mutation in the $tRNA^{Leu(UUR)}$ gene . To check if this increase in the mutation level had consequences on the expression of HKII, we performed Western blot and observed that the levels of this enzyme were higher in this new cybrid clone (Fig. 39).

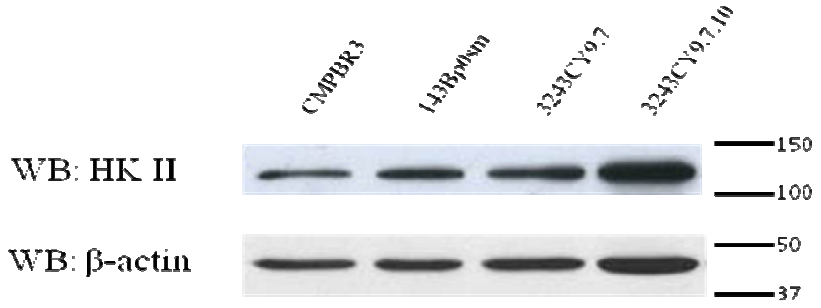

Figure 39: HKII expression in 3243CY9.7.10: Molecular weight markers are indicated in kDa. A representative immunoblot of two experiments is shown.

3.2.1.2.3 mRNA levels

The 143Bρ0sm showed the highest levels of enzyme transcripts, except for GLUT3 and LDH-A. In fact, this cell line displayed the lowest value of LDH-A mRNA and the only one to differ, with statistic significance (Fig 40). The mRNA levels of HKII are lower in CMPBR3 and 3243CY9.7, but 3243CY9.7.10 has higher levels (Fig. 41). Both mutant cybrids have lower transcripts of GLUT3 and GLUT4, compared to CMPBR3. GLUT1 was higher in 3243CY9.7.10 (Fig. 42). In the case of PDK1, all the cybrids displayed mRNA levels significantly lower than 143B and 143Bρ0sm (Fig. 43). G6PD mRNA levels showed a decrease with the mutation in 3243CY9.7 cell line but these statistically significant difference was lost in 3243CY9.7.10 (Fig. 44).

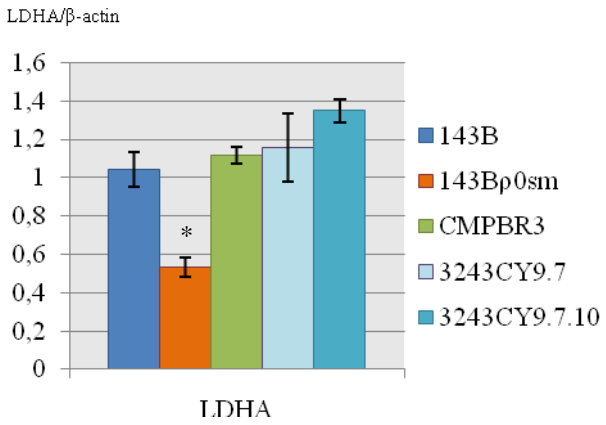

Figure 40: Real-Time PCR results for LDHA in cybrid cell lines. Data is normalized for β-actin expression and correspond to 3 experimental replicas. Bars, standard deviation; columns, mean. Statistical significance is indicated with an asterisk ($p<0.05$). Data were subjected to one-way ANOVA and a posterior Tukey test.

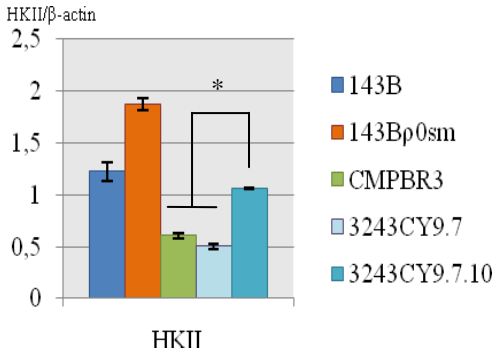

Figure 41: Real-Time PCR results for HKII in cybrid cell lines:. Data is normalized for β-actin expression and correspond to 3 experimental replicas. Bars, standard deviation; columns, mean. Statistical significance is indicated with an asterisk ($p<0.05$). Data were subjected to one-way ANOVA and a posterior Tukey test.

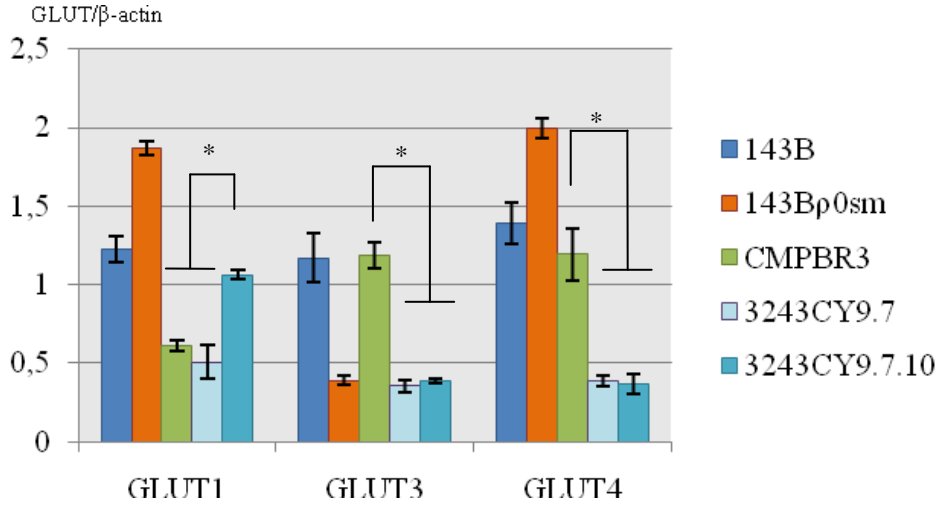

Figure 42: Real-Time PCR results for GLUT1, 3 and 4 in cybrid cell lines. Data is normalized for β-actin expression and correspond to 3 experimental replicas. Bars, standard deviation; columns, mean. Statistical significance is indicated with an asterisk ($p<0.05$). Data were subjected to one-way ANOVA and a posterior Tukey test.

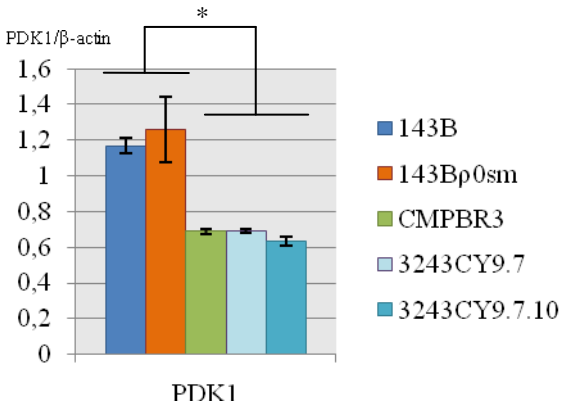

Figure 43: Real-Time PCR results for PDK1 in cybrid cell lines.. Data is normalized for β-actin expression and correspond to 3 experimental replicas.. Bars, standard deviation; columns, mean. Statistical significance is indicated with an asterisk ($p<0.05$). Data were subjected to one-way ANOVA and a posterior Tukey test.

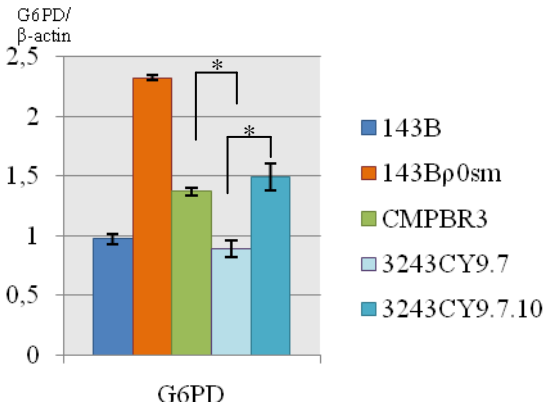

Figure 44: Real-Time PCR results for G6PD in cybrid cell lines. Data is normalized for β-actin expression and correspond to 3 experimental replicasBars, standard deviation; columns, mean. Statistical significance is

indicated with an asterisk ($p<0.05$). Data were subjected to one-way ANOVA and a posterior Tukey test.

Concerning SDHB silencing, the mRNA levels of HKII, GLUT 3, GLUT4, PDK1 and LDH-A increased in a statistically significant manner. GLUT1 and G6PDH levels were also higher in B1.4, compared to TR30013.1, but not statistically significant. However, we observed that the mRNA levels of SDHB were lower in B1.4 than in TR30013.1, but not statistically significant (Figs. 45, 46, 47 and 48).

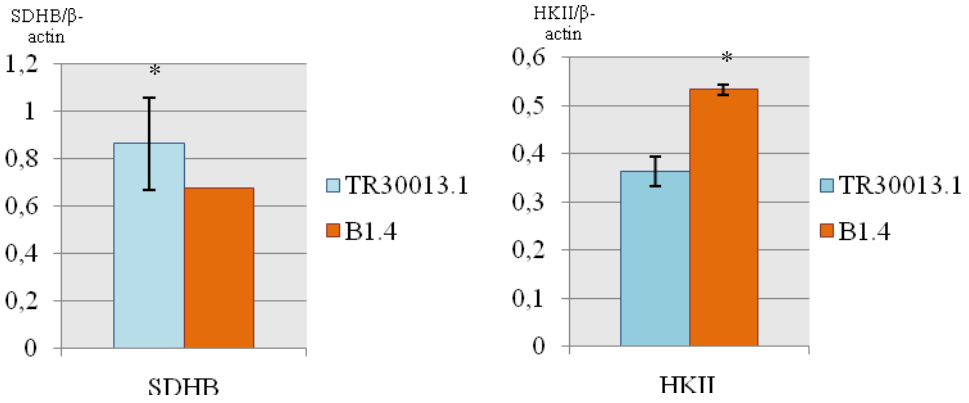

Figure 45: Real-Time PCR results for SDHB and HKII in SDHB silenced (B1.4) and control (TR30013.1) cell lines. Data is normalized for β-actin expression and correspond to 3 experimental replicas Bars, standard deviation; columns, mean. Statistical significance is indicated with an asterisk ($p<0.05$). Data were subjected to Mann-Whitney test.

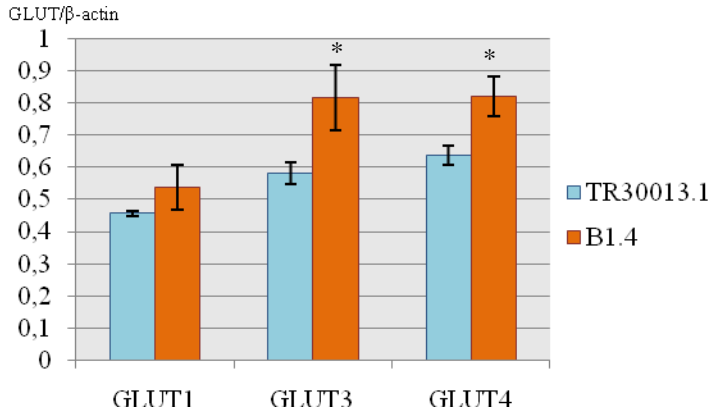

Figure 46: Real-Time PCR results for GLUT1, 3 and 4 in SDHB silenced (B1.4) and control (TR30013.1) cell lines. Data is normalized for β-actin expression and correspond to 3 experimental replicas. Bars, standard deviation; columns, mean. Statistical significance is indicated with an asterisk ($p<0.05$). Data were subjected to Mann-Whitney test.

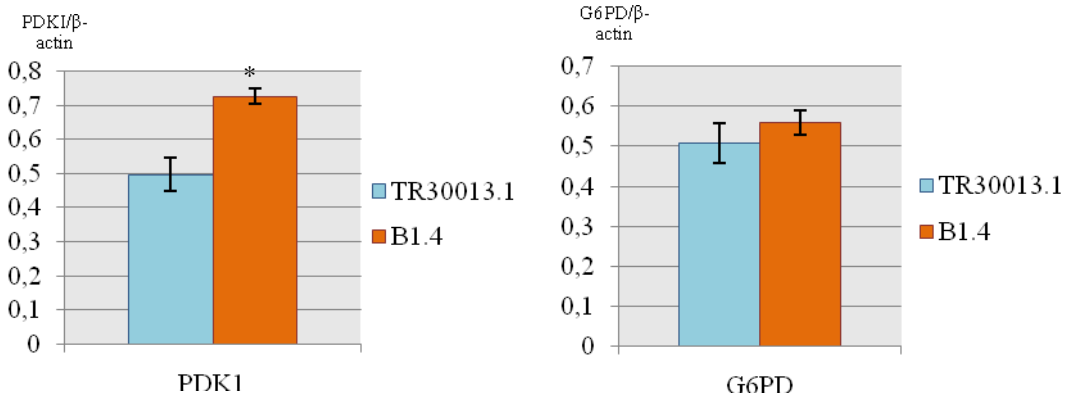

Figure 47: Real-Time PCR results for PDK1 and G6PD in SDHB silenced (B1.4) and control (TR30013.1) cell lines. Data is normalized for β-actin expression and correspond to 3 experimental replicas. Bars, standard

deviation; columns, mean. Statistical significance is indicated with an asterisk ($p<0.05$). Data were subjected to Mann-Whitney test.

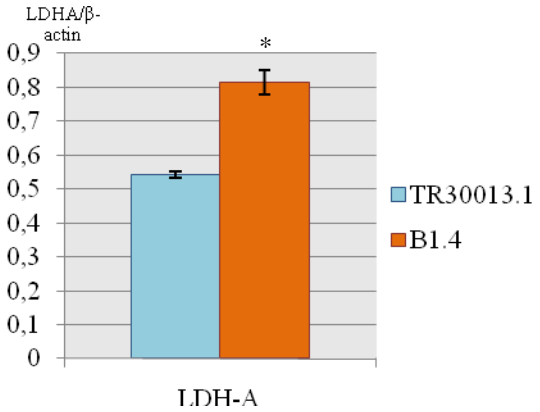

Figure 48: Real-Time PCR results for LDHA in SDHB silenced (B1.4) and control (TR30013.1) cell lines. Data is normalized for β-actin expression and correspond to 3 experimental replicas. Bars, standard deviation; columns, mean. Statistical significance is indicated with an asterisk ($p<0.05$). Data were subjected to Mann-Whitney test.

3.2.2 Cellular phenotype associated to tumourigenesis

3.2.2.1 Cell growth

One of the most studied hallmarks of cancer is the increased replicative potential of tumour cells.

To study the growth of 143B, 143Bρ^{0}sm, CMPBR3, 3243CY9.7 and 3243CY9.7.10 (hereafter designated as cybrid cell lines), cells were counted over time. We were unable to use the thymidine analogue, 5-bromo-2-deoxyuridine (BrdU), to assess cell

proliferation, because 143B cell line, as well as all cell lines derived from it, are thymidine kinase 1-deficient. Thymidine kinase 1 is a cytosolic enzyme that catalyzes the phosphorylation of thymidine and BrdU destinated for nuclear DNA synthesis (Magnusson *et al.*, 2003).

The population doubling time (PDT) is a parameter that characterizes a cell line in terms of growth in the exponential phase. It is the time, in hours, necessary for cells to duplicate their number (Davis, 1994). The PDT calculated for the 3243CY9.7 and 3243CY9.7.10 mutant cybrids as well as for CMPBR3 wild-type cybrids, the parental cell line (143B) and the 143Bρ^{0}sm showed that the latter was the one with highest PDT, followed by cybrids 3243CY9.7.10. The PDT of 3243CY9.7 and CMPBR3 was identical and 143B presented the lowest value meaning it was the one with the highest growth rate. However, these differences were not statistically significant (Fig. 49).

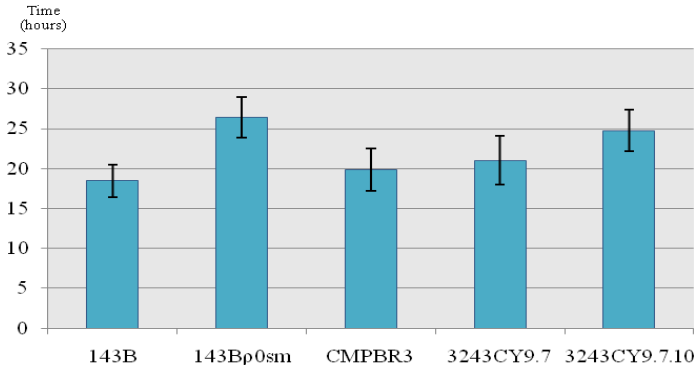

Figure 49: Cellular growth (PDT) of cybrid cell lines. Bars, standard deviation; columns, mean. Data were subjected to one-way ANOVA and a posterior Tukey test.

3.2.2.2 Cell death

Apoptosis plays a critical role in cancer development and in the cellular response to therapeutic approaches. Despite the fact that the exact role of pathogenic mtDNA mutations in cellular apoptotic response remains unclear, apoptosis is tightly linked to the metabolic condition of the cells and the glucose metabolism has been considered "at the crux of the death pathways" (King and Gottlieb, 2009). Considering this information, the rate of cell death was evaluated in cybrid cell lines, taking advantage of the TUNEL assay.

Cell death, examined by TUNEL assay, was evaluated in cybrid cell lines in response to a well-known apoptotic inducer, staurosporine (STS). The concentration of STS that reflected more the differences between cell lines was 50nM (data not shown). 4 hours after the addition of STS all cell lines behave similarly: they appeared stressed as the cellular volume appeared diminished, membranes disrupted and it was noticed the appearance of vacuoles, as concluded by the microscope visualization (Fig. 50).

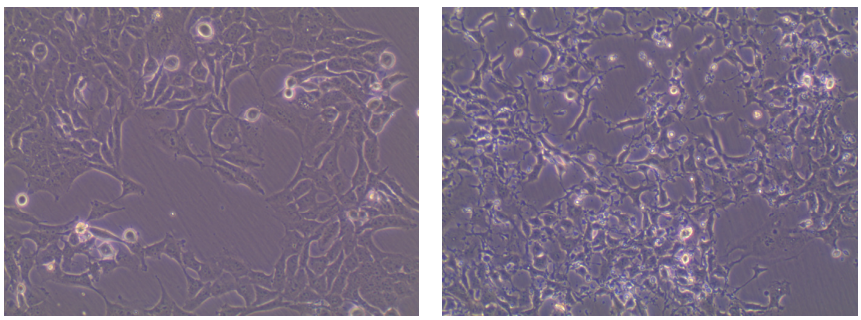

Figure 50: Treatment of cells with the apoptosis inductor STS: morphologic analysis by inverted microscope. (A) Cells not treated and (B) STS 50nM-treated cells. Figures of 143B exemplifying the aspect of all cell lines.

Cell death levels were compared with a negative control where no enzyme (terminal transferase) was added to the reaction.

Observing the histograms and determining the geometric mean of the curve of each cell line, we were able to confirm that staurosporine increased cell death in all cell lines, relatively to the basal levels (no stimuli). However, 143B and CMPBR3 cell lines had a greater increase in cell death with the addition of the drug, comparing 3243CY9.7 and 143Bρ^{0}sm, which showed almost no basal levels of death and only a small increase facing an apoptotic-stimuli (Figs. 51 and 52).

143B

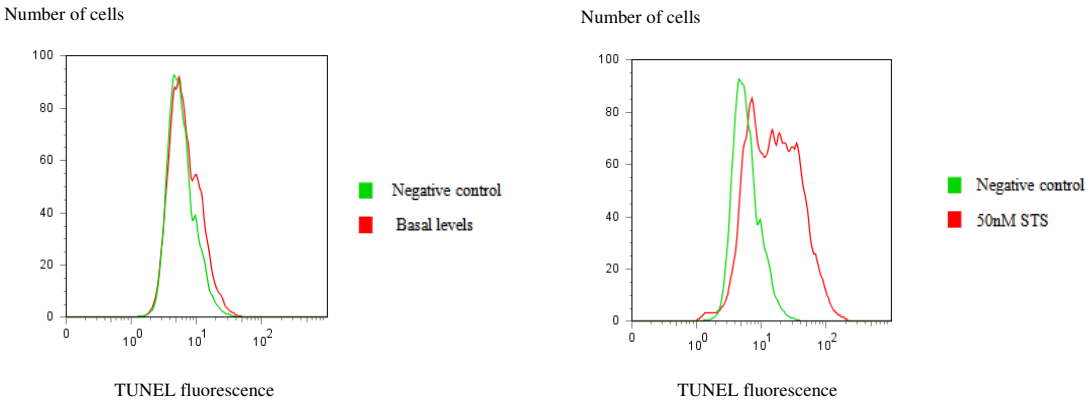

143Bρ^{0}sm

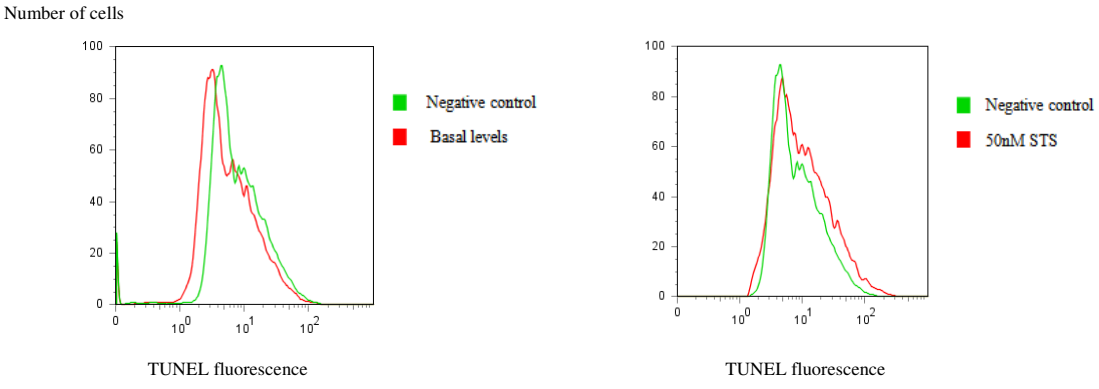

CMPBR3

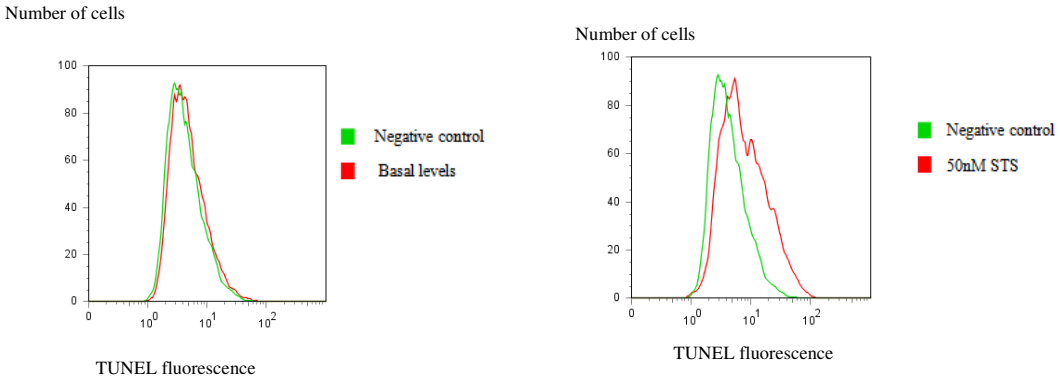

3243CY9.7

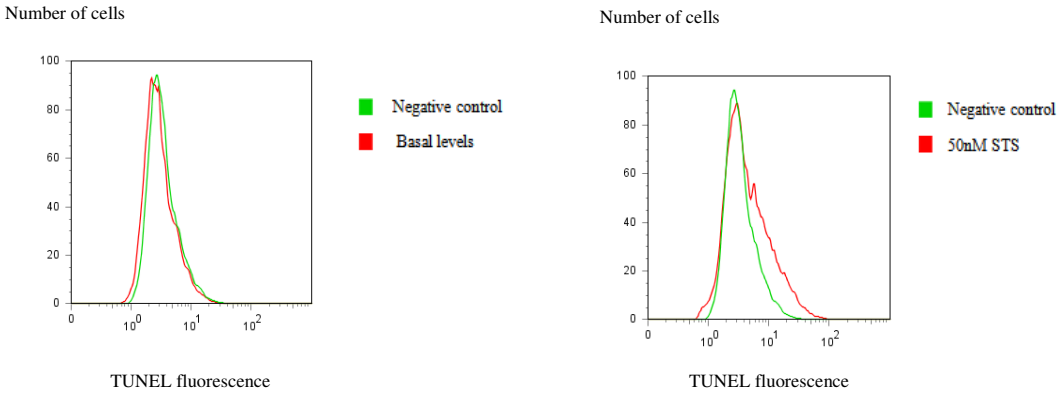

Figure 51: Cell death cybrid cell lines. Histograms represent the distribution of the fluorescence of the cell population, reflecting the increment of cell death from basal conditions to 50nM-STS treatment.

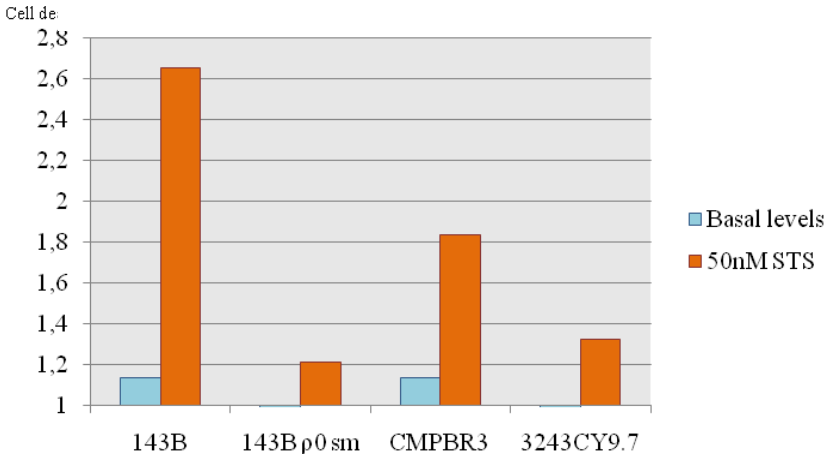

Figure 52: Cell death in cybrid cell lines. Bars represent the quantification of the geometric mean of the histograms of each cell line. Data was normalized to the negative control (TUNEL reaction in the absence of the enzyme). Data are expressed as fold-change in respect to β-actin and negative control.

3.2.2.3 Motility and migration

The ability to invade and metastasize is probably the most important aspect in determining the aggressiveness of tumour cells. Cancer dissemination involves, among other aspects, migration through the extracellular matrix towards blood and lymphatic vessels (Pani *et al.*). It has been suggested that the glycolytic switch can be crucial for the ability of cell to spread at distance (Pani *et al.*). Hence, we determined the migration and motility capacity of cybrid cell lines. To address individual cell motility, cells were plated at a low density and the length of the route described by the cells and the type of movement was assessed; regarding migration, cells were plated at confluency and we measured the period of time required to progress a micrometre (1µm) towards the inside of a scratch. Migration was not evaluated as the time needed to close a scratch because

cells did not move together in a block but instead moved individually or in small groups.

It was observed that 3243CY9.7 and 3243CY9.7.10 had increased individual motility than 143B, 143Brho0sm and CMPBR3 as seen by the increased length of the route that each cell described (Fig X and X)); in addition, 3243CY9.7 and 3243CY9.7.10 had also increased migratory capacity than 143B, 143Brho0sm and CMPBR3 as measured by the increased speed in progressing inside a scratch (Figs. 53 and 54).

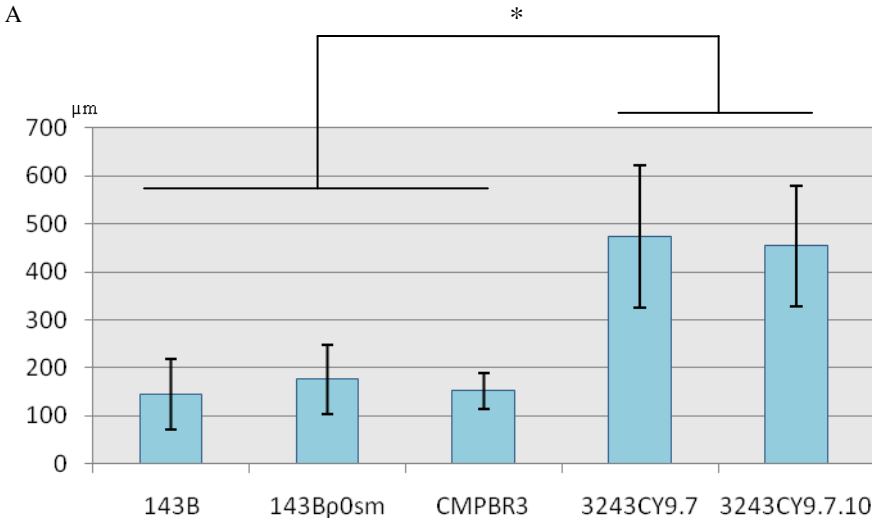

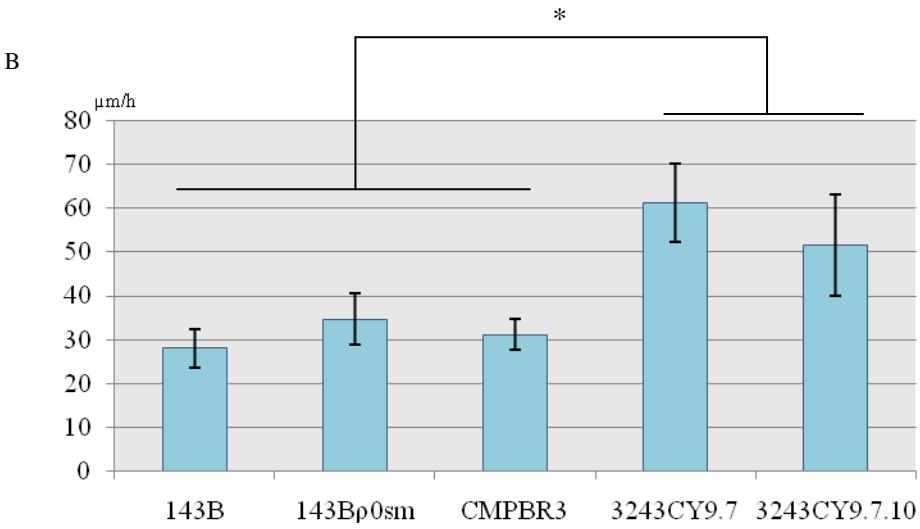

Figure 53: Motility and migration of cybrid cell lines. Data are expressed as micrometre and micrometre per hour, respectively and are result of five measurements. Bars, standard deviation; columns, mean. Statistical significance is indicated with an asterisk ($p<0.05$). Data were subjected to one-way ANOVA and a posterior Tukey test.

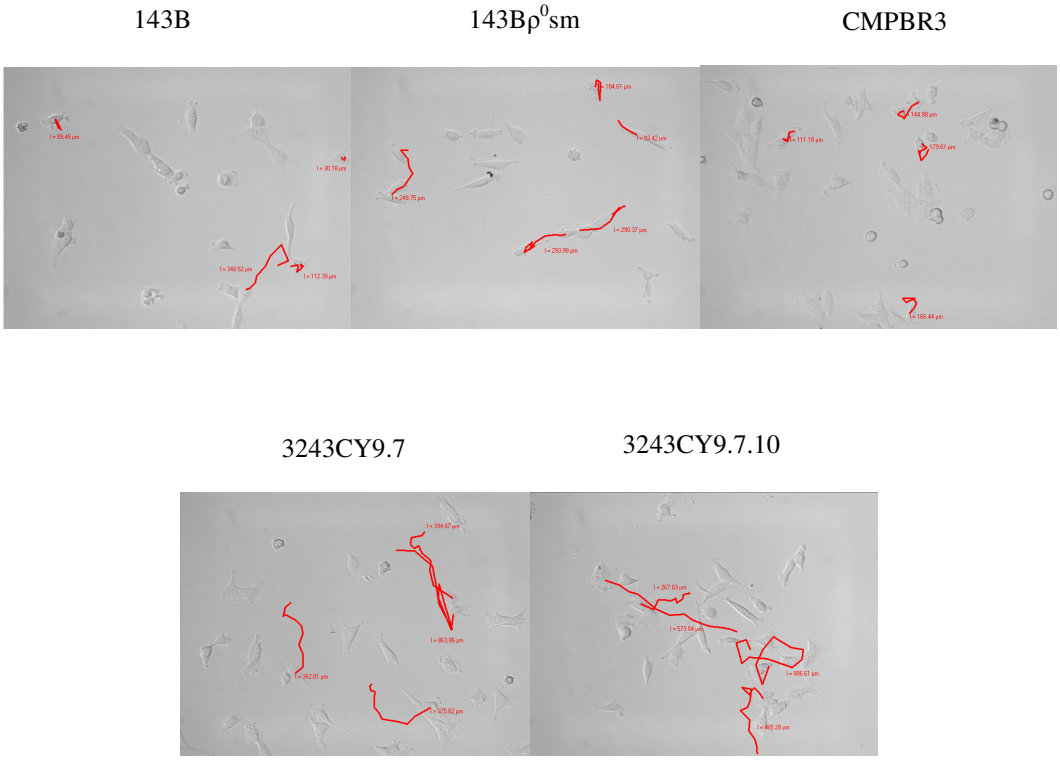

Figure 54: Individual cell motility: movement described by the cybrid cell lines. The red lines represent the total movement of a single cell during 14h.

3.3 *In vivo* Experiments

Cells behave differently in an artificial situation, like *in vitro* culture which has dramatic differences, namely concerning oxygen and nutrients, when compared with the natural environment in which they are inserted. This microenvironment is even more important

when nutrient and oxygen concentrations are direct linked to the effect on study (Gatenby and Gillies, 2004). To investigate the functional importance of the mtDNA OXPHOS proteins *in vivo*, a mouse xenograft model was used. The cybrid 3243CY9.7 and the controls 143Bρ^{0}sm and CMPBR3 were injected subcutaneously in the dorsal flanks of five nude mice with identical number of cells ($1.0x10^6$).

Injection of 3243CY9.7 cells resulted in the development of tumours in all five mice, one tumour per mouse, whereas with the inoculation of 143Bρ^{0}sm and CMPBR3 cell lines no visible tumours were detected in any of the five mice (Table III).

Table III: Tumours developed in the 5 mice after injection of each cell line.

Cell line	**Number of tumours**
CMPBR3	0/5
143Bρ^{0}sm	0/5
3243CY9.7	5/5

Tumour growth was monitored over time. Tumours derived from the mutant cybrids were a mass of cells, either single or composed by two lobules. The volume of the all 5 tumours increased over time (Figs. 55 and 56).

Figure 55: Macroscopic aspect of the tumours excised from the 5 euthanized mice, 42 days after injection with the cybrid 3243CY9.7 (one tumour per mouse).

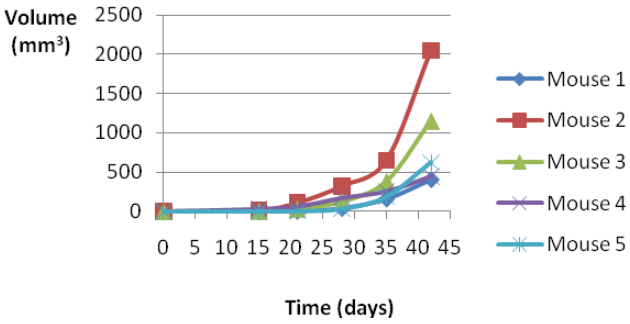

Figure 56: Growth rate (volume) of the tumours in the 5 mice injected with the cybrid 3243CY9.7 cell line. Tumour measurements were performed on day 15, 21, 28, 35 and 42 post-injection.

Two of the tumours (mice 3 and 5) appeared to have invaded deeply the adjacent tissue, while the others were individualized. When the morphologic characteristics of the lungs of these mice with apparent invasion were examined macroscopically, the lung of mouse 3 showed a congestive aspect with whitish areas.

After a hematoxiline/eosine (H&E) staining of the lungs, visualization under a light microscope revealed partial loss of the alveolar structure in mouse 3. In addition, in the mice 4 and 5 we could observe the presence of metastases as shown in Fig. 57. In both pictures mitotic figures can be observed (arrows).

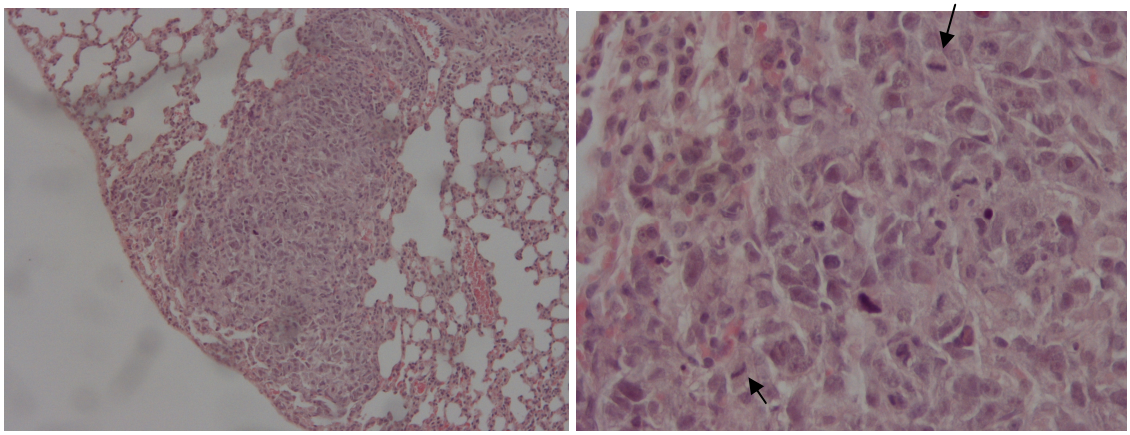

100x 200x

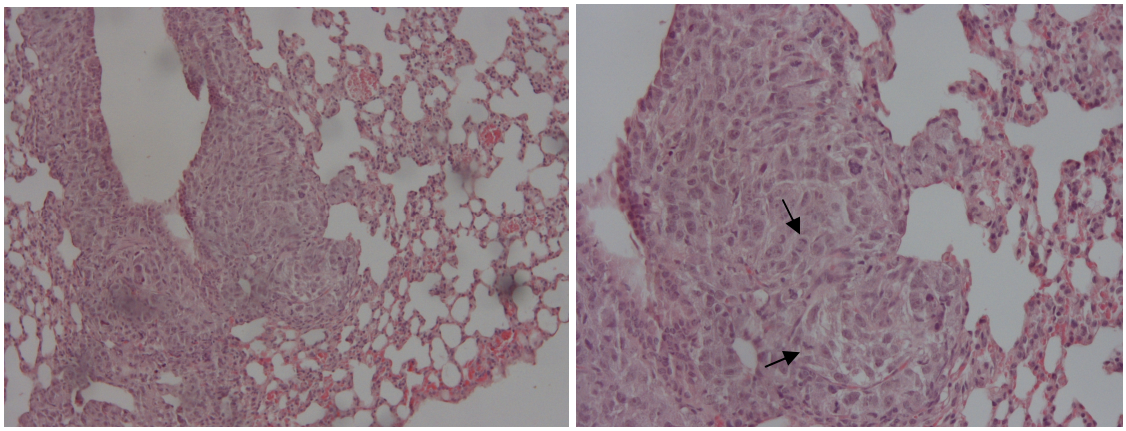

100x 200x

Figure 57: Lung metastases in mouse 5: microphotographs representative of H&E staining sections showing metastases with the presence of mitotic figures (arrows).

Upon sequencing analysis of DNA from the extracted tumours, we confirmed that they all harboured the mtDNA mutation under study (A3243T in $tRNA^{Leu(UUR)}$ gene) (Fig. 58).

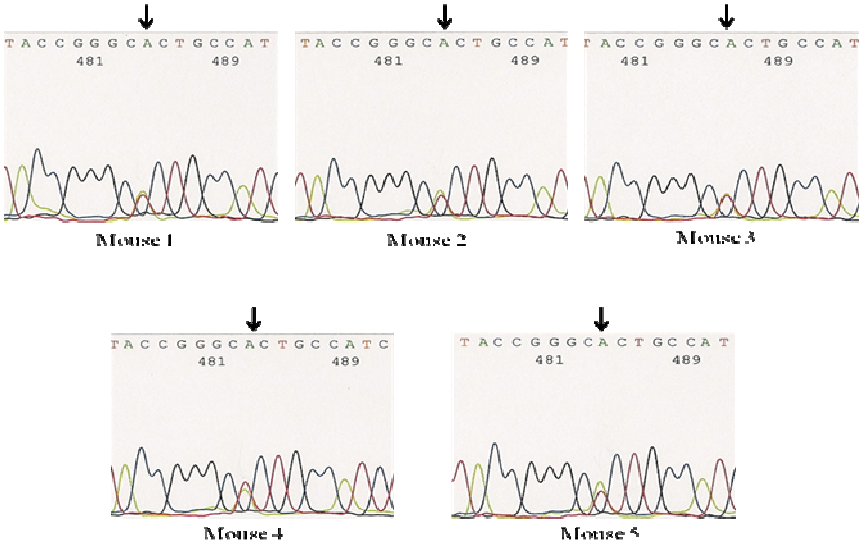

Figure 58: Sequence analysis of the $tRNA^{Leu(UUR)}$ gene in the 5 mice injected with the cybrid 3243CY9.7: electropherograms showing the A-to-T transition at mtDNA nucleotide position 3243, according to the Cambridge Reference Sequence. The arrows point the substitution place.

Chapter 4 Discussion

Otto Warburg, complemented by other authors, have shown that human tumours frequently present enhancement of the glycolytic pathway for energy production (and other cellular needs, as anabolic metabolism), even though ample supply of oxygen is present to support mitochondrial OXPHOS function (DeBerardinis *et al.*, 2008; Warburg, 1956).

One of the hypotheses which may explain the "Warburg effect" is that cancers accumulate defects, more or less deleterious, in mitochondrial respiration and therefore in ATP generation from OXPHOS. These defects can arise from mutations that occur either in the mtDNA itself or in nuclear-encoded mitochondrial proteins and would result in enhanced glycolysis, since ATP generation from OXPHOS would not be possible.

Other authors claim that tumour cells appear to be capable of performing respiration, but the rate of OXPHOS is reduced by a dramatic increase in glycolysis and lactate production, meaning that decreased mitochondrial OXPHOS would not be the cause of accelerated glycolysis but rather other genetic or environmental alterations (referencia Frezza, 2009).

Almost certainly, there is no universal way of achieving the Warburg effect and mitochondrial dysfunction can function as either cause or bystander/consequence. Warburg himself did not contradict the idea that tumours cannot use mitochondrial respiration. In fact, he emphasised that there is a division of labour in energy production rather than an exclusively reliance of tumours on glycolysis for energy production (Warburg, 1956). In our way of thinking, a genetic cause for mitochondrial dysfunction,

particularly in genes encoding OXPHOS and Krebs cycle proteins could be the breaker of the "equilibrium" favouring glycolysis.

It is widely recognized that mutations in mtDNA are a common observation in human tumours and many reports have shown that mtDNA mutations can impair the function of OXPHOS (Brandon *et al.*, 2006; Lee and Wei, 2009). It has also been demonstrated that mtDNA mutations and mitochondrial dysfunction may contribute to tumour progression by enhancing the survival, proliferation and metastatic potential of tumour cells (Frezza and Gottlieb, 2009; Lee and Wei, 2009).

The genes that encode the subunits of SDH complex (also known as OXPHOS complex II) protein are considered to be tumour suppressors; this enzyme has also been categorized as "housekeeping" and makes the bridge between OXPHOS and Krebs cycle. In fact, germline mutations in SDHA, B, C or D (the genes that encode the four SDH subunits) and in the newly described SDH5, were found to cause hereditary paraganglioma and phaeochrocytoma (Burnichon *et al.*, ; Gottlieb and Tomlinson, 2005; Hao *et al.*, 2009). Glycolysis and mitochondrial dysfunction is thought to be an intermediate in the process SDH-caused neoplasias (Gottlieb and Tomlinson, 2005).

Taking all of this into account, our goal was to study the role of genetic mitochondrial dysfunction in the acquisition of the "Warburg effect". The models used had either a mtDNA mutation in *ND1* or in $tRNA^{Leu(UUR)}$ gene or silencing of the SDHB protein.

Our results point to an important role of mitochondrial dysfunction for the metabolic shift towards aerobic glycolysis typical of tumour cells; in addition cells harbouring a mtDNA mutation in the $tRNA^{Leu(UUR)}$ gene display a higher tumourigenic potential,

suggesting that loss mitochondrial OXPHOS function is important in tumour development/progression.

4.1 Cell lines

For the cybrid construction we began by using XTC.UC1 cell line mtDNA because it harbours a mutation in the mtDNA gene *ND1* (encodes a complex I subunit). A number of studies have demonstrated the relation of defective complex I and OXPHOS, with this *ND1* mutation; however, a metabolic analysis has never been done, to our knowledge. Inactivation of complex I, the most studied OXPHOS complex and the one most commonly affected in human tumours, would allow us to understand deeply the relation between complex I deficiency and cancer metabolism.

In XTC.UC1 was given more emphasis to the *ND1* mutation, despite this cell line harbour other mutation in cyt *b* gene. However, only with the establishment of the stable cybrid cell line is possible to analyse the levels of both mutations and investigate which one is the responsible for the phenotype.

On the other hand, it could be interesting to compare the dysfunction of a specific complex with compromised OXPHOS with alterations in all the complexes. In fact, we were able to construct a cybrid cell line with a mutation in the $tRNA^{Leu(UUR)}$ gene – A3243T mutation. This transition has not been studied intensively. However, its functional effects on the tRNA gene may resemble the ones from a most common mutation in the same base - A3243G transition in the $tRNA^{Leu(UUR)}$ – that probably leads to an alteration in the tertiary structure of the tRNA or to reduced secondary

modifications and a consequent metabolism instability and diminished charging by the leucyl-tRNA synthetase (Chomyn *et al.*, 2000).

Complex II and its subunits would also be a natural target of our study. It is part of the Krebs cycle that connects glucose metabolism in the cytosol to OXPHOS in the mitochondria and its subunits considered as tumour suppressor genes; therefore it is a natural model of altered metabolism and inherited tumourigenesis.

4.1.1 Selection of the mtDNA mutation of interest

XTC.UC1 cell line is an immortalized cell line derived from a metastasis of a thyroid carcinoma that harbours two mtDNA mutations, making it a good model for studying the role of these in mitochondrial dysfunction (Bonora *et al.*, 2006).

The XTC.UC1 cell line batch that we have displayed a lower level of *ND1* mutation (about 50%), comparing to the study of Bonora *et al*. (2006) where the *ND1* mutation was found to be heteroplasmic with 94.3% presence of the mutated allele (Bonora *et al.*, 2006). When we produced cybrids from XTC.UC1, the resulting clones showed very low levels of the mutation, thus no effects would be observed. To overcome this problem, we decided to increase the mutation load in the XTC.UC1 and our attempts were successful. The supplementation of the medium of the cell lines with uridine and achievement of successive serial dilutions led to an increase in the number of mtDNA copies with the mutations. This might be related to the fact that a defective OXPHOS renders cells auxotrophic for pyrimidines because dihydroorotate dehydrogenase (and enzyme that catalyzes the fourth step in the *de novo* biosynthesis of pyrimidine) is

located in the inner mitochondrial membrane and intimately associated to the respiratory chain (Knecht and Loffler, 2000). We can also assume that, if adding uridine to the medium where cells are being cultured results in higher levels of the mtDNA mutation, it probably means that these mutations disrupt the functionality of the respiratory chain. This approach was also applied to the cybrids with the A3243T mutation in the $tRNA^{Leu(UUR)}$ gene and may also have contributed to the selection of higher levels of mutation in this cybrid cell line.

In the case of the *ND1* mutation, the mechanism behind this method may be not only an artificial selection, since only those clones with higher levels of mutation were chosen; a phenomenon of natural selection must be present as well. This hypothesis was supported by the finding that all the growing clones had higher levels of the *ND1* mtDNA mutation, when compared to the XTC.UC1 (cultured in medium with uridine).

There has been a lot of debate concerning the dynamics of mtDNA mutations. In cancer and in mtDNA diseases, both homoplasmic and heteroplasmic mtDNA mutations have been observed. It has been defended that tumours *in vivo* are under selective constrains that act positively in mtDNA mutations that promote tumour progression (Zhidkov *et al.*, 2009). Some mutant mtDNA may actually have a replicative advantage over wild-type mtDNA. Even though the *in vitro* environment is very different from *in vivo*, this selective advantage may also be present in cell culture, under appropriate conditions. Carew and Huang (2002) suggested some possible mechanisms by which heteroplasmic mutations may be selected: if a mutation confers cell growth/survival advantage or facilitates mtDNA replication, such mutation is likely to survive the selection. Depending on the duration and the degree of growth/survival advantage, the cells

carrying the "advantageous" mtDNA mutation may eventually become dominant and evolve to establish a homoplasmic mutant state. A growth/survival advantage may also be acquired through a second event such as additional DNA alterations caused by ROS (Fig. 59).

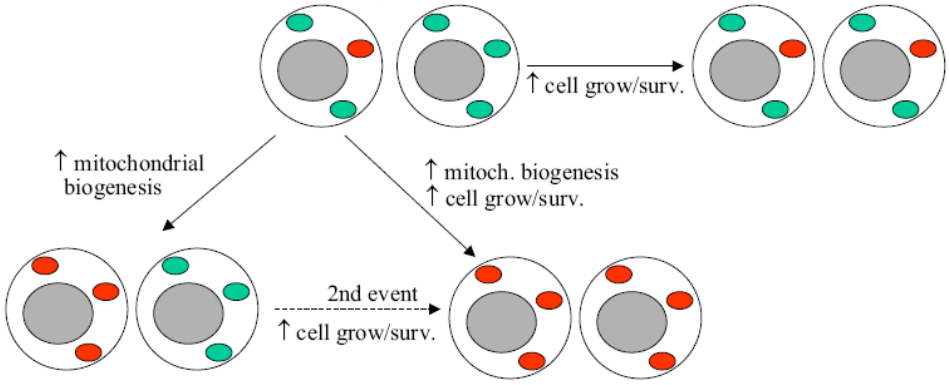

Figure 59: Mechanism of selection of mtDNA mutations (adapted from (Carew and Huang, 2002).

Other authors stand for the idea that the accumulation of mtDNA mutations in tumours is due to its monoclonal origin and these mutations are in fact selected against (Khaidakov and Shmookler Reis, 2005). It has been also stated that because cells continually fuse and divide mitochondria, any given mitochondrion within a heteroplasmic cell will likely contain both mutant and wild-type mtDNA. This premixing leads to reduced fluctuations in mutant/wild-type mtDNA ratios in the daughter cells and diminishes the likelihood of producing homoplasmy (Chan, 2006). However, this mechanism of mitochondrial fusion and fission it is not a guarantee of heteroplasmy, it varies within the tissue involved and it mitochondrial subcellular heterogeneity as been discussed (Chan, 2006; Wikstrom *et al.*, 2009). On the other

hand, Park *et al*. (2009) demonstrated that a heteroplasmic and not homoplasmic, mitochondrial DNA mutation in complex I promotes tumorigenesis.

In another perspective, Coller *et al.* (2001), using computer modelling, defended that homoplasmy of mtDNA mutations in human tumours can be achieved entirely by chance through unbiased mtDNA replication and sorting during cell division without selection for physiological advantage (Coller *et al.*, 2001).

As we were unable to obtain a stable cybrid cell line with the mutation in *ND1* gene within a threshold required to cause a biochemical or phenotypic consequence, the study was not continued. Currently, efforts are been made in order to solve this problem.

4.2 Metabolic phenotype

The first step in order to check for the role of mitochondrial proteins dysfunction in the Warburg effect was to investigate whether the established cell lines presented this aerobic glycolysis metabolism. Thus, we studied the flux of some key metabolites in energy production, by assessing their levels in the culture medium of cells undergoing the exponential growth phase. More secretion of a metabolite was regarded as an increase in intracellular production and more uptake as more consume. This would allow us to infer the active metabolic pathways in each cell line. The conclusions are, however, made with the reservations because we lack replicates confirming these results.

Warburg recognized in the 20s that malignant cells produce large amounts of lactic acid, because of the ATP production through conversion of glucose to lactate (Warburg *et al.*, 1927). Lactic acidosis is also a typical biochemical hallmark of mitochondrial diseases

and it is widely used in the diagnosis of mitochondrial encephalomyopathies (DiMauro and Schon, 2001). This secretion of lactate in accompanied by a high rate of glucose uptake, phenomenon that is exploited by PET imaging (Kubota, 2001). Nevertheless, this glucose uptake must be associated with lactate secretion, to be sure that glycolysis products are been targeted towards lactate production. 3243CY9.7 cybrids and SDHB-silenced cell lines were analysed in terms of the glucose and lactate fluxes across the membrane. For a better understanding of the active metabolic pathways, the main enzymes were studied in terms of expression, either by real-time PCR and Western blotting. It is important to state that the Western blot analysis was done using protein isolated from the same cells used in the measurement of the main fluxes across the plasma membrane, while the real-time PCR was performed later, using RNA isolated from the same cell lines but with different passage.

Despite the fact that glucose uptake and lactate secretion noticed seemed to be lower in the 3243CY9.7 cybrid than the wild-type cybrids (CMPBR3), the rate of lactate secretion per glucose uptake was higher. The SDHB silencing also resulted in a slightly increase in the rate of lactate secretion per glucose uptake. An important note is that the values of the rate lactate-glucose obtained are positive, meaning more lactate is being secreted than glucose uptaken. Moreover, and most importantly, when compared to parallel studies in our lab (data not published) concerning a non-tumourigenic but also transformed (GRIM-19 silencing) cell line (with the adequate reservation due to the differences between the cell lines), these values are elevated. This might indicate that, from the beginning, tumourigenic nature of 143B cell line (and consequently, all of its derivatives), it already presents an altered metabolism, i.e., increased glycolysis.

We also hypothesised that if both 3243CY9.7 cybrid and SDHB silenced cell lines displayed high levels of glycolysis compared with respective controls, this may related to expression of enzymes in the glycolytic pathway. An increased rate of glucose uptake has been correlated with the upregulation of glucose transporters and HKII, which control the glycolytic flux at the transport and phosphorylation steps (Burt *et al.*, 2001; Mamede *et al.*, 2005). All the enzymes studied have been suggested as molecular targets of cancer metabolism (Tennant *et al.*).

Most work on glucose transporters and cancer concerns GLUT1. GLUT1 is ubiquitously expressed in many tumour types, but rarely expressed in corresponding benign tissue. Moreover, it is considered an intrinsic marker of hypoxia and also a predictor of poor prognosis in some tumours (Airley *et al.*, ; Kunkel *et al.*, 2003). GLUT-1 expression was associated with the invasive ability of human breast cancer cells (Grover-McKay *et al.*, 1998) and with a lower infiltration of CD8(+) effector cells in renal cell carcinoma tissue (Singer *et al.*). It has been shown that this protein plays an important role in regulating glycolytic flux (Rivenzon-Segal *et al.*, 2003). GLUT3 is also consistently expressed at high levels in cancer cells (Yamamoto *et al.*, 1990). The role of GLUT4 in cancer has not been much explored. GLUT4 expression was found to be significantly increased in ovarian invasive carcinoma compared to expressions in both benign and borderline tumour, although not significantly correlated with the degree of differentiation or stage of ovarian cancer (Shibata *et al.*, 2005). On the other hand, it was found to have a decreased expression in a sarcoma cell line (Chiaramonte *et al.*, 1998).

HK are the enzymes that catalyse the phosphorylation of glucose to G6P, preventing the efflux of glucose from the cell. During the neoplastic transformation, HKII is over-expressed and the expression of other hexokinases is reduced. This over-expression can be caused by genetic amplification, mRNA stabilization, promiscuous activation of the promoter and epigenetics. It is also under discussion the role of HKII in immortalization of cells (Mathupala *et al.*, 2009).

LDH-A is upregulated in tumours (Goldman *et al.*, 1964). Fantin et al. (2006) showed that mammary tumour cells rely on LDH-A activity even when oxygen is not limiting. Its downregulation also leads to an increase in OXPHOS and O_2 consumption (Fantin *et al.*, 2006).

PDH is another enzyme that is correlated with the rate lactate secretion. PDH activity is regulated by pyruvate dehydrogenase kinase (PDK) that is able to phosphorylate and inactivate PDH. The upregulation of PDK has been correlated with poor prognosis in head and neck squamous tumours (Wigfield *et al.*, 2008).

PDK has been used as an approach for cancer therapy with dichloroacetate (DCA). DCA is a small molecule inhibitor of PDK currently approved for treatment of congenital lactic acidosis. This component inactivates PDK, leaving PDH active and resulting in activation of OXPHOS; this, in turn, leads to apoptosis either increasing the flux through the electron transport chain which results in release of cyt c by membrane depolarization and by increment of ROS production leading to potassium ion efflux and caspase activation (Bonnet *et al.*, 2007).

Aerobic glycolysis is thought to be just one component of the metabolic transformation. One of the theories about the advantages of glycolysis in tumourigenesis is the creation of intermediates for anabolic reactions. For example, G6P can be used in glycogen and pentose-phosphate pathway. This last pathway plays a crucial role in, among others, NADPH regeneration and formation of ribose-5-phosphate, essential molecules for anabolism (fatty acids and acid nucleic synthesis). This deviation is influenced by G6PD, which is responsible for G6P entry in this pathway. We observed that neither 3243CY9.7 cybrid nor SDHB-silenced cell lines displayed statistically significant increase in the transcription levels of this G6PD. However, this lack of over-expression does not mean that glycolytic carbon is not been diverted towards ribose-5-phosphate synthesis, because of the existence of the non-oxidative pathway (DeBerardinis *et al.*, 2008).

4.2.1 SDHB silenced cell line

In the SDHB silenced cells the protein levels and mRNA levels seem to be concordant allowing the correlation between mRNA levels with the studied fluxes of metabolites. In order to simplify the interpretation of the results, higher mRNA levels are assumed, in the case of lack of protein analysis, as leading to higher functional protein levels. However, we are aware that mRNA expression does not directly correlate with the amount of the corresponding protein since there are mechanisms of degradation of mRNA and regulatory processes of enzymatic activity.

Our results showed increased transcription of GLUT 3 and 4 genes, which may explain the higher glucose uptake of B1.4. GLUT1 does not seem to be associated with SDHB

silencing. As glucose is the principal energy source for cancer cells, the up-regulation glucose transporters could bring a survival advantage to cancer cells by increasing glucose uptake in environments of low glucose concentration. Increased LDH-A transcription may be related with the increased lactate secretion observed in B1.4 cell line. It was also observed in B1.4 an increase in transcription of HKII enzyme and a correspondent increased expression (although this last not statistically significant), suggesting that this enzyme might be playing a role in facilitating an high glycolytic activity. This is also supported by other two observations: there does not seem to be differences in mRNA levels of G6PD, meaning that glucose is not being diverted towards the oxidative pentose phosphate pathway; nevertheless this is not the only enzyme responsible for the converting of glucose intermediates into the ribose-5-phosphate synthesis. Besides, higher PDK mRNA levels can be correlated with inhibition of PDH, accumulation of pyruvate in cytoplasm and its conversion in lactate. An inhibition of pyruvate oxidation would redirect metabolic flux to cytosolic pyruvate metabolism and consequently lactate production.

All this supports the observed increased lactate production per unit of consumed glucose.

Even though we did not observe a significant silencing of SDHB at mRNA or protein level, it was observed a decrease of mRNA level. In addition, during the assay of the fluxes of the metabolites, SDHB was silenced by the first timepoints, but not at T5, where the measurements were made. The differences in transcription levels of glycolytic enzymes may suggest that the SDHB knockdown caused metabolic alterations that persist even when the silencing is lost.

The decrease of expression of SDHB with its silencing, although not statistically significant, together with the data suggesting that this shRNA against SDHB was successful, allowing to infer that SDHB silencing alters the cellular metabolism, increasing glycolysis. The repetition of these experiments will permit to obtain more conclusive data concerning the role of SDHB protein in cellular metabolism.

4.2.2 A3243T cybrids

Cybrid cell line 3243CY9.7 showed an increased rate of lactate secretion per glucose uptaken, suggesting increased rate of glycolysis. The levels of HKII were similar concerning mRNA, but increased concerning protein (not statistically significant) We did not observe, however, differences in the levels of GLUT or LDH-A, when compared to CMPBR3, confirmed by protein analysis in the case of GLUT1. PDK mRNA levels did not differ and G6PD even seemed to be decreased in 3243CY9.7. So, there seems to be an incongruence between these observations and the elevated lactate production per molecule of glucose consumed, comparing to CMPBR3 which suggests that most of the consumed glucose is being directed towards lactate formation. The increase in HKII protein levels may explain the higher rate of lactate secretion per uptake of glucose. It may be that, in 3243CY9.7 cell line, the mRNA transcripts are more stable leading to higher rates of translation, comparing to CMPBR3. Nevertheless, these results need further confirmation and the enzymes activity needs to be assessed.

All together, the mtDNA mutant 3243CY9.7 cybrids seem to present a more glycolytic phenotype than wt CMPBR3 cybrids. The lack of exuberance of this phenotype may be attributable to the wild-type mtDNA copies present in mitochondria of A3243T cybrids

that are masking its effects. Studies performed with the mutation in $tRNA^{Leu(UUR)}$ gene (not clear if it is the same mutation or the A3243G mutation) showed that a protective effect against the mutation was exerted in cybrids with levels of residual wild-type mtDNA above 6% (Chomyn *et al.*, 1992).

In fact, it seems that the mutation levels are crucial. After the assay of the fluxes of the metabolites was performed, a new clone harbouring a higher level of A3243T mutation was isolated – 3243CY9.7.10. mRNA analysis revealed that, concerning HKII and GLUT1, there was a statistically significant increase, comparing to CMPBR3 and even with 3243CY9.7. The Western blot analysis for HKII confirms real-time PCR results. On the other hand, the glucose that predictably is being more uptaken by the cell seems to be diverted towards ribose-5-phosphate synthesis due to the increased levels of mRNA levels of G6PD. This might indicate that in fact there is a threshold of the mtDNA mutation levels, that when surpassed, turn the effects much more evident.

The mRNA results for 3243CY9.7.10 are more similar to those observed for $143B\rho^0$sm. The latter had more transcription of HKII, GLUT1, GLUT 4, PDK1 and G6PD than CMPBR3. It also showed higher glucose uptake and lactate secretion, but the lactate secretion per glucose uptake was lower. It seems that mtDNA depletion leads to a higher uptake of glucose and posterior input into glycolysis but its carbons are then after deviated to the pentose phosphate pathway (and probably others), explaining the lower lactate secretion per glucose unit. $143B\rho^0$sm also showed decreased mRNA levels of LDH-A. This may seem contradictory with the increased lactate secretion and also with our observation during cell culture in which the medium where this cell line was

cultured seemed more acidified. We propose that the increased lactate secretion may be due to higher expression of other isoforms of lactate dehydrogenase.

In optimal growth conditions, more pronounced differences between enzyme expression would be expected, however, since 143B and all other lines are osteosarcoma-derived, the levels of the studied enzymes are already overexpressed. In addition, the conditions used in these experiments do not resemble the tumour environment *in vivo*.

4.2.3 Glutamine metabolism

Glutamine metabolism in cancer cells has been target of much investigation in the last years. Tumour cells consume large amounts of glutamine (Sauer *et al.*, 1982). It was proposed that the glutamine metabolism satisfies crucial aspects of metabolic transformation, allowing cells to use glucose carbon to build nucleic acids and lipids. This is important in very proliferative cells like tumour cells. As referred before (see Introduction Section), glutamine metabolism provides both anaplerotic and NADPH demands of growth and at the same time it allows the production of ATP by glycolysis and mitochondria and in part contributes for protein synthesis (Fig. 60). Many studies have demonstrated that tumours consume large amounts of glutamine and "glutaminolysis" has been even considered as a hallmark of tumour cell (Medina, 2001).

Therefore, the glutamine uptake and glutamate secretion rates were also evaluated. Higher glutamine and glutamate fluxes with SDHB silencing, together with the increased lactate secretion suggest that there might be an increased metabolism of

glutamine to lactate or referred as glutaminolysis. These differences were, however, not noticed in 3243CY9.7 cybrid.

Once more, the cancer cell lines used in this work have glutamine consumption and glutamate secretion rates much higher (to a 10-fold level) than a non-tumourigenic cell line (data not published).

In order to clarify the glutamine metabolism, future work must be conducted. It would be necessary, for example, to analyse the expression of glutaminases that deamidate glutamine to form glutamate and ammonia.

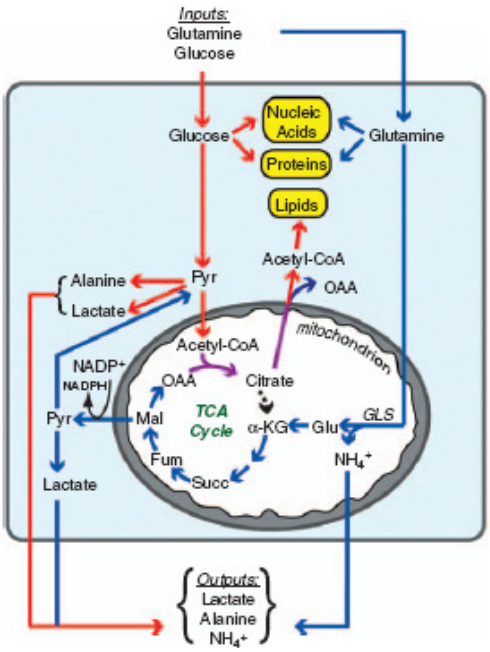

Figure 60: Interaction of glucose and glutamine pathways (DeBerardinis and Cheng).

Given the results we have so far, it becomes evident that the mitochondrial respiration needs to be assessed in order to confirm that the A3243T mutation/SDHB silencing are

indeed causing mitochondrial dysfunction. There is, however, some literature concerning this issue. A3243T transition in the $tRNA^{Leu(UUR)}$ was shown to reduce the activity of mitochondrial oxidative phosphorylation complexes (Shaag *et al.*, 1997). Some studies have been conducted concerning the most commonly found A to G transition in the same base (3243) and marked differences were observed concerning respiratory activity of cybrids with A3243G mutation compared to the parental 143B and with wild-type cybrids (Chomyn *et al.*, 1992). Besides, the successful selection of this mutated cybrids with medium complemented with uridine performed in our study indicates that this mutation leads to a dysfunctional OXPHOS chain. Biochemical analyses have demonstrated that mutations in SDHB lead to loss of a functional enzyme complex and a defective respiratory chain (King *et al.*, 2006). ρ^0 cells are incapable of producing energy through oxidative phosphorylation due to the absence of all mitochondrially-encoded proteins (King and Attardi, 1989). ρ^0 cells rely exclusively on glycolysis for energy (Davis *et al.*, 1996).

4.3 *In vivo* oncogenic capability and in *vitro* tumourigenic phenotypes

Having the appropriate cellular models for mitochondrial dysfunction and partially analysed their metabolism, we were also interested in assessing the ability of the A3243T cybrid cell lines to develop tumours in nude mice and see whether this ability was correlated with cell growth, cell death and migration/motility capacity.

Cybrid cell lines transplantation into nude mice has been employed previously to investigate the role of mtDNA in tumourigenesis (Petros *et al.*, 2005). Our results from the inoculation of mice with 3243CY9.7 cybrid cell line together with wt cybrids

(CMPBR3) and 143Bρ^0sm were very patent. All mice injected with 3243CY9.7 cybrid cell line, developed tumours while no mouse inoculated with CMPBR3 did. Injection of 143Bρ^0sm cells did not cause the growth of tumours as well. These results clearly demonstrate the tumourigenic potential of this specific mutation *in vivo* in comparison to mtDNA depletion and wild-type mtDNA.

In contrast, Morais *et al*. (1994) reported that ρ^0 cells could form tumours (Morais *et al.*, 1994). This may be because in the previous study ethidium bromide was used for depletion of mtDNA can also change the nDNA, affecting some cellular phenotype essential for tumour formation. Moreover, they have not compared cybrids with wild type or mutant mtDNA. This is a very relevant issue because mtDNA mutations arise spontaneously in somatic cells at a relative high rate. Another possible reason for the discrepancy of the results, may lie in the way of administrating the cells: our ρ^0 cell line may not be capable of forming tumours subcutaneously but when cells are injected via intradermic or intravenous, the result may be different (Morais *et al.*, 1994). In the work of Shidara *et al.* (2005) it was shown that ρ^0HeLa cells are able to form tumours, although the settlement frequency was very low (Shidara *et al.*, 2005).

There was no selection against the mutation, because all the tumours excised exhibit it. In fact, in four out of five tumours, the load of mutation seemed to increase slightly.

In addition to the capacity of forming a tumour mass *in vivo*, we could also have some hints concerning the aggressiveness of these tumours. It was clear that in two mice the tumours were invading the adjacent tissue and we could observe the presence of lung metastases also in two mice (one of them also displays invasion of surrounding tissues)

suggesting that the cells that give rise to the tumours *in vivo* possess the ability to invade and metastasize.

These results show that the observed oncogenic properties are independent of the cell nuclear background, even though, we do not exclude the possibility that mutant mtDNA may influence the expression of nDNA-encoded genes involved in cell proliferation or apoptosis. Cells devoid of mtDNA (143Bρ^{0}sm) are not able to form tumours *in vivo,* a condition which could be reverted by the repopulation with mutant mtDNA (3243CY9.7), but not with wt mtDNA (CMPBR3).

Such a clear difference concerning tumour formation *in vivo* should also reflect distinct properties, namely concerning proliferation and apoptosis. In addition, to be able to invade and metastasize, as observed in three out of five mice, cells must possess capabilities in terms of motility and migration.

4.3.1 Cell growth

Our results show that, in the conditions used, the mtDNA mutation in 3243CY9.7 cybrid cell line does not alter the growth rate, being identical to CMBR3. 143Bρ^{0}sm cells showed the highest population doubling time, meaning they take more time to double their population number. This result suggests that the absence of mtDNA delays cell cycle progression. Some cross-talk between the nuclear and the mitochondrial genome might be involved. Our results are in agreement with recent data (Mineri *et al.*, 2009).

In the results, only one replicate was presented due to the fact that during the experiments, we were not able to plate equal cell densities and, consequently, these experiments cannot be considered that way. However, these results were coherent with the observations during cell culture.

4.3.2 Cell death

Programmed cell death is an important biological process involved in embryonic development, maintenance of homeostasis and in several physiological and pathological events in humans. One of the hallmarks of cancer is precisely programmed cell death evasion (Hanahan and Weinberg, 2000).

Programmed cell death is tightly linked to the metabolic condition of the cell, particularly to glucose metabolism (King and Gottlieb, 2009) and mitochondria has been long accepted as having a central role in both these processes (Frezza and Gottlieb, 2009; Tait and Green). It is known that the glycolytic shift in tumour cells makes the outer mitochondrial membrane less susceptible to permeabilization and thereby the cells more resistant to mitochondrially-mediated cell death (reviewed in (Gogvadze *et al.*).

Our TUNEL results indicate that 3243CY9.7 cybrids with the A3243T mtDNA mutation affecting $tRNA^{Leu(UUR)}$ gene are more resistant to STS-induced cell death, comparing to wt mtDNA cybrids (CMPBR3), as measured by the lower levels of DNA breaks. Other authors have also reached to the conclusion that mutations in the mitochondrial genome confer apoptosis resistance. In these studies, cybrids with *MTATP6* (complex V), *ND4* (complex I) and $tRNA^{Leu(CUN)}$ (Kulawiec *et al.*, 2009;

Mizutani *et al.*, 2009; Shidara *et al.*, 2005). On the other hand, there are contradictory evidences (Liu *et al.*, 2004).

In terms of cell death, the effect of the A3243T mtDNA mutation (3243CY9.7 cybrid cell line) and of total mtDNA depletion (143Bρ^{0}sm) seems similar. 143Bρ^{0}sm cell line displayed very low levels of basal cell death and showed to have a higher resistance to induced apoptosis, compared to the parental cell line (143B) and CMPBR3. A mitochondrial dysfunction caused by total depletion of mtDNA (as in 143Bρ^{0}sm) can lead to apoptosis resistance, because it prevents tumour cells from undergoing cell death through mechanisms that involve OXPHOS complexes. For example, complex I was found to integrate a caspase-independent apoptotic pathway, in which granzyme A specifically cleaves subunit NDUFS3 of complex I, resulting in increased generation of ROS, disruption of the mitochondrial transmembrane potential and cell death (Martinvalet *et al.*, 2008). This is also in accordance to the results from our laboratory in which 143Bρ^{0}sm cell lines produces almost no ROS (data not shown).

If, in fact, mitochondrial dysfunction through mtDNA mutations can have a role in decrease susceptibility to apoptosis, as ours results tend to show, this could be used for sensitizing tumour cells to cancer therapy. However, this still under debate as Singh *et al*. (1999) reported that ρ^0 cells were resistance some types of cancer therapy whereas others authors demonstrated that a functioning OXPHOS chain was required for cell sensitivity (Joshi *et al.*, 1999; Singh *et al.*, 1999). This experiment has, yet, to be repeated to confirm this tendency.

As 3243CY9.7 cybrid revealed to be more resistant to cell death, even though they did not show enhanced cell growth *in vitro* - probably evasion of apoptosis was the key

hallmark for the acquisition of growth advantage, presumed by the higher tumourigenic capacity. However, most certainly this is not the only characteristic responsible for tumours formation; otherwise 143B ρ^0sm would have the same result as the cybrids.

4.3.3 Motility, migration and metastization

As stated before, migration and motility are cell features that influence the ability of tumours cell to invade and metastasize. We saw that mutated cybrids presented higher motility and migration rates, compared to parental cells, wt cybrids and 143Bρ^0sm cells.

The role of these two processes alone is not well studied, while invasion, which already implies the capacity of degrading the extracellular matrix, is far more studied. Invasion and migration are, indeed, quite different processes and may imply different pathways: cells that have increased migration and motility capability may not be very invasive and highly invasive cells may not migrate a lot. Our results show, however, that high migration/motility rates may be correlated to increased capability to invade new tissues and metastasize.

By microscopic observation, two of five mice were found to have lung metastasis. The presence of metastases was inferred from the morphologic characteristics of the lung cells stained with H&E and will be confirmed by specific markers of human tumour cells, such as GLUT1 or HKII. Macroscopically, we could also observe the presence of invasion, suggesting that these tumours display an aggressive behaviour. Most likely, we will observe the presence of metastases in other organs of the mice injected with the 3243CY9.7 after an exhaustive search.

Although we did not investigate the mechanism responsible for conferring a higher metastatic ability to cybrid cell line, this issue has been debated for some years. On the one hand, motility is highly influenced by connections between the cytoskeleton and intercellular junctions. Some evidences point to an interaction between cytoskeleton elements and mitochondria (Leterrier *et al.*, 1994). ROS production has been correlated with the cytoskeleton dynamics, as well as with other events that compose the process of metastasizing (Pani *et al.*). In fact, in 3243CY9.7 cybrid cell line it was detected high levels of ROS, comparing to CMPBR3 (data not shown).

One of the links that has been established between the "Warburg effect" and metastatic process concerns acidification of the extracellular matrix. A glycolytic metabolism in the presence of oxygen leads to accumulation of lactate and to acidification of the extracellular space. The cells that are capable of resist to this acidification will probably display a significant selective advantage against surrounding normal cells, leading to enhanced invasiveness. Acidification of the extracellular space is thought to favour matrix degradation and increase the expression of angiogenic factors (Pani *et al.*).

A very interesting study stressed the role of mtDNA mutations in tumour metastasis. By exchanging the mtDNA of two mouse cell lines with different metastatic potentials, the capability to metastasize *in vivo* accompanied the mtDNA (Ishikawa *et al.*, 2008).

4.4 MtDNA depletion vs. mtDNA mutations

The majority of the results showed that the metabolic effects and the ones associated with tumourigenesis of mtDNA depletion are different from the ones resulting from

mtDNA mutations. This was evident in the metabolic phenotype, although a higher level of mutation (3243CY9.7.10) approximated the cybrid metabolic phenotype to the one resulting from total depletion (143Bρ0sm), and also in the migration/motility ability and the oncogenic capability to form tumours *in vivo*. The exception was, apart from cell growth, cell death which may be explained by the strongest role of mitochondria in this process.

Total depletion of mtDNA in 143Bρ0sm cell line may cause a complete absence of the respiratory chain, whereas cell harbouring the mtDNA $tRNA^{Leu(UUR)}$ mutation may still have some residual activity. This should be proved by assessing the respiration capacity of mitochondria and analysing the activity of each complex individually

4.5 Cybrid technology

The cybrid approach has been described as essential to overcome the fact that bulk of cancer properties are regulated by nuclear-encoded genes. In fact, it revealed to be a useful approach to investigate the cellular phenotype associated with mtDNA mutations.

Apart from others, cybrid analysis has the advantage of studying the effects of the entire mitochondria in the same nuclear background regardless of the mutation status in the mtDNA. Besides cybrid technology generates a situation that is less artificial than an upregulation of a gene or abolishing its transcription.

4.6 Signalling pathways

In this work, the aim was not to unravel the mechanisms behind mitochondrial dysfunction that lead to the "Warburg effect", but rather to prove that there is a correlation and this is important for the oncogenic process.

When the literature is reviewed, two important molecules stand out: HIF-1 and ROS.

One of the possibilities for the metabolic and oncogenic changes induced by primary mitochondrial dysfunction is mediated by HIF-1. Silencing SDHB protein can lead to an increase in the intracellular accumulation of succinate. This metabolite is a competitive inhibitor of prolyl hydroxylases, which are enzymes that usually targets HIF-1α for destruction in an oxygen dependent-fashion. A decreased availability of this enzyme to hydroxylate HIF-1α results in an inhibition of the interaction with VHL and consequently the inhibition of its degradation (Guzy *et al.*, 2008; Selak *et al.*, 2005) (Fig. 61).

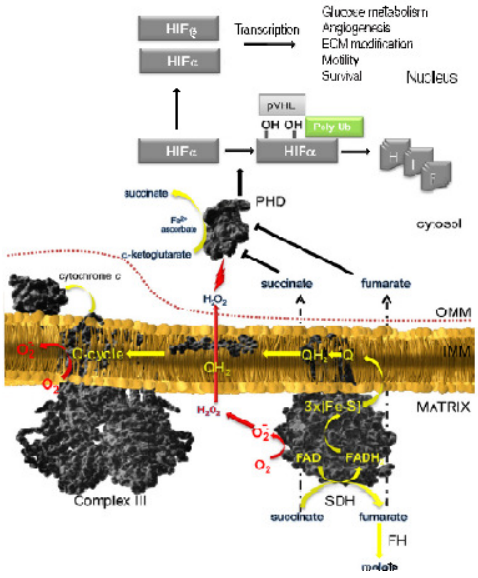

Figure 61: SDH and FH in stabilization of HIF-1α (adapted from Frezza and Gottlieb, 2009; Gottlieb and Tomlinson, 2005).

HIF-1α may also be stabilized by ROS (Pani *et al.*). ROS are generated as a toxic by-product of mitochondrial OXPHOS (Murphy, 2009). MtDNA mutations and mitochondrial dysfunction have been related with higher ROS production (Petros *et al.*, 2005). This is supported by experiments performed in our laboratory that showed higher production of ROS in 3243CY9.7 cybrid cell line, compared with wt cybrids, CMPBR3 (data not published). Although, this assay was not done for SDHB-silenced cell lines, Guzy *et al.* (2008) have shown that inhibition of SDHB cause an increased in oxidant stress (Guzy *et al.*, 2008).

Once stabilized, HIF can be responsible for both the metabolic and tumourigenic alterations that we observed. In fact, HIF leads to activation of transcriptional responses associated to glycolysis and general metabolism, growth factor signalling, immortalization, genetic instability, tissue invasion and metastasis and angiogenesis (Fig. 62).

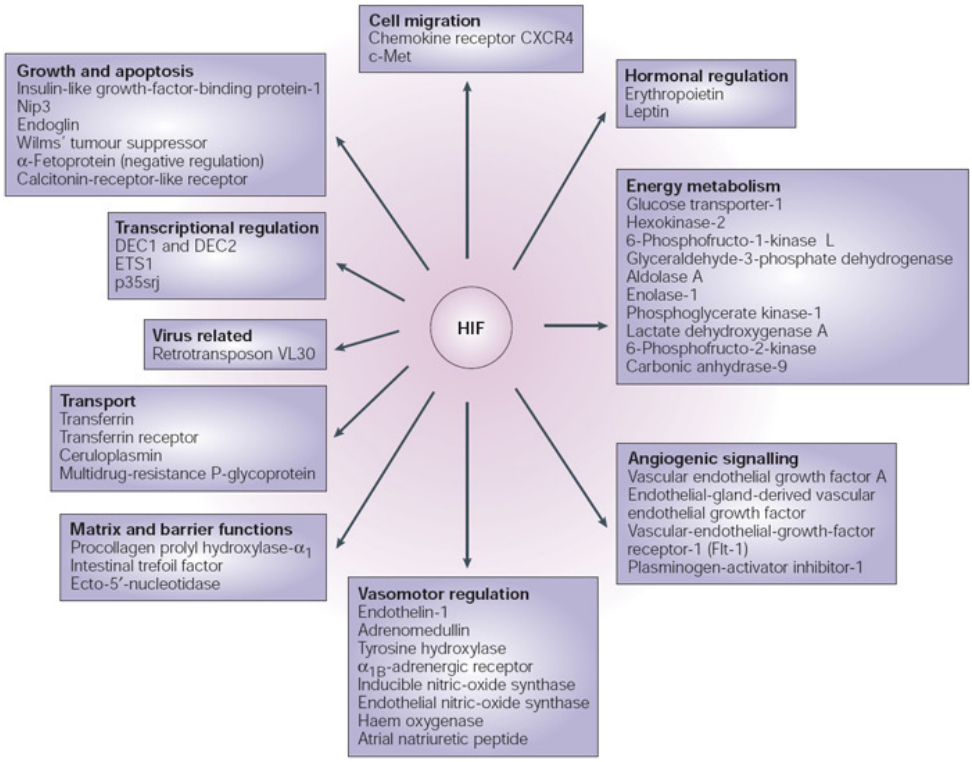

Figure 62: HIF-1 target genes (Schofield and Ratcliffe, 2004).

ROS positively contribute to tumourigenesis in different ways. They have been involved in signal transduction of mitogenic and survival inputs by growth factor receptors (Weinberg *et al.*). They drive genomic damage and genetic instability. ROS signalling by adhesion molecules and changes in cytoskeleton promotes cell motility and shape the tumour microenvironment by inducing inflammation/repair and angiogenesis. ROS have been correlated with all the classical six hallmarks of cancer. However, it should be pointed out that ROS can also function as tumour suppressors (Pani *et al.*).

Together, these evidences point to the fact that mitochondrial dysfunction may activate pathways involved in metabolic shift and development and maintenance of a malignant

phenotype. The role of ROS and HIF in mediating mitochondrial dysfunction and the "Warburg effect" and tumourigenesis deserves deeper understanding because of its promising contribution to antineoplastic therapeutic approaches and prevention for this complex disease that is cancer.

4. 7 Conclusions and future perspectives

The "Warburg effect" is the oldest known phenotype and one of the most common, if not the most common in human tumours. Although it has been shown that a majority of cancer cell lines harbour mutant mitochondrial proteins, it has not yet been determined how mitochondrial dysfunction contributes to tumourigenesis.

In this project we aimed to develop a cell line model of mitochondrial OXPHOS/Krebs cycle dysfunction that could allow us to study the importance of mitochondria in tumour cell metabolism, namely in the Warburg effect, as well as in tumour development. Although we have not yet built a stable cybrid cell line with a *ND1* (complex I gene) mutation, the construction of cybrids with the $tRNA^{Leu(UUR)}$ A3243T mutation was successful as well as SDHB silencing in wild-type cybrids. Our data demonstrated a link between mitochondrial dysfunction and induction of an aerobic, glycolytic and malignant phenotype.

In this study, the "Warburg effect" in mitochondrial dysfunction models was investigated superficially. The goal was precisely the identification of a number of different areas/properties/pathways that deserve further investigation at a more detailed level. For example, it became clear that the putative effects of mitochondrial

dysfunction depend on the environment in which cells are inserted, as seen by the drastic difference in tumour formation *in vivo.*

This area of study is intrinsically associated with the microenvironment in which cell are growing. In order to bring cellular culture conditions closer to *in vivo*, the assays will be performed in hypoxic conditions and lower glucose concentration. .

The metabolic phenotype analysis should be repeated and complemented with other enzymes. It would be very interesting to trace the carbon atoms using some carbon labelling, in order to have a more precise idea of the active metabolic pathways. The lack of replicates in cellular growth, cell death should also be filled. It will be very important to investigate cellular invasion.

Results of the transcription levels of main enzymes of energetic metabolism point out for altered metabolism in A3243T cybrid 3243CY9.7.10. It is imperative to analyse the metabolic phenotype of this cybrid, as well as its oncogenic properties *in vitro* and *in vivo*.

Chapter 5 References

Acebo P, Giner D, Calvo P, Blanco-Rivero A, Ortega AD, Fernandez PL *et al* (2009). Cancer abolishes the tissue type-specific differences in the phenotype of energetic metabolism. *Transl Oncol* **2:** 138-45.

Addabbo F, Montagnani M, Goligorsky MS (2009). Mitochondria and reactive oxygen species. *Hypertension* **53:** 885-92.

Airley R, Evans A, Mobasheri A, Hewitt SM Glucose transporter Glut-1 is detectable in peri-necrotic regions in many human tumor types but not normal tissues: Study using tissue microarrays. *Ann Anat* **192:** 133-8.

Alberts BJ, Alexander; Lewis, Julian; Raff, Martin; Roberts, Keith; Walter, Peter (2002). *Molecular Biology of the Cell*, 4th edn. Garland Science: New York.

Amuthan G, Biswas G, Zhang SY, Klein-Szanto A, Vijayasarathy C, Avadhani NG (2001). Mitochondria-to-nucleus stress signaling induces phenotypic changes, tumor progression and cell invasion. *EMBO J* **20:** 1910-20.

Bayley JP, Devilee P, Taschner PE (2005). The SDH mutation database: an online resource for succinate dehydrogenase sequence variants involved in pheochromocytoma, paraganglioma and mitochondrial complex II deficiency. *BMC Med Genet* **6:** 39.

Bayona-Bafaluy MP, Manfredi G, Moraes CT (2003). A chemical enucleation method for the transfer of mitochondrial DNA to rho(o) cells. *Nucleic Acids Res* **31:** e98.

Bonnet S, Archer SL, Allalunis-Turner J, Haromy A, Beaulieu C, Thompson R *et al* (2007). A mitochondria-K+ channel axis is suppressed in cancer and its normalization promotes apoptosis and inhibits cancer growth. *Cancer Cell* **11:** 37-51.

Bonora E, Porcelli AM, Gasparre G, Biondi A, Ghelli A, Carelli V *et al* (2006). Defective oxidative phosphorylation in thyroid oncocytic carcinoma is associated with pathogenic mitochondrial DNA mutations affecting complexes I and III. *Cancer Res* **66:** 6087-96.

Boss DS, Olmos RV, Sinaasappel M, Beijnen JH, Schellens JH (2008). Application of PET/CT in the development of novel anticancer drugs. *Oncologist* **13:** 25-38.

Brandon M, Baldi P, Wallace DC (2006). Mitochondrial mutations in cancer. *Oncogene* **25:** 4647-62.

Burnichon N, Briere JJ, Libe R, Vescovo L, Riviere J, Tissier F *et al* SDHA is a tumor suppressor gene causing paraganglioma. *Hum Mol Genet* **19:** 3011-20.

Burt BM, Humm JL, Kooby DA, Squire OD, Mastorides S, Larson SM *et al* (2001). Using positron emission tomography with [(18)F]FDG to predict tumor behavior in experimental colorectal cancer. *Neoplasia* **3:** 189-95.

Canter JA, Kallianpur AR, Parl FF, Millikan RC (2005). Mitochondrial DNA G10398A polymorphism and invasive breast cancer in African-American women. *Cancer Res* **65:** 8028-33.

Carew JS, Huang P (2002). Mitochondrial defects in cancer. *Mol Cancer* **1:** 9.

Carroll VA, Ashcroft M (2005). Targeting the molecular basis for tumour hypoxia. *Expert Rev Mol Med* **7:** 1-16.

Chae HJ, Kang JS, Byun JO, Han KS, Kim DU, Oh SM *et al* (2000). Molecular mechanism of staurosporine-induced apoptosis in osteoblasts. *Pharmacol Res* **42:** 373-81.

Chan DC (2006). Mitochondria: dynamic organelles in disease, aging, and development. *Cell* **125:** 1241-52.

Chatterjee A, Mambo E, Sidransky D (2006). Mitochondrial DNA mutations in human cancer. *Oncogene* **25:** 4663-74.

Chiaramonte R, Bartolini E, Testolin C, Comi P (1998). Regulation of the human glut4 gene expression in tumor RD18 cell line. *Pathobiology* **66:** 191-5.

Chomyn A, Enriquez JA, Micol V, Fernandez-Silva P, Attardi G (2000). The mitochondrial myopathy, encephalopathy, lactic acidosis, and stroke-like episode syndrome-associated human mitochondrial tRNALeu(UUR) mutation causes aminoacylation deficiency and concomitant reduced association of mRNA with ribosomes. *J Biol Chem* **275:** 19198-209.

Chomyn A, Lai ST, Shakeley R, Bresolin N, Scarlato G, Attardi G (1994). Platelet-mediated transformation of mtDNA-less human cells: analysis of phenotypic variability among clones from normal individuals--and complementation behavior of the tRNALys mutation causing myoclonic epilepsy and ragged red fibers. *Am J Hum Genet* **54:** 966-74.

Chomyn A, Martinuzzi A, Yoneda M, Daga A, Hurko O, Johns D *et al* (1992). MELAS mutation in mtDNA binding site for transcription termination factor causes defects in protein synthesis and in respiration but no change in levels of upstream and downstream mature transcripts. *Proc Natl Acad Sci U S A* **89:** 4221-5.

Coller HA, Khrapko K, Bodyak ND, Nekhaeva E, Herrero-Jimenez P, Thilly WG (2001). High frequency of homoplasmic mitochondrial DNA mutations in human tumors can be explained without selection. *Nat Genet* **28:** 147-50.

Crabtree HG (1929). Observations on the carbohydrate metabolism of tumours. *Biochem J* **23:** 536-45.

Czarnecka AM, Golik P, Bartnik E (2006). Mitochondrial DNA mutations in human neoplasia. *J Appl Genet* **47:** 67-78.

Darzynkiewicz Z, Galkowski D, Zhao H (2008). Analysis of apoptosis by cytometry using TUNEL assay. *Methods* **44:** 250-4.

Davis AF, Ropp PA, Clayton DA, Copeland WC (1996). Mitochondrial DNA polymerase gamma is expressed and translated in the absence of mitochondrial DNA maintenance and replication. *Nucleic Acids Res* **24:** 2753-9.

Davis JM (1994). *Basic Cell Culture – A Practical Approach*. Oxford University Press: New York.

DeBerardinis RJ, Cheng T Q's next: the diverse functions of glutamine in metabolism, cell biology and cancer. *Oncogene* **29:** 313-24.

DeBerardinis RJ, Sayed N, Ditsworth D, Thompson CB (2008). Brick by brick: metabolism and tumor cell growth. *Curr Opin Genet Dev* **18:** 54-61.

DiMauro S, Schon EA (2001). Mitochondrial DNA mutations in human disease. *Am J Med Genet* **106:** 18-26.

Fantin VR, St-Pierre J, Leder P (2006). Attenuation of LDH-A expression uncovers a link between glycolysis, mitochondrial physiology, and tumor maintenance. *Cancer Cell* **9:** 425-34.

Favaro E, Nardo G, Persano L, Masiero M, Moserle L, Zamarchi R *et al* (2008). Hypoxia inducible factor-1alpha inactivation unveils a link between tumor cell metabolism and hypoxia-induced cell death. *Am J Pathol* **173:** 1186-201.

Fischer K, Hoffmann P, Voelkl S, Meidenbauer N, Ammer J, Edinger M *et al* (2007). Inhibitory effect of tumor cell-derived lactic acid on human T cells. *Blood* **109:** 3812-9.

Frezza C, Gottlieb E (2009). Mitochondria in cancer: not just innocent bystanders. *Semin Cancer Biol* **19:** 4-11.

Gasparre G, Porcelli AM, Bonora E, Pennisi LF, Toller M, Iommarini L *et al* (2007). Disruptive mitochondrial DNA mutations in complex I subunits are markers of oncocytic phenotype in thyroid tumors. *Proc Natl Acad Sci U S A* **104:** 9001-6.

Gatenby RA, Gillies RJ (2004). Why do cancers have high aerobic glycolysis? *Nat Rev Cancer* **4:** 891-9.

Gogvadze V, Zhivotovsky B, Orrenius S The Warburg effect and mitochondrial stability in cancer cells. *Mol Aspects Med* **31:** 60-74.

Goldman RD, Kaplan NO, Hall TC (1964). Lactic Dehydrogenase in Human Neoplastic Tissues. *Cancer Res* **24:** 389-99.

Goto Y, Nonaka I, Horai S (1990). A mutation in the tRNA(Leu)(UUR) gene associated with the MELAS subgroup of mitochondrial encephalomyopathies. *Nature* **348:** 651-3.

Gottlieb E, Tomlinson IP (2005). Mitochondrial tumour suppressors: a genetic and biochemical update. *Nat Rev Cancer* **5:** 857-66.

Grover-McKay M, Walsh SA, Seftor EA, Thomas PA, Hendrix MJ (1998). Role for glucose transporter 1 protein in human breast cancer. *Pathol Oncol Res* **4:** 115-20.

Guzy RD, Sharma B, Bell E, Chandel NS, Schumacker PT (2008). Loss of the SdhB, but Not the SdhA, subunit of complex II triggers reactive oxygen species-dependent hypoxia-inducible factor activation and tumorigenesis. *Mol Cell Biol* **28:** 718-31.

Hanahan D, Weinberg RA (2000). The hallmarks of cancer. *Cell* **100:** 57-70.

Hao HX, Khalimonchuk O, Schraders M, Dephoure N, Bayley JP, Kunst H *et al* (2009). SDH5, a gene required for flavination of succinate dehydrogenase, is mutated in paraganglioma. *Science* **325:** 1139-42.

Harris AL (2002). Hypoxia--a key regulatory factor in tumour growth. *Nat Rev Cancer* **2:** 38-47.

Horton TM, Petros JA, Heddi A, Shoffner J, Kaufman AE, Graham SD, Jr. *et al* (1996). Novel mitochondrial DNA deletion found in a renal cell carcinoma. *Genes Chromosomes Cancer* **15:** 95-101.

Hsu PP, Sabatini DM (2008). Cancer cell metabolism: Warburg and beyond. *Cell* **134:** 703-7.

Isaacs JS, Jung YJ, Mole DR, Lee S, Torres-Cabala C, Chung YL *et al* (2005). HIF overexpression correlates with biallelic loss of fumarate hydratase in renal cancer: novel role of fumarate in regulation of HIF stability. *Cancer Cell* **8:** 143-53.

Ishii T, Yasuda K, Akatsuka A, Hino O, Hartman PS, Ishii N (2005). A mutation in the SDHC gene of complex II increases oxidative stress, resulting in apoptosis and tumorigenesis. *Cancer Res* **65:** 203-9.

Ishikawa K, Takenaga K, Akimoto M, Koshikawa N, Yamaguchi A, Imanishi H *et al* (2008). ROS-generating mitochondrial DNA mutations can regulate tumor cell metastasis. *Science* **320:** 661-4.

Jones RG, Thompson CB (2009). Tumor suppressors and cell metabolism: a recipe for cancer growth. *Genes Dev* **23:** 537-48.

Joshi B, Li L, Taffe BG, Zhu Z, Wahl S, Tian H *et al* (1999). Apoptosis induction by a novel anti-prostate cancer compound, BMD188 (a fatty acid-containing hydroxamic acid), requires the mitochondrial respiratory chain. *Cancer Res* **59:** 4343-55.

Kaipparettu BA, Ma Y, Wong LJ Functional effects of cancer mitochondria on energy metabolism and tumorigenesis: utility of transmitochondrial cybrids. *Ann N Y Acad Sci* **1201:** 137-46.

Kamb A, Wee S, Lengauer C (2007). Why is cancer drug discovery so difficult? *Nat Rev Drug Discov* **6:** 115-20.

Kato H, Miyazaki T, Nakajima M, Takita J, Kimura H, Faried A *et al* (2005). The incremental effect of positron emission tomography on diagnostic accuracy in the initial staging of esophageal carcinoma. *Cancer* **103:** 148-56.

Khaidakov M, Shmookler Reis RJ (2005). Possibility of selection against mtDNA mutations in tumors. *Mol Cancer* **4:** 36.

King A, Gottlieb E (2009). Glucose metabolism and programmed cell death: an evolutionary and mechanistic perspective. *Curr Opin Cell Biol* **21:** 885-93.

King A, Selak MA, Gottlieb E (2006). Succinate dehydrogenase and fumarate hydratase: linking mitochondrial dysfunction and cancer. *Oncogene* **25:** 4675-82.

King MP, Attardi G (1989). Human cells lacking mtDNA: repopulation with exogenous mitochondria by complementation. *Science* **246:** 500-3.

Knecht W, Loffler M (2000). Inhibition and localization of human and rat dihydroorotate dehydrogenase. *Adv Exp Med Biol* **486:** 267-70.

Kruse B, Narasimhan N, Attardi G (1989). Termination of transcription in human mitochondria: identification and purification of a DNA binding protein factor that promotes termination. *Cell* **58:** 391-7.

Kubota K (2001). From tumor biology to clinical Pet: a review of positron emission tomography (PET) in oncology. *Ann Nucl Med* **15:** 471-86.

Kulawiec M, Owens KM, Singh KK (2009). Cancer cell mitochondria confer apoptosis resistance and promote metastasis. *Cancer Biol Ther* **8:** 1378-85.

Kumar B, Koul S, Khandrika L, Meacham RB, Koul HK (2008). Oxidative stress is inherent in prostate cancer cells and is required for aggressive phenotype. *Cancer Res* **68:** 1777-85.

Kunkel M, Reichert TE, Benz P, Lehr HA, Jeong JH, Wieand S *et al* (2003). Overexpression of Glut-1 and increased glucose metabolism in tumors are associated with a poor prognosis in patients with oral squamous cell carcinoma. *Cancer* **97:** 1015-24.

Lazarou M, Thorburn DR, Ryan MT, McKenzie M (2009). Assembly of mitochondrial complex I and defects in disease. *Biochim Biophys Acta* **1793:** 78-88.

Le A, Cooper CR, Gouw AM, Dinavahi R, Maitra A, Deck LM *et al* Inhibition of lactate dehydrogenase A induces oxidative stress and inhibits tumor progression. *Proc Natl Acad Sci U S A* **107:** 2037-42.

Lee HC, Wei YH (2009). Mitochondrial DNA instability and metabolic shift in human cancers. *Int J Mol Sci* **10:** 674-701.

Leterrier JF, Rusakov DA, Nelson BD, Linden M (1994). Interactions between brain mitochondria and cytoskeleton: evidence for specialized outer membrane domains

involved in the association of cytoskeleton-associated proteins to mitochondria in situ and in vitro. *Microsc Res Tech* **27:** 233-61.

Liang CC, Park AY, Guan JL (2007). In vitro scratch assay: a convenient and inexpensive method for analysis of cell migration in vitro. *Nat Protoc* **2:** 329-33.

Lima J, Teixeira-Gomes J, Soares P, Maximo V, Honavar M, Williams D *et al* (2003). Germline succinate dehydrogenase subunit D mutation segregating with familial non-RET C cell hyperplasia. *J Clin Endocrinol Metab* **88:** 4932-7.

Liu CY, Lee CF, Hong CH, Wei YH (2004). Mitochondrial DNA mutation and depletion increase the susceptibility of human cells to apoptosis. *Ann N Y Acad Sci* **1011:** 133-45.

Lodish HB, Arnold; Matsudaira, Paul; Kaiser, Chris A.; Krieger, Monty; Scott, Matthew P.; Zipursky, Lawrence and Darnell, James (2004). *Molecular Cell Biology*, 5th edn. Freeman: USA.

Lopez-Rios F, Sanchez-Arago M, Garcia-Garcia E, Ortega AD, Berrendero JR, Pozo-Rodriguez F *et al* (2007). Loss of the mitochondrial bioenergetic capacity underlies the glucose avidity of carcinomas. *Cancer Res* **67:** 9013-7

Luft R, Ikkos D, Palmieri G, Ernster L, Afzelius B (1962). A case of severe hypermetabolism of nonthyroid origin with a defect in the maintenance of mitochondrial respiratory control: a correlated clinical, biochemical, and morphological study. *J Clin Invest* **41:** 1776-804.

Magnusson J, Orth M, Lestienne P, Taanman JW (2003). Replication of mitochondrial DNA occurs throughout the mitochondria of cultured human cells. *Exp Cell Res* **289:** 133-42.

Malmqvist U, Arner A, Uvelius B (1991). Lactate dehydrogenase activity and isoform distribution in normal and hypertrophic smooth muscle tissue from the rat. *Pflugers Arch* **419:** 230-4.

Mamede M, Higashi T, Kitaichi M, Ishizu K, Ishimori T, Nakamoto Y *et al* (2005). [18F]FDG uptake and PCNA, Glut-1, and Hexokinase-II expressions in cancers and inflammatory lesions of the lung. *Neoplasia* **7:** 369-79.

Martinvalet D, Dykxhoorn DM, Ferrini R, Lieberman J (2008). Granzyme A cleaves a mitochondrial complex I protein to initiate caspase-independent cell death. *Cell* **133:** 681-92.

Mathupala SP, Ko YH, Pedersen PL (2009). Hexokinase-2 bound to mitochondria: cancer's stygian link to the "Warburg Effect" and a pivotal target for effective therapy. *Semin Cancer Biol* **19:** 17-24.

Maximo V, Soares P, Lima J, Cameselle-Teijeiro J, Sobrinho-Simoes M (2002). Mitochondrial DNA somatic mutations (point mutations and large deletions) and mitochondrial DNA variants in human thyroid pathology: a study with emphasis on Hurthle cell tumors. *Am J Pathol* **160:** 1857-65.

Maximo V, Sobrinho-Simoes M (2000). Hurthle cell tumours of the thyroid. A review with emphasis on mitochondrial abnormalities with clinical relevance. *Virchows Arch* **437:** 107-15.

McGowan KM, Long SD, Pekala PH (1995). Glucose transporter gene expression: regulation of transcription and mRNA stability. *Pharmacol Ther* **66:** 465-505.

Medina MA (2001). Glutamine and cancer. *J Nutr* **131:** 2539S-42S; discussion 2550S-1S.

Medina RA, Owen GI (2002). Glucose transporters: expression, regulation and cancer. *Biol Res* **35:** 9-26.

Mineri R, Pavelka N, Fernandez-Vizarra E, Ricciardi-Castagnoli P, Zeviani M, Tiranti V (2009). How do human cells react to the absence of mitochondrial DNA? *PLoS One* **4:** e5713.

Mizutani S, Miyato Y, Shidara Y, Asoh S, Tokunaga A, Tajiri T *et al* (2009). Mutations in the mitochondrial genome confer resistance of cancer cells to anticancer drugs. *Cancer Sci* **100:** 1680-7.

Mochiki E, Kuwano H, Katoh H, Asao T, Oriuchi N, Endo K (2004). Evaluation of 18F-2-deoxy-2-fluoro-D-glucose positron emission tomography for gastric cancer. *World J Surg* **28:** 247-53.

Morais R, Zinkewich-Peotti K, Parent M, Wang H, Babai F, Zollinger M (1994). Tumor-forming ability in athymic nude mice of human cell lines devoid of mitochondrial DNA. *Cancer Res* **54:** 3889-96.

Moreno-Sanchez R, Rodriguez-Enriquez S, Marin-Hernandez A, Saavedra E (2007). Energy metabolism in tumor cells. *FEBS J* **274:** 1393-418.

Mueller MM, Fusenig NE (2004). Friends or foes - bipolar effects of the tumour stroma in cancer. *Nat Rev Cancer* **4:** 839-49.

Murphy MP (2009). How mitochondria produce reactive oxygen species. *Biochem J* **417:** 1-13.

Pani G, Galeotti T, Chiarugi P Metastasis: cancer cell's escape from oxidative stress. *Cancer Metastasis Rev* **29:** 351-78.

Parr RL, Maki J, Reguly B, Dakubo GD, Aguirre A, Wittock R *et al* (2006). The pseudo-mitochondrial genome influences mistakes in heteroplasmy interpretation. *BMC Genomics* **7:** 185.

Parry DM, Pedersen PL (1983). Intracellular localization and properties of particulate hexokinase in the Novikoff ascites tumor. Evidence for an outer mitochondrial membrane location. *J Biol Chem* **258:** 10904-12.

Pathania D, Millard M, Neamati N (2009). Opportunities in discovery and delivery of anticancer drugs targeting mitochondria and cancer cell metabolism. *Adv Drug Deliv Rev* **61:** 1250-75.

Pavlides S, Tsirigos A, Vera I, Flomenberg N, Frank PG, Casimiro MC *et al* Transcriptional evidence for the "Reverse Warburg Effect" in human breast cancer tumor stroma and metastasis: similarities with oxidative stress, inflammation, Alzheimer's disease, and "Neuron-Glia Metabolic Coupling". *Aging (Albany NY)* **2:** 185-99.

Pedersen PL (2007). Warburg, me and Hexokinase 2: Multiple discoveries of key molecular events underlying one of cancers' most common phenotypes, the "Warburg Effect", i.e., elevated glycolysis in the presence of oxygen. *J Bioenerg Biomembr* **39:** 211-22.

Petros JA, Baumann AK, Ruiz-Pesini E, Amin MB, Sun CQ, Hall J *et al* (2005). mtDNA mutations increase tumorigenicity in prostate cancer. *Proc Natl Acad Sci U S A* **102:** 719-24.

Pries AR, Cornelissen AJ, Sloot AA, Hinkeldey M, Dreher MR, Hopfner M *et al* (2009). Structural adaptation and heterogeneity of normal and tumor microvascular networks. *PLoS Comput Biol* **5:** e1000394.

Rivenzon-Segal D, Boldin-Adamsky S, Seger D, Seger R, Degani H (2003). Glycolysis and glucose transporter 1 as markers of response to hormonal therapy in breast cancer. *Int J Cancer* **107:** 177-82.

Robey IF, Lien AD, Welsh SJ, Baggett BK, Gillies RJ (2005). Hypoxia-inducible factor-1alpha and the glycolytic phenotype in tumors. *Neoplasia* **7:** 324-30.

Saffran HA, Pare JM, Corcoran JA, Weller SK, Smiley JR (2007). Herpes simplex virus eliminates host mitochondrial DNA. *EMBO Rep* **8:** 188-93.

Samudio I, Fiegl M, Andreeff M (2009). Mitochondrial uncoupling and the Warburg effect: molecular basis for the reprogramming of cancer cell metabolism. *Cancer Res* **69:** 2163-6.

Sauer LA, Stayman JW, 3rd, Dauchy RT (1982). Amino acid, glucose, and lactic acid utilization in vivo by rat tumors. *Cancer Res* **42:** 4090-7.

Schofield CJ, Ratcliffe PJ (2004). Oxygen sensing by HIF hydroxylases. *Nat Rev Mol Cell Biol* **5:** 343-54.

Schwarzbach MH, Hinz U, Dimitrakopoulou-Strauss A, Willeke F, Cardona S, Mechtersheimer G *et al* (2005). Prognostic significance of preoperative [18-F] fluorodeoxyglucose (FDG) positron emission tomography (PET) imaging in patients with resectable soft tissue sarcomas. *Ann Surg* **241:** 286-94.

Selak MA, Armour SM, MacKenzie ED, Boulahbel H, Watson DG, Mansfield KD *et al* (2005). Succinate links TCA cycle dysfunction to oncogenesis by inhibiting HIF-alpha prolyl hydroxylase. *Cancer Cell* **7:** 77-85.

Semenza GL, Jiang BH, Leung SW, Passantino R, Concordet JP, Maire P *et al* (1996). Hypoxia response elements in the aldolase A, enolase 1, and lactate

dehydrogenase A gene promoters contain essential binding sites for hypoxia-inducible factor 1. *J Biol Chem* **271:** 32529-37.

Semenza GL, Wang GL (1992). A nuclear factor induced by hypoxia via de novo protein synthesis binds to the human erythropoietin gene enhancer at a site required for transcriptional activation. *Mol Cell Biol* **12:** 5447-54.

Seppet E, Gruno M, Peetsalu A, Gizatullina Z, Nguyen HP, Vielhaber S *et al* (2009). Mitochondria and energetic depression in cell pathophysiology. *Int J Mol Sci* **10:** 2252-303.

Shaag A, Saada A, Steinberg A, Navon P, Elpeleg ON (1997). Mitochondrial encephalomyopathy associated with a novel mutation in the mitochondrial tRNA(leu)(UUR) gene (A3243T). *Biochem Biophys Res Commun* **233:** 637-9.

Shaw RJ (2006). Glucose metabolism and cancer. *Curr Opin Cell Biol* **18:** 598-608.

Shibata K, Kajiyama H, Mizokami Y, Ino K, Nomura S, Mizutani S *et al* (2005). Placental leucine aminopeptidase (P-LAP) and glucose transporter 4 (GLUT4) expression in benign, borderline, and malignant ovarian epithelia. *Gynecol Oncol* **98:** 11-8.

Shidara Y, Yamagata K, Kanamori T, Nakano K, Kwong JQ, Manfredi G *et al* (2005). Positive contribution of pathogenic mutations in the mitochondrial genome to the promotion of cancer by prevention from apoptosis. *Cancer Res* **65:** 1655-63.

Singer K, Kastenberger M, Gottfried E, Hammerschmied CG, Buttner M, Aigner M *et al* Warburg phenotype in renal cell carcinoma: High expression of glucose-transporter 1 (GLUT-1) correlates with low CD8(+) T-cell infiltration in the tumor. *Int J Cancer*.

Singh KK, Kulawiec M, Still I, Desouki MM, Geradts J, Matsui S (2005). Inter-genomic cross talk between mitochondria and the nucleus plays an important role in tumorigenesis. *Gene* **354:** 140-6.

Singh KK, Russell J, Sigala B, Zhang Y, Williams J, Keshav KF (1999). Mitochondrial DNA determines the cellular response to cancer therapeutic agents. *Oncogene* **18:** 6641-6.

Smolkova K, Plecita-Hlavata L, Bellance N, Benard G, Rossignol R, Jezek P Waves of gene regulation suppress and then restore oxidative phosphorylation in cancer cells. *Int J Biochem Cell Biol*.

Sutovsky P, Moreno RD, Ramalho-Santos J, Dominko T, Simerly C, Schatten G (1999). Ubiquitin tag for sperm mitochondria. *Nature* **402:** 371-2.

Swerdlow RH (2007). Mitochondria in cybrids containing mtDNA from persons with mitochondriopathies. *J Neurosci Res* **85:** 3416-28.

Swietach P, Vaughan-Jones RD, Harris AL (2007). Regulation of tumor pH and the role of carbonic anhydrase 9. *Cancer Metastasis Rev* **26:** 299-310.

Tait SW, Green DR Mitochondria and cell death: outer membrane permeabilization and beyond. *Nat Rev Mol Cell Biol* **11:** 621-32.

Tennant DA, Duran RV, Gottlieb E Targeting metabolic transformation for cancer therapy. *Nat Rev Cancer* **10:** 267-77.

van den Ouweland JM, Lemkes HH, Ruitenbeek W, Sandkuijl LA, de Vijlder MF, Struyvenberg PA *et al* (1992). Mutation in mitochondrial tRNA(Leu)(UUR) gene in a large pedigree with maternally transmitted type II diabetes mellitus and deafness. *Nat Genet* **1:** 368-71.

Vander Heiden MG, Cantley LC, Thompson CB (2009). Understanding the Warburg effect: the metabolic requirements of cell proliferation. *Science* **324:** 1029-33.

Vazquez A, Liu J, Zhou Y, Oltvai ZN Catabolic efficiency of aerobic glycolysis: the Warburg effect revisited. *BMC Syst Biol* **4:** 58.

Wallace DC (2005). A mitochondrial paradigm of metabolic and degenerative diseases, aging, and cancer: a dawn for evolutionary medicine. *Annu Rev Genet* **39:** 359-407.

Warburg O (1956). On the origin of cancer cells. *Science* **123:** 309-14.

Warburg O, Wind F, Negelein E (1927). The Metabolism of Tumors in the Body. *J Gen Physiol* **8:** 519-30.

Weinberg F, Hamanaka R, Wheaton WW, Weinberg S, Joseph J, Lopez M *et al* Mitochondrial metabolism and ROS generation are essential for Kras-mediated tumorigenicity. *Proc Natl Acad Sci U S A* **107:** 8788-93.

WHO. (2010).

Wigfield SM, Winter SC, Giatromanolaki A, Taylor J, Koukourakis ML, Harris AL (2008). PDK-1 regulates lactate production in hypoxia and is associated with poor prognosis in head and neck squamous cancer. *Br J Cancer* **98:** 1975-84.

Wikstrom JD, Twig G, Shirihai OS (2009). What can mitochondrial heterogeneity tell us about mitochondrial dynamics and autophagy? *Int J Biochem Cell Biol* **41:** 1914-27.

Wittenhagen LM, Kelley SO (2002). Dimerization of a pathogenic human mitochondrial tRNA. *Nat Struct Biol* **9:** 586-90.

Yamamoto T, Seino Y, Fukumoto H, Koh G, Yano H, Inagaki N *et al* (1990). Over-expression of facilitative glucose transporter genes in human cancer. *Biochem Biophys Res Commun* **170:** 223-30.

Yan H, Parsons DW, Jin G, McLendon R, Rasheed BA, Yuan W *et al* (2009). IDH1 and IDH2 mutations in gliomas. *N Engl J Med* **360:** 765-73.

Yeung SJ, Pan J, Lee MH (2008). Roles of p53, MYC and HIF-1 in regulating glycolysis - the seventh hallmark of cancer. *Cell Mol Life Sci* **65:** 3981-99.

Zhidkov I, Livneh EA, Rubin E, Mishmar D (2009). MtDNA mutation pattern in tumors and human evolution are shaped by similar selective constraints. *Genome Res* **19:** 576-80.

Zhou S, Kachhap S, Sun W, Wu G, Chuang A, Poeta L *et al* (2007). Frequency and phenotypic implications of mitochondrial DNA mutations in human squamous cell cancers of the head and neck. *Proc Natl Acad Sci U S A* **104:** 7540-5.

Zielke A, Tezelman S, Jossart GH, Wong M, Siperstein AE, Duh QY *et al* (1998). Establishment of a highly differentiated thyroid cancer cell line of Hurthle cell origin. *Thyroid* **8:** 475-83.